Universitetet i Stavanger

DET TEKNISK-NATURVITENSKAPELIGE FAKULTET

MASTEROPPGAVE

Studieprogram/spesialisering: Master of Science in Petroleum Engineering Production technology	Høstsemesteret, 2014... Åpen
Forfatter: Ole Divino Randmæl	…… (signatur forfatter)
Fagansvarlig: Mesfin Agonafir Belayneh Veileder(e):	
Tittel på masteroppgaven: Engelsk tittel: Challenges of a Floating Production Unit in in the Arctic.	
Studiepoeng:30	
Emneord: FPU FPSO ARCTIC ICE LOADS ICE ACTIONS ICE MECHANICS	Sidetall: 90 + vedlegg/annet:8 Stavanger, 13.01/2014 dato/år

UNIVERSITETET I STAVANGER

Challenges of a Floating Production Unit in in the Arctic

By Ole Divino Randmæl

Contents

I Abstract

The challenging conditions in the deep water Arctic (>100) demands solutions that still have to be develop in order to successfully operate.

In terms of production units the FPSO seems like the most likely solution to use in deep water areas where the distance from shore is too long to build a subsea to shore solution. The ship-shaped FPSO is the only one that have been proven and tested in real waters of the suggested options. It demands however substantial ice management in order to operate safely in Shtokman condition waters. A cylindrical FPSO has no need of weathervaning and requires less ice management. However its open water skills are still questionable and the Cylindrical FPSO-ICE is still a concept only model tested so far. In the arctic the cone shape downward structure near the waterline is to prefer due to the lower ice actions. The rapid climate change offers a problem in terms of for casting and predicting environmental condition when designing for an offshore field for an operating period over several years. The ice properties of the ice ridge are of limited knowledge. This may lead a conservative design of the production units which will increase the cost in an already cost full field development design.

II Acknowledgement

This thesis has been written mostly in Svalbard while taking courses in Arctic Technology. I would like to thank the UNIS in Svalbard for holding inspiring courses in Arctic Technology.

I would like to thank my professors in UNIS, Jan Otto Larsen, Sveinung Løset and Aleksey Marchenko for holding interesting courses and taking me on wonderful fieldwork and laboratory work to get hands on experience in an arctic environment.

I would also send my outmost gratitude to my supervisor Mesfin Agonafir Belayneh which has believed in me, sent me valuable input to my thesis and kept me motivated to finish in the time of need.

My biggest thanks goes to my parents whom I owe everything to, even though it's been a tough year they have supported, encouraged and kept my spirits up and been a solid rock. Thank you.

1 Introduction

This thesis presents a review of challenges on the FPU system in arctic environment. In the report, the basics of ice physics along with the engineering design calculation methods are outlined.

1.1 Background

1.1.1 What is Arctic?

The arctic can have several definitions dependent on the topic it is mentioned in, but it is common to refer the Arctic geographically by the places that has no higher than 10 degrees isotherm in July in the northern hemisphere , or by latitude everything above 66˚N. In this thesis we will refer the Arctic to wherever one encounters Arctic conditions on the northern hemisphere.

1.1.2 What are Arctic Conditions?

The weather conditions in the arctic can be characterized as extreme with respect to temperatures which can drop to -70˚C and by strong winds and huge waves. These factors combined together give one of the most hostile working and living conditions in the world. On top of that the sea has drifting or fixed ice which means operating in these waters could be quite challenging.

1.1.3 What are the opportunities and challenges?

The society today is now looking towards the Arctic to build infrastructure and explore for hydrocarbons and valuable minerals. Offshore constructions will be more and more important in the Arctic since the increase of global temperature makes previously unreachable areas, now accessible. Climatic changes will not only challenge human lively hoods in the Arctic, but also will provide us with new opportunities. The arctic has been warmed up during the last decades with 2.5 degrees Celsius increase of a mean temperature (SWIPA, 2011). This substantial rise of temperature is the key factor in the creation of the new arctic reality

The results of the warming are evident:

- Snow cover extent and duration is decreasing all over the arctic.
- Glaciers, ice caps and the Greenland ice sheet are melting faster.
- Permafrost is thawing
- The sea ice is diminishing both in thickness and extent in summer season.

Even though the sea ice, snow and the ice caps are highly variable and there are regional differences, the changes we see go beyond natural variability. Within the last decade the changes in arctic cryosphere seems to have accelerated.

The following sites are prospective for offshore oil and gas exploration and production in the Arctic and cold regions:

- Beaufort sea
- Grand Banks
- Sea of Okhotsk
- Bohai Sea
- Pecora Sea
- Barents Sea

- Caspian Sea

The Arctic is believed to be an area with the highest unexplored hydrocarbon (HC) potential in the world. By 2035 the demand for oil and gas will grow globally by 18% and 44%, respectively. 60% of planned oil and gas production in 2035 will be from fields not yet found and discovered (A Zolutikin-AT-327 2013)

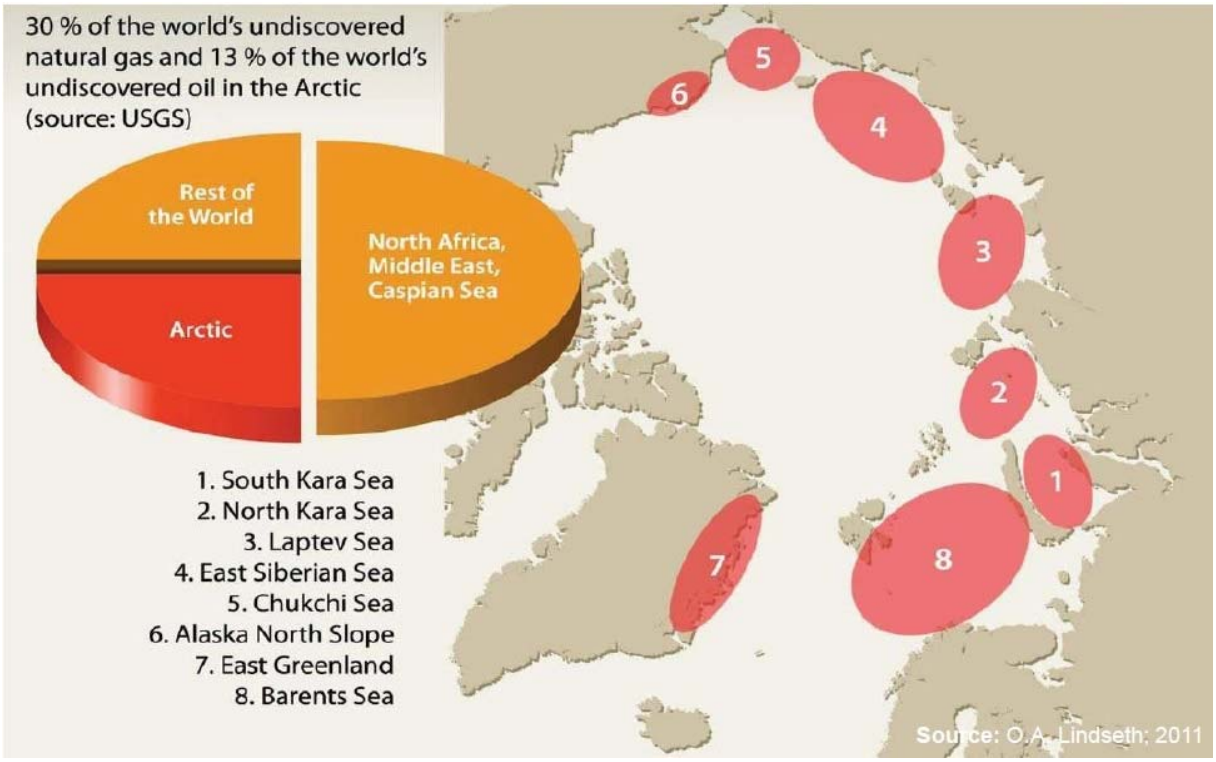

Figure 1 (O.A. Lindseth)

According to USGS, 30% of the world's natural gas and 13% of the world's undiscovered oil is situated in the Arctic.

The challenges in project development in the arctic is however just as big as the opportunities. The challenges of developing Arctic offshore fields can be listed as following but not limited to:

- Severe climate conditions
- Presence of ice
- High economic cost
- Long distance transport of oil and gas
- Lack of technology ,competence and experience in offshore field development
- Deficit of qualified personnel
- Environmental risks that is not yet fully understood
- The energy response time in a remote location must be shortened

In arctic drilling operations it is necessary to plan operations on avoiding contact with sea ice when the ocean is ice free. However, since the summer is short there is insufficient time to complete an exploration in ice free conditions. So the petroleum industry today is actually faced by the decision between avoiding the ice, or to operate in it. The biggest risk can be to operate with open water

equipment under the assumption that ice can be avoided completely. With the changing climate it is difficult to predict whether ice will interact with the platform or not.

During the exploration phase one has to make sure one learns to operate in contact with sea ice in order to increase exploration efficiency. The regional weather, ocean and ice conditions and dynamics must be learned during the first years in the area of the exploration.

During the production phase one can apply the lessons learned in the exploration phase. If the environment is not fully understood, and the operating in contact with sea ice is not mastered the production phase design tends to be overly conservative. This results in highly expensive solutions. The result can be compromises in the production up-time achieved, making the platform less efficient or even not worth to run.

In the arctic, it is important that the operations in contact with ice are built in to the plans from the start of the exploration project. This will maximize the efficiency of not only the exploration, but also the production phase. Since the 1970's, dozens of exploration wells have been drilled in the arctic without unacceptable accidents.

With that being said, it becomes more important to investigate the properties of ice and ice mechanics. With respect to offshore constructions it becomes more prominent to understand ice mechanics in order to build structures that will sustain environmental loads and failure will be prevented as an example due to floating icebergs or drifting ice floes. For instance, with drifting sea ice or ice bergs, design evaluations has to be made in order for the offshore constructions to withstand ice loads which can crate forces up to several megaNewton on a structure. An example of an ice resisting offshore structure is the Moliqpak platform in Sakhalin, Russia. This platform is designed to withstand the moving ice outside the stationary structure.

Figure 2 Moliqpac platform(http://www.oilrig-photos.com/)

However, in areas where icebergs appear frequently, further strengthening becomes impossible or economic unprofitable. So maybe mobile platforms will be seen as a more profitable solution for hydrocarbon field exploitations in the Arctic region. The use of a floating production unit (FPU) allows to decrease the design of ice loads level, which makes it more profitable economically and decreasing risks of accidents.

1.2 Objective

The objective of this thesis is to get an overview over the challenges that comes with field development in the deeper Arctic waters with respect to ice action

1.3 Methodology

The thesis presents an introduction of basic ice mechanics and an overview over alternate floating production units used in the Arctic. I have spent the semester in Svalbard taking courses of Arctic technology which the theory of this thesis is supported on. Following courses was taken:

- *AT-301*
  Arctic Infrastructures in a Changing Climate (10 ECTS)
- *AT-332*
  Physical Environmental Loads on Arctic Coastal and Offshore Structures (10 ECTS)
- *AT-327*
  Arctic Offshore Engineering (10 ECTS)

Both field and case work has been done in the courses and especially an extensive experimental laboratory week with respect to ice properties is described in this thesis. My objective of this thesis is to get knowledge about the challenges there is to developing an Arctic field in the high artic. Before this thesis started I had no knowledge about ice mechanics, field development or construction, so it was a nice chance to broaden my view besides the actual petroleum technology aspect.

2 FPSO unit system designs and Technology

With difference to stationary platforms, a floating production units (FPU) is not fixed to the sea bed by gravity. It is evident that where the water depth and environmental loads are not favorable for fixed structures, a FPU may be the desired choice in terms of practical reasons but also economically. The floaters are designed to take of the hydrocarbons produced from subsea wells with risers of either flexible composite or rigid steel material with a flexible configuration.

While the loads from the deck on fixed structures are transmitted through the bottom founded foundation, the loads from the deck on a floating structure are supported by buoyancy forces of the hull supporting the deck. Following table summarizes the main differences between bottom-founded structures and floating structure design (Chakratrti S.K. 2005):

Function	Bottom-Supported	Floating
Payload support	Foundation-bearing capacity	Buoyancy
Well access	“rigid” conduits(conductors), surface wellheads and controls	“dynamic” risers, subsea wellheads and subsea or surface controls
Environmental loads	Resisted by strength of structure and foundation, compliant structure inertia	Resisted by vessel inertia and stability, mooring strength
Installation	Barge(dry) transport and launch, upend, piled foundations	Wet or dry transport, towing to site and attachment to pre-installed moorings
Regulatory and design practices	Oil industry practices and government petroleum regulations	Oil industry practices, government petroleum regulations and Coast Guard & International Maritime regulations

2.1 Types of FPU’S

There are several types of floating production units and the units which are particularly used for deep water are types such as the FPSO, Semi-submersible, TLP and SPAR.

FPSO

The FPSO is a term that stands for floating production, storage and offloading unit. If the FPU had drilling abilities also the abbreviation would be FPDSO. The shape of an FPSO can vary either if it is shaped like a ship or like a cylindrical buoy. The FPSO has relatively shallow drafts but a relatively large water plane area which provides space for topside equipment for processing and storage of oil and gas.

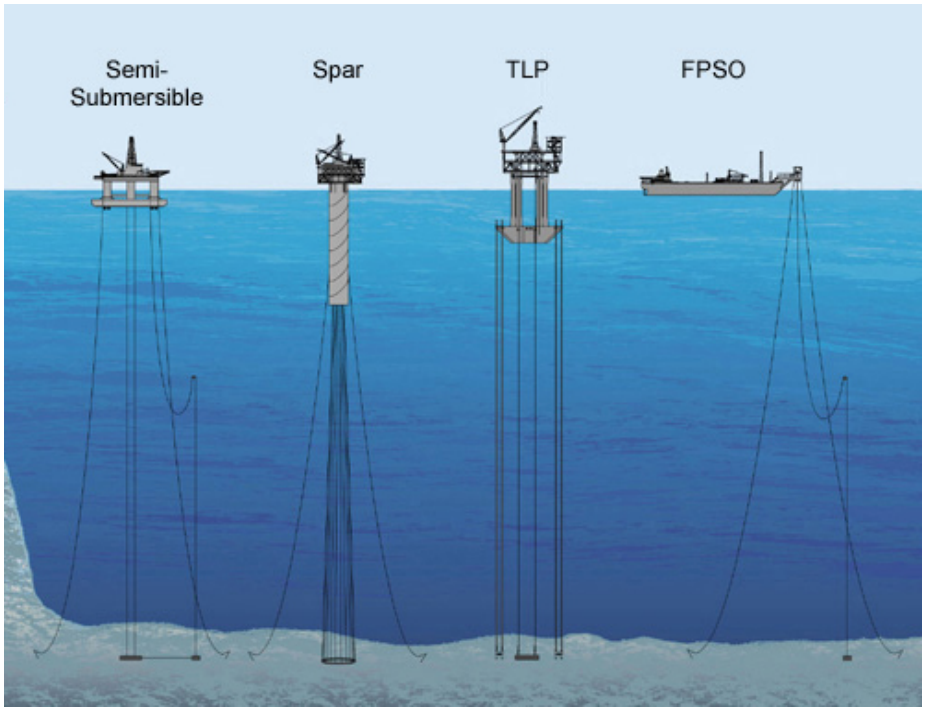

Figure 3 Types of floater solutions (http://www.modec.com/)

Semi-submersible

A semi-submersible is a floating unit which consists of a top side deck that comes in several designs. It is typically stabilized by columns with submerged lower hulls which are semi-submerged to a predetermined draft during operations. Compared to a FPSO the semi-submersible has a small water plane area.

TLP

A tension leg platform (TLP) somewhat resembles the gravity based structures. However it is fully buoyant but vertically moored to the sea floor with tension legs.

SPAR

This floater is also moored to the sea floor like the TLP, however the spar has a deep draft and a moderate to small waterplane area and is characterized by the long and often cylindrical vertical columns. Due to its length the SPAR cannot be pulled into position up right. Therefore it is transported so that the draft is in a horizontal position before the hull is ballasted so that it comes into a vertical position. The topside of the SPAR is connected once the draft is in its position and vertical. In general the SPAR is anchored to the sea floor with multiple tout mooring lines.

2.2 Functional requirements

The type of chosen FPSO depends of the functional requirements that the project area of interest requires. From a general point of view, one can consider the design process as a spiral (fig 4). The functional requirements of a FPSO consist depends on many factors in which each of the factors become better defined once you come further in to the spiral(AP RP2T, 2010). But to make it simple the basic functional requirements that all floaters must have is that it must be stable, safe and usable for its task. The buoyancy of the floater must be equal to the loads from the topside, the moorings and the risers. And especially in an Arctic environment the design of the FPSO must be able to withstand environmental loads in order to keep motions, stability and station keeping to a minimum criterion.

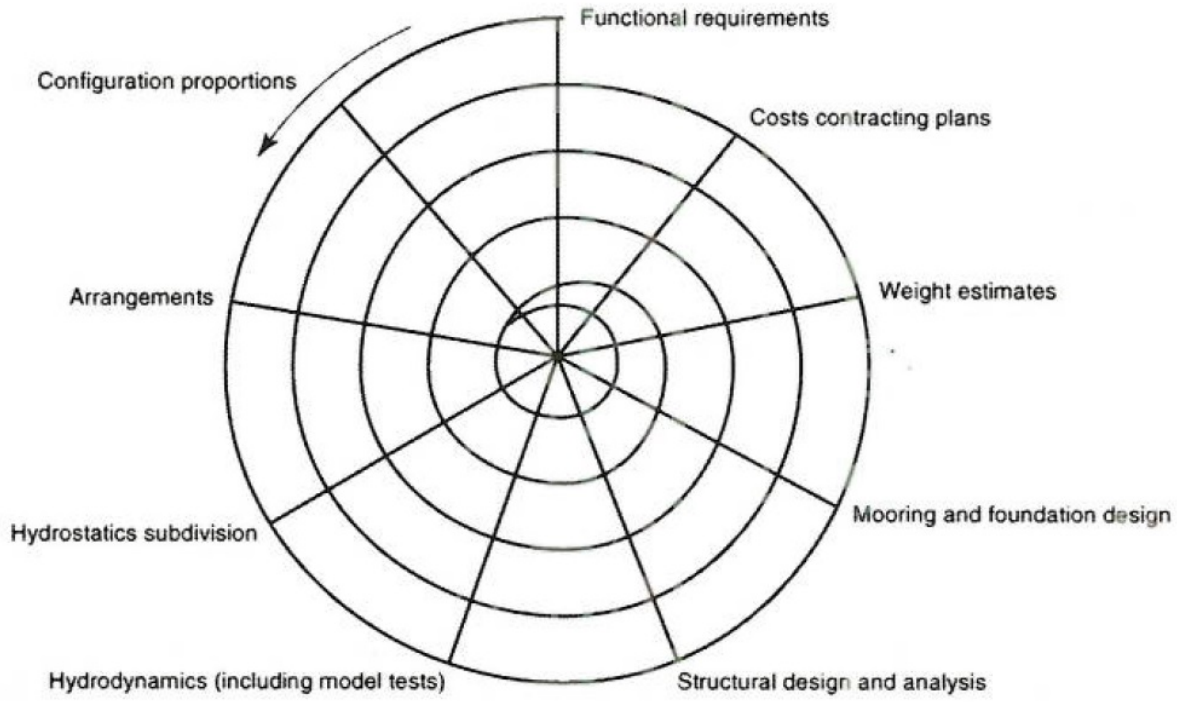

Figure 4 Design process spiral (AP RP2T, 2010)

In the following the functional requirements of a floater will be listed (Chakratrti S.K. 2005):

2.2.1 Topsides weight and dimensions

One of the most important requirements of a floater is the ability to carry its own weight. As mentioned, the buoyancy must be equal to the loads from the topside, the moorings and the riser. The topside weight includes the loads from the facilities on deck which must be carried by the hull. The weight may vary depending on the state the floater is in, either it is drilling, producing, being transported, fully stored with petroleum, etc. So as well as determining the weight of the deck structure, deck area, drilling and producing equipment, etc. it is important to determine the properties of the produced fluids since they affect the topside weight. By calculating the maximum possible topside weight one can determine the maximum buoyancy one must have available on the floater.

2.2.2 Environmental Conditions

The environmental conditions of the region that the FPSO will operate in must be investigated. It is no good idea to be designing a FPSO to be prepared for tempered waters like the south pacific when it is going to be used in the high Arctic and vice versa. Over dimensioning a floater will give unnecessary expenses economically, and under dimensioning a floater might be fatal and lead to accidents. It is common practice to specify a design criteria based on a 100 year return period, which is based on a probability of events happening, weather it is huge waves, strong winds, strong currents or icebergs.

2.2.3 Water depth and Geotechnical Properties

The water depth and the soil properties of the sea bed dictate especially how the floater should be moored. Depending on the soil the anchors must be design to have a good attachment to the sea bed. A FPSO over 20m depth cannot be moored to the sea bed the same way as over a depth of 1000m. The depth of the water dictates how the mooring lines should be distributed.

2.2.4 Risers

A typical riser for bottom-founded structures is fixed and not flexible. For the floater it is often that the riser is flexible but also has the ability to produce and drill. And one of the most fundamental issues in planning a deep-water field is the choice of either a wet tree or dry tree. With the use of flexible risers is associated with wet trees. The SPAR and the TLP are the only floaters that utilize a dry tree of the fleet of floaters (Ronalds and Lim, 2001). The design of the floater decides whether the tension of the floater is to be carried by the vessel or by other means and it is important to identify the scenarios of failures that leads to tensions and stroke of the riser like a broken mooring line or a flooded compartment of the hull.

2.3 FPSO Specifications

Further in this chapter the specifications of floating production storage and offloading system will be reviewed. A FPSO can have several different appearances, either if it is a converted tanker or a purpose built vessel. The firs obvious difference that separates the FPOS from each other is the shape of the hull. The FPSO can either be ship shaped or designed as a mono hull with a cylindrical shape. What they have in common is that they are equipped with hydrocarbon processing facilities installed on deck and can process both oil and gas with the possibility to store it as well.

2.3.1 FPSO Hull design

The size of a FPSO is determined by the hull size in which again is determined by following four parameters (Chakratrti S.K. 2005):

1. *Provision of oil storage capacity compatible with the production rate and offloading arrangements, i.e. shuttle tanker turnaround time.*
2. *Provisions of topsides space for a safe layout of the process plant, accommodations and utilities.*
3. *Provision of displacement and ballast capacity to reduce the effects of motions on process plant and riser systems.*
4. *Provisions of space for the production turret(bow, stern or internal), and the amount of hull storage capacity lost as a consequence(new-build or conversion)*

The shape of the hull much determines how the environmental loads will affect the floater. A converted tanker will typically have the length to breadth ratio of about 6:1, this design favors the motion to go forward. However, the FPSO'S are not required to do that so the new purpose built FPSO would often have another type of hull shape than of a tanker. It is now standard to design a FPSO as a permanently moored vessel and then make adjustments from that depending on the purpose and environment the FPSO would operate in.

2.3.2 Topside

The deck structure of an FPSO consists of production and processing units, accommodation for the workers, production turret and other equipment. On a ship shaped FPSO the turret is placed either on the back (stern) or the front (bow) of the ship depending on several factors as, safety hazards, capacity issues, ship handling etc. Some FPSO, typically the circular mono-hulls do not have the turret topside but make use of an external turret.

2.3.3 Positioning system

Due to the fact that the floater is not fixed into position in the same way as a bottom founded structure, the FPSO is subjected to loads that can give translational and rotational motions. To describe the directions of motions and movement a coordinate system is used. The translational and rotational motions can be translated into a xyz coordinate system where the motions can be named as following: Surge(X), sway(Y), heave(Z), roll(X-axis), pitch(Y-axis) and yaw(Z-axis).

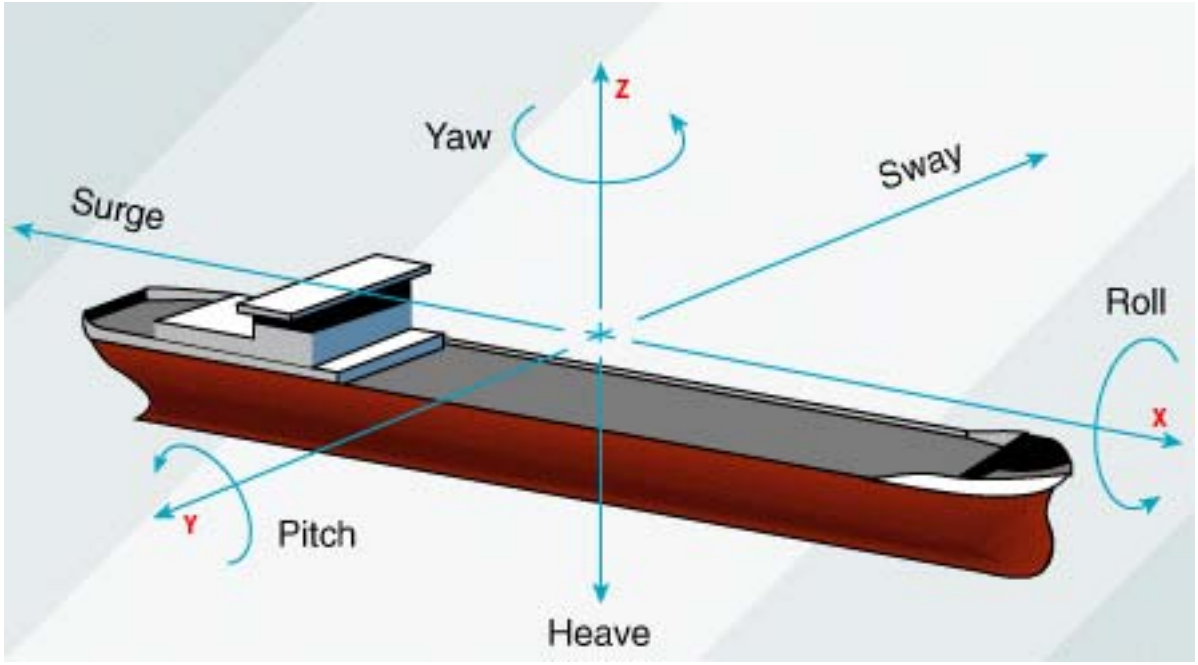

Figure 5 Position coordinad axis (www.ogj.com)

In order to keep the FPSO stable and stationary the mooring and positioning system is vital. There are several types of mooring systems and in the following a review of the most common types will be done.

An important feature to keep the FPSO stationary is the mooring or positioning of the floater. In order to describe the types of positioning system, we can divide the types into three groups.

2.3.3.1 Spread mooring lines

This type of mooring system consists of lines that are firmly embedded to the seafloor. The FPSO are moored with the lines attached in the bow and stern in such way that the boat is prevented from yawing or weathervane. One can further subdivide the spread mooring system to two more types.

Catenary mooring

With this type of mooring the mooring forces is obtained mainly from the net weight of the spread catenary mooring. This means that due to the weight of the lines itself, steel or chains, the line will have a slope in such way that the forces will have a horizontal direction at the sea bed.

Tout mooring

Tout mooring is defines as when the mooring lines is arranged straight rather than a slope, and is adjusted by high initial mooring forces obtained from the elastic elongation of these lines. In order to have this ability the lines used are lighter than the catenary steel lines or chains. This method is preferred at deep water fields due to the angle of the lines.

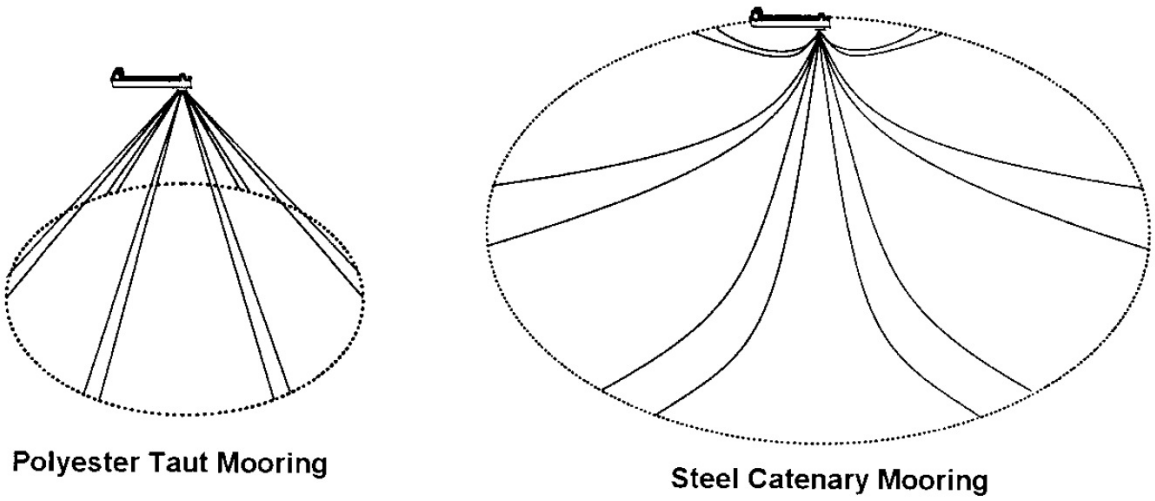

Figure 6 taut mooring vs catenary mooring (Chakratrti S.K. 2005)

2.3.3.2 Single point mooring

Single point mooring system is a system that allows a unit to weathervane due to the change of environmental conditions. There are several types of single point mooring systems and some of them can be subdivided into the following.

Catenary anchor leg mooring

Consist of a large buoy connected to mooring points along the sea bed. The unit is moored to the buoy by mooring lines or an inelastic yoke construction.

Single anchor mooring

Consist of the mooring structure with buoyancy which is positioned at or near the water surface, and is connected to the sea bed. The unit is then moored to the buoy by mooring lines or an inelastic yoke construction.

Turret mooring

There are several types of turret concepts that can be used. A can be turret installed internally within the floater, or externally at the stern or the bow. Even a disconnectable turret that is moored to the seabed by a spread mooring system can be used under the floater.

2.3.3.3 Dynamic positioning

Rather than mooring a floater to a fixed position, an alternate option can be used. The dynamic positioning (DP) system is basically based on that the floater has thrusters which are mounted in such way that thy give force thrust in both longitudinal, transverse directions and torque around a vertical axis so that the floater remains fixed over a desired position. The DP system keeps track on data from different sensors which measures motions and conditions created by environmental features so that the thrusters can counteract undesirable motions to keep the floater stable and in place.

2.3.4 Turret design

The turret system allows the vessel to freely weathervane around the turret, which is fixed by moorings to the sea bed. There is a wide selection of FPSO turrets in the market today. The placement of the turret greatly affects the floaters performance in terms of handling. For example, it is easier for the FPSO to weathervane into equilibrium if the turret is placed either on the stern or the bow under non-collinear environments compared to if the turret is placed in the middle of the boat. However, having the turret at the bow or the stern will increase vessel pitch that again may lead to opposing effect on the mooring line tensions in the line dynamic mooring analysis (Chakratrti S.K. 2005). The turret also affects the FPSO design in other ways such as loss of cargo tank volume, longitudinal strength of the floater, riser design amongst other factors.

2.3.5 Offloading

The produced gas and oil must be able to be offloaded and transported to the marked. The offloading can be done in several ways to a shuttle tanker with a hose using equipment such as a offloading reel, trailing hose, loading buoy and more. Depending on the configuration of the FPSO the offloading can take place from either the stern or the bow or if it is a cylindrical FPSO simply from the either side of the floater. The configuration of offloading procedures becomes important under harsh environmental condition due to the risk of pulling forces on the offloading hose.

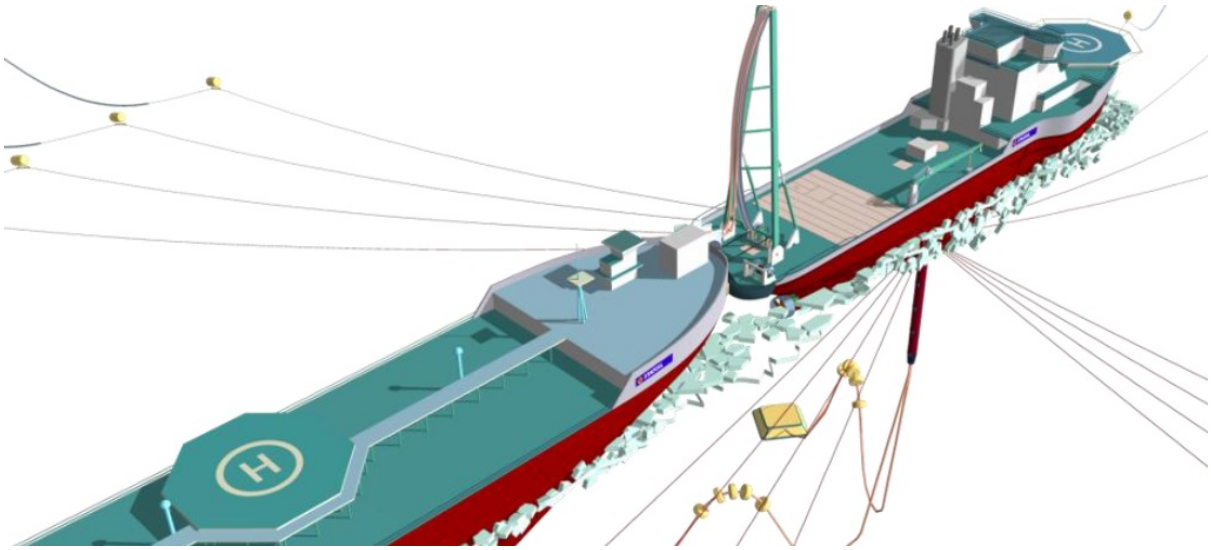

Figure 7 FPSO offloading concept (S. Løset 2011)

3 Ice Mechanics

3.1 Formation of Ice

3.1.1 Properties of ice

There are 12 crystalline forms of ice, in which in this thesis we are going to study the crystalline ice, Ih. Ice Ih is termed ordinary ice whose hexagonal crystal symmetry is reflected in the shape of snowflakes. This type of ice is the stable form at normal temperatures and pressures. The way the water molecule is bent determines how the molecules fit together in a crystal. Each oxygen atom has two hydrogen atoms attached to it at the distance of 0.95 Å, forming an angle of 104.31°. The presence of two lone-pair electron orbitals makes sure that the H_2O molecule is non-linear and form an approximately a tetrahedral system with two bonding orbitals. The angle between bonds is about 109,30°, and the units of oxygen and hydrogen in ice differ only slightly from the molecular structure of water.

Pauling (Pauling 1935)proposed a statistical model for the structure of ice Ih based upon the Bernal-Fowler ice rules :

- Each oxygen atom has two hydrogen atoms attached to it at distances of about 0.95 Å, thereby forming a water molecule.
- Each water molecule is oriented so that its two hydrogen atoms are directed approximately towards two of the four oxygen atoms that surround it tetrahedral.
- The orientation of adjacent water molecules is such that only one hydrogen atom lies between each pair of oxygen atoms.
- Under ordinary ice conditions ice Ih can exist in any one of a large number of configurations, each corresponding to certain distribution of the hydrogen atoms with respect to the oxygen atoms.

It forms in a shape of a hexagonal prism. Each layer of the prism consists of 6 oxygen atoms bonded with each other by two hydrogen atoms. Each layer is then bonded to the next layer by one hydrogen atom. This layer defines the basalt layer, or the a-axis in the structure. The c-axis is perpendicular to the basalt plane. The fundamental building block of the crystal structure of ice is the unit cell. By stacking unit cells face to face in perfect alignment, the complete 3D crystallographic structure is constructed.

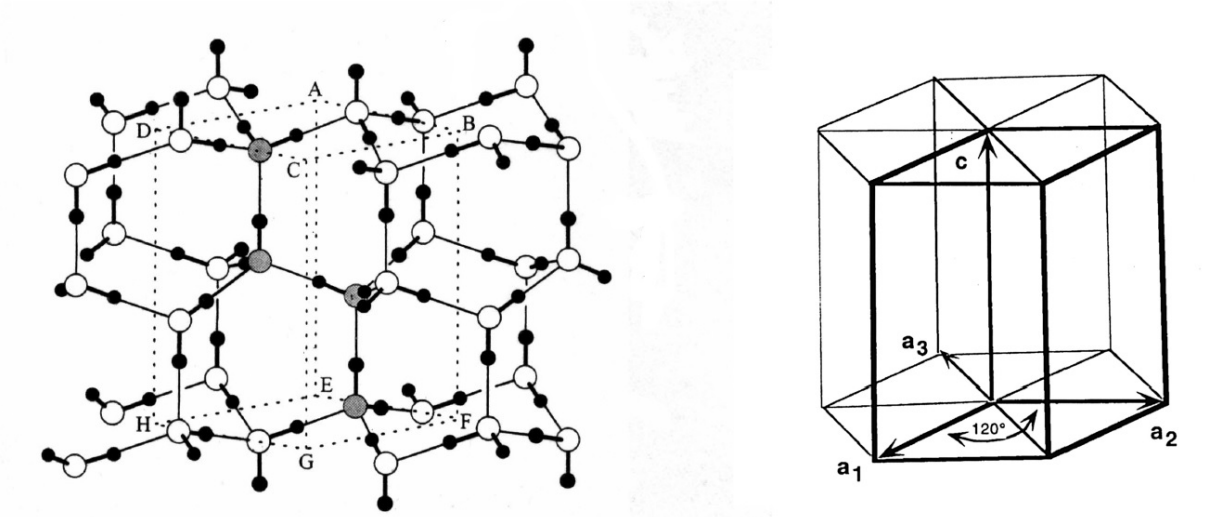

Figure 8 Structure of the ice crystal, hexagonical shape on the right side (S.Løset Ice compendium 1998)

Properties of the unit cell:

•A parallelepiped (6 parallelograms).
•The ribs a have a length 4.51 Å and the ribs along the c-axis have a length 7.35 Å.
•The 8 O-atoms on the vertices are each shared between 8 unit cells.
•The 4 O-atoms on the edges are each shared Between 4 unit cells.
•There are 2 O-atoms within the unit cell, consequently, there are exactly 4 O-atoms in a unit cell.

The basal planes at the top and bottom are shared between stacking unit cells. Thus, there are 2 basal planes inside the unit cell.
Each O-atom has 3 H-bonds in the basal plane, and only 1 H-bond perpendicular to the Basal plane, i.e. along the c-axis. Consequently, fracture along the basal plane involves the rupture of 2 H-bonds in the unit cell, while fracture along any plane normal to the basal plane requires the breaking of at least 4 H-bonds. Thus, hexagonal ice fails by gliding and cleaving along the basal plane, rather than by fracturing along the c-axis. Thus, ice is an **anisotropic** material. The c-axis is the only axis of symmetry in the Ih lattice, thus the thermal conductivity, elastic stiffness and atomic diffusivity are isotropic perpendicular to the c-axis.

The Ih lattice has a relative open structure, so the water molecules can get closer and packed in a random matter together if the lattice breaks down. This is the reason why liquid water is denser than ice, which leads to the ice actually floating on top of the water.
If we look at sea water there is some slight differences than in fresh water. When sea water freezes, the salt is expelled completely from the first flat ice platelets that form. Therefor we can get pure ice cover in the sea. Due to its size, NaCl ions cannot fit in the Ih lattice and neither do they fit into the ice crystals as interstitial molecules. So when seawater freezes over, the ice crystals reject the salt into the water surrounding the ice, increasing the salinity of the surrounding water. Some of the rejected salts forms brine pockets in the ice and some are mixed with the underlying water. The salinity influences the strength of the ice by making it more porous. The salt in the ice is also rejected slowly during the lifetime of the ice, in the melting season the pockets grows and may form channels that drain the salts out

The Ih crystal which obeys the Bernal-Fowler rules is an ideal ice crystal. An ideal perfect ice crystal would be difficult to permanently deform. However, in nature the ice crystals often have deformations as shown in. These deformations are responsible for giving the creeping properties of ice. There are several ways the crystal structure of ice may deviate from the ideal Ih lattice structure. The following table gives a brief summary of the most common defects in the ice structure (Løset Ice compendium,1998) .The defects are grouped into the types of defects:

- Point defect - defect at one water molecule
- Line defect – defect along of line of water molecules
- Plane defect – defect along a plane of water molecules.

3.1.2 Types of Ice formations

The soluble chemicals from the soil and rock are carried out from the rain that lands on land and carries the solution out to the sea. When the ocean evaporates, most of the dissolved solution is left behind giving the sea a typical salinity of 34.5 ppt. The salinity in the sea causes the seawater to have a freezing point below zero degrees. For the value of 34.5 ppt. the water freezes over first when its -

1.8°C and the first ice crystals start to from at 1.9°C. A certain amount of super cooling is required to form the first ice crystal.

When the ocean is calm, only the top layer is super cooled.
The first ice that forms is the primary layer; in this layer the c-axis of the ice structure is randomly oriented. The initially formed ice crystals will grow into the form of hexagonal needles whose c-axes are parallel to the needle axis. The orientation of these needle-formed crystals in water is generally completely random. The needles will tend to grow along the basal plane into the water, i.e. across the width of the needle. At small temperature gradients crystallization proceeds slowly which leads to that the initial needles will float horizontally and the c-axis will take a horizontal orientation. At larger temperature gradients (usual) - a more rapid solidification which leads to that the initial needles will interlock, and the c-axis will become randomly orientated

Usually at sea, wind and waves will agitate the surface layer, mixing the initial ice crystals near the air-water interface with the water beneath, causing super cooling to extend to deeper levels. Thus, instead of the initial ice crystals staying near the air-water interface, they are suspended in the super cooled water column. This suspension of ice crystals may occur up to several meters. Natural nucleation of the initial crystals in the super cooled water column will then cause the formation of so-called frazil particles in the form of small discoids or fine spiculae. These discoids and fine spiculae of ice stay suspended in water and are known as frazil ice. Frazil ice has a grain size < 2 mm, and abrasion and rotation of the frazil particles relative to one another results in a random *c*-axis orientation.

3.1.3 Ice features in arctic waters

When speaking of sea ice it can be divided in the age of the ice itself.

- Young ice is ice that has grown up to 30 cm in thickness. This ice type has not yet survived a melting summer.
- First year ice has developed from young ice and is defined as ice which has no more than one winter's growth. First year ice can be as thick as 2m.
- Old ice is defined as sea ice which has survived at least one summers melt with a typical thickness up to 3m or more. Most topographic features are smoother than on first year ice. Old ice can be sub divided into second-year ice and multi-year ice.

Ice floe - An ice floe is defined as an relatively flat piece of sea ice which can be sub divided with respect to horizontal size as follows:

- Giant floe- Over 10km across
- Vast floe – in the range of 2-10 km across
- Big floe – 500 -2000m across
- Medium floe – 100-500m across
- Small floe – 20-100m across
- Ice cake/broken ice – any relatively flat piece of sea ice less than 20m across.

Iceberg – A massive piece of ice originated from a glacier which can vary greatly in shape and sizes. Usually protruding more than 5m above sea level and can either be floating or grounded. Ice bergs

can be described with respect to shapes as tabular, dome-shaped, sloping, pinnacled, and weathered or glacier bergs.

Bergy bit – A large piece of floating glacier ice generally showing less than 5m above sea-level but more than 1m and is normally about 100-300m^2 in area.

Ice field – Area of floating ice which consist any size of floes that is greater than 10km across.

Ice patch – Area of floating-ice that is less than 10 km across.

Ice-surface features

Level-ice – Sea ice which has not been affected by deformation.

Deformed ice – A general term for ice which has been squeezed together and in places forced both upwards and downwards. Deformed ice can be subdivided further into:

- *Rafted ice* – Type of deformed ice formed by on piece overriding another.
- *Ridge* – A line or wall of broken ice forced up by pressure. The submerged volume of broken ice under a ridge, forced downward by pressure is termed an ice keel.
- *Consolidated ridge* – A ridge in which the base has frozen together.
- *Ridged ice* – Ice piled randomly one piece over another in the form of ridges and walls. Usually found in first year ice.
- *Rubble field*- An area of extremely deformed sea ice of unusual thickness formed during the winter by the motion drift against or around a protruding rock, islet or obstruction.

3.2 Failure Modes

When we want to consider the structural design for a platform we need to think about two types of ice actions. The global and the local ice action loads.

When looking at the local ice action we consider only a smaller part of the contact area, a smaller contact area gives a higher local pressure. This small area is typically in a size up to 2m^2.

If we look at the overall strength and stability of the structure, we look at the global action, which is the action exerted on the whole structure at any instant time. The global ice action depends on two factors which is the effective contact area and the local stresses or the nominal contact area and the effective pressures between the ice and the structure if the effective contact area is not specified.

The main problem when it comes to predicting conditions causing a failure of an ice feature in the vicinity of a structure can be formulated as follows(S.Løset 2006):

“for a given structure form, the ice properties and environmental conditions it is necessary to find the action required to fail an ice feature”

Even though there are two main factors that affect the global load, there are several factors that affect the contact area and the stresses. A following figure shows roughly how things depend on each

other with respect to ice actions.

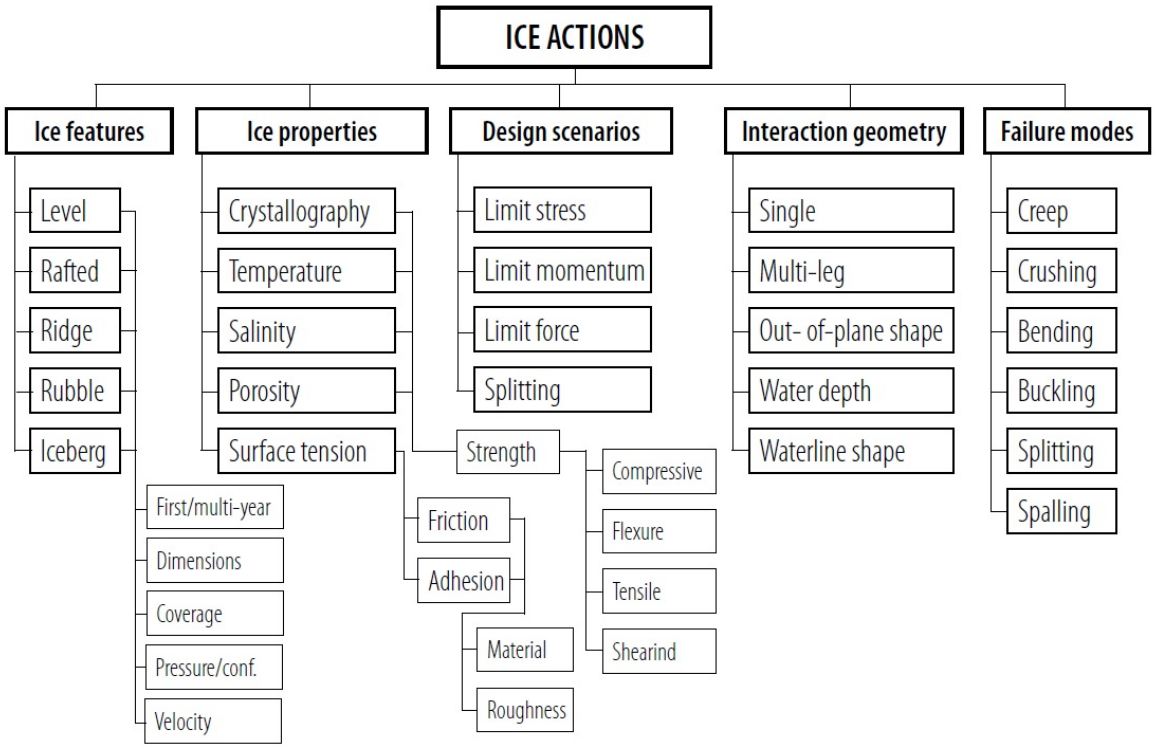

Figure 9 Parameters that affect the ice action (Løset et al. 2006)

Since ice is a material that does not behave purely elastic or viscous, it does not readily lend itself into framework of classical mechanics. Under stress application an ice sample displays a combination of responses (Sanderson 1988).

Ice shows an instantaneous elastic response, but also immediately begins to creep at a time dependent rate. In addition, ice is an extremely brittle material if the stress of the ice is high enough or applied long enough.

When talking about mechanical properties of ice, it is most important to distinguish between brittle and ductile behavior. It is convenient to divide the treatment of ice properties into two parts (Sanderson 1988):

- Continuum behavior – elastic and ductile creep deformation without fracture or rupture
- Fracture behavior – brittle and ductile-brittle in which cracks form

Laboratory test on ice is usually a uniaxial compression, uniaxial tension or an indentation test.

The indentation test gives a realistic picture of interaction between a construction and ice. Failure mode during indentation depends principally on two things: the rate of indentation, defined as U/D and aspect ratio D/h. U is relative velocity of ice, D is the width of the indenter, and h being the vertical thickness of ice. With indentation tests carried out by scientists in the past, a variety of failure modes were observed(Sanderson 1988):

- **a)** *Creep*: at low indentation rates, deformation is entirely in the continuum mode with no formation of cracks. The stress associated with creep deformation is dependent on indentation rate, strain rate, aspect ratio and on any type of ice anisotropy involved.
- **b)** *Radial cracking*: At high aspect-ratio (ratio between the diameter of the indenter and height of the ice sheet) and above a certain stress level, formation of radial cracks is commonly observed.
- **c)** *Buckling:* If the ice sheet is thin it is more prone to elastic buckle formation. The buckles are unstable and rapidly lead to the formation of circumferential cracks.
- d) *Circumferential cracks* may form as a result of elastic buckling. In other case they may form due to an overall applied out of plane bending movement from eccentric loading conditions.

In addition to these global failure modes two local failure modes can be also named (S.Løset 2006):

- **e)** *Spalling* also known as flaking, is observed as in-plane horizontal crack that grows away from the contact zone and fragments of ice break away upwards and downwards and divides the ice sheets into layers. During high indentation rates and low aspect ratio the event of local spalling is frequently observed.
- **f)** *Crushing:* During crushing the ice at the contact zone is pulverized to a powder and extruded upwards and downwards.

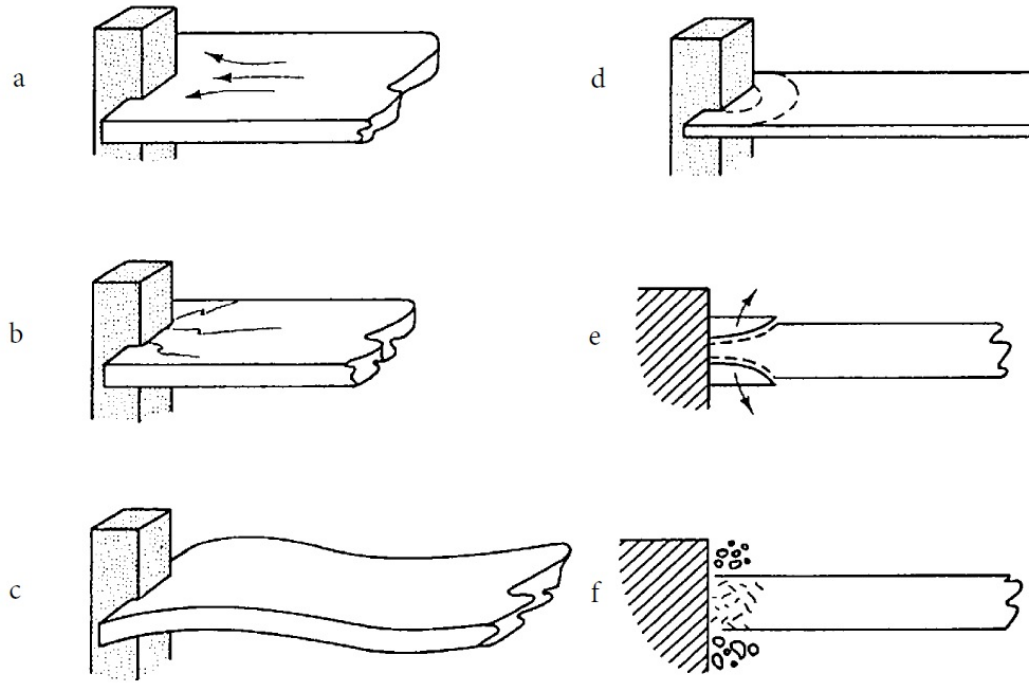

Principle failure mechanisms observed during laboratory indentation experiments: (a) — creep, (b) — radial cracking, (c) — buckling, (d) — circumferential cracking, (e) — spalling, (f) — crushing (Sanderson, 1988).

Figure 10

3.3 Ice actions

The type of failure is affecting the magnitude of the ice action. If the ice failures by crushing it will give a larger ice action than if the ice fails by flexure. The design features of structure makes an impact on what kind of failure the ice feature will experience. Following parameters may determine the failure mode for the sea ice:

- The ice thickness
- Presence of ridges
- The velocity of the ice feature
- Temperature of the ice
- Shape of the structure

The shape of the structure is one important parameter to determine the failure mode. A vertical structure will be more prone to ice action by crushing failure while sloping structures are more prone to ice actions by bending failure. That is why vertical structures generally experience larger ice actions than sloping structures. However, the complexity and composition of the failure modes in the end determines the magnitude of the action.

For the interaction scenarios it is useful to consider the limiting mechanisms. Looking at the design scenario we can from the figure 11 see that there are 4 different scenarios that has to be considered.

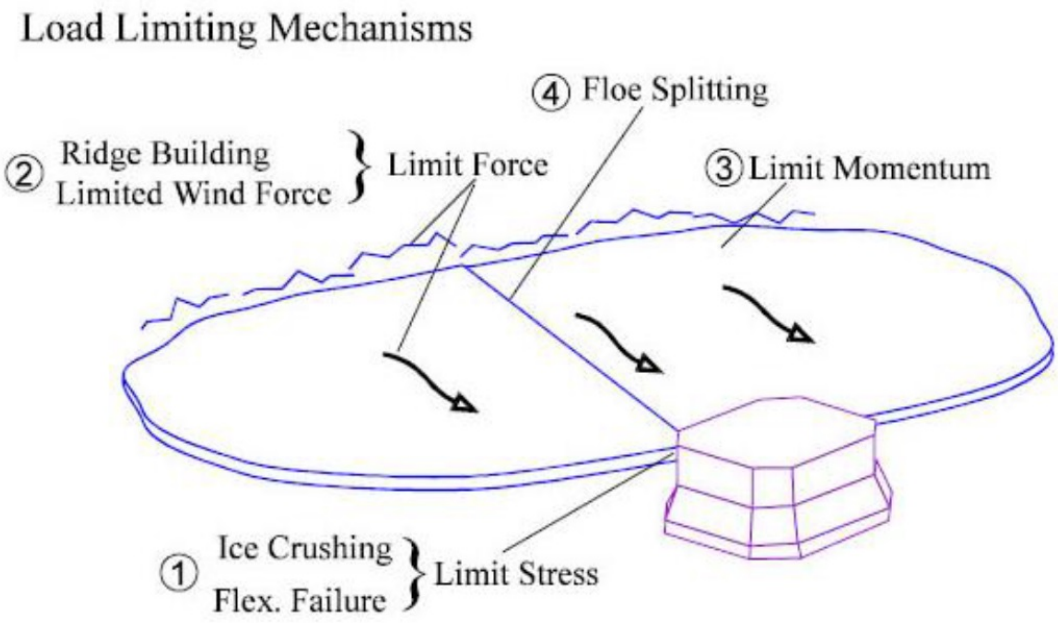

Figure 11 Loading limiting mechanisms (S. Løset lecture AT-327)

Limit stress

The ice failure mechanism that occurs adjacent to the structure controls the ice actions. The limit stress scenario represents the maximum stress of the ice that leads the ice to fail and completely surrounds the structure. This often controls the maximum external load applied to the structure.

Limit momentum

This scenario occurs when the kinetic energy of the ice feature limits the ice action. The limit momentum scenario describes the case when an ice feature like an isolated floe, ice island or an iceberg, does not have the velocity enough to make the structure penetrate the ice. The ice feature will just rest in front of the structure after the structure has insignificantly has penetrated the ice. If the structure is relatively thin and the concentration of ice is low, the ice feature will travel around the obstacle. However if the concentration of ice is high enough, the force build up will eventually lead to a limit force scenario

Limit force scenario

During the limit force scenario following alternatives can happened:

1. Wind and current actions accumulates over the surfaces of the halted ice and are transmitted to the structure. From rest, the velocity of the ice slowly increases making the structure penetrate the ice.
2. If the ice action is rather low, rafting riding and jam formation might occur if the surrounding ice is weaker than the adjacent ice floe.

Splitting

This scenario occurs when an ice feature hits the structure in such way that the ice splits in to pieces. Among the mentioned scenarios this has usually the lowest action.

The shape of the structure is an important factor in determining the ice action. A brief over loads from ice on vertical, sloping and multi legged structures will be given in the following.

4.3.1 Ice actions on vertical structures

The shape of the structure is an important factor in determining the ice action. A brief over loads from ice on vertical, sloping and multi legged structures will be given in the following

4.3.2.1 Limit stress scenario

If we consider a vertical monopod in which the ice exerts on. The load applied to the structure with respect to the limit stress scenario would be

$$F = h \int_{-\pi/2}^{\pi/2} \sigma_c cos\varphi RD\varphi = h\sigma_c 2R = \sigma_c Dh$$

where σ_c is the unconfined compressive strength of ice, D is the diameter of the structure, R is the radius of the structure and h is the ice thickness of the incoming ice(12).

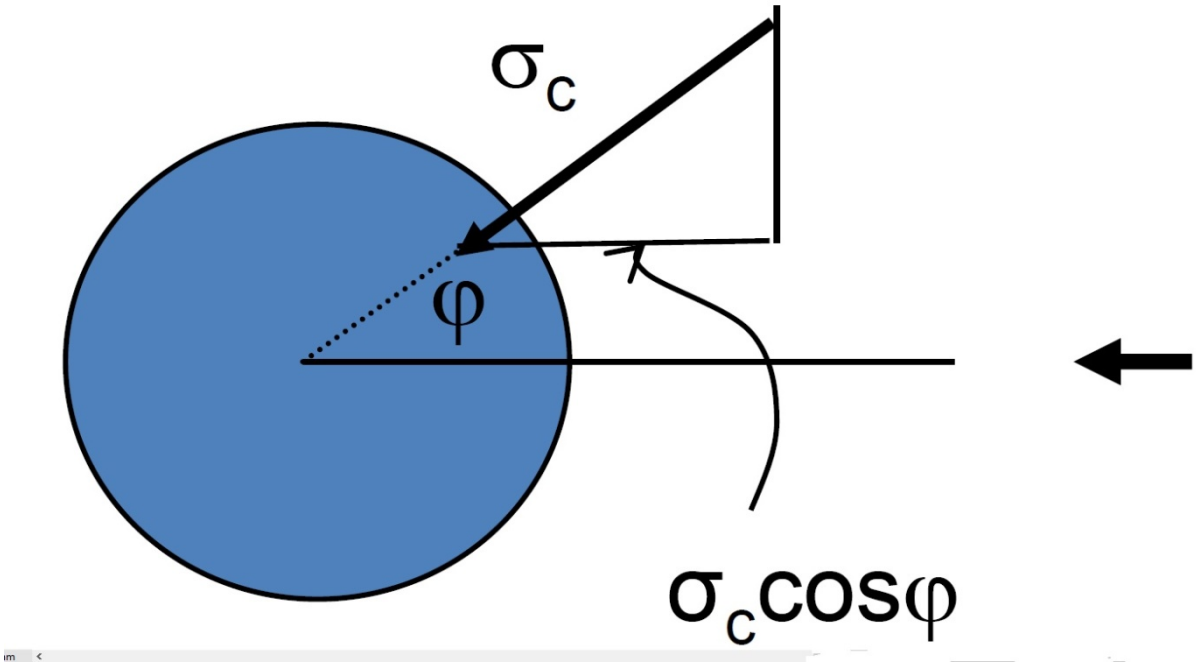

Figure 12 Limit stress physical figure (S. Løset AT-327 lecture)

This formula is however not valid in nature due to following reasons(S.Løset 2006):

- Applied pressure load on the structure can never be evenly distributed over the whole entire contact surface as well as the maximal strength cannot be achieved simultaneously over the whole contact surface.
- The unconfined compressive strength of ice varies in different points of the contact surface.
- Besides the normal stresses, there are also tangential stresses acting due to friction between the contact surfaces. At some contact points it may be a tangential stress and another point it could be tensile.
- The unconfined compressive strength of ice varies in different points of the contact surface.
- Other factors that are not taken accounted for in this formula include ice velocity, form of the structural cross section, ice pr0operties, ice sheet edge roughness etc.

A more accurate formula which is one of the most used formulas today is the Korzhavin (1962) formula.

This formula can be written in the form of:

$$F = IKm\sigma_c Dh$$

F is a total load on the structure. I is an indentation factor which takes into account the crystallographic structure of ice, its properties, the aspect ratio and the influence of the stress/strain field on strength. K is a “contact factor” which takes into account the imperfect contact ratio between the ice sheet and the structure. D is the structure diameter; h is the ice thickness and σ_c is the uniaxial compressive strength of ice. A shape factor “m” is also introduced if the surface of the

contact structure has a different shape than a flat surface. For instance, the shape factor of a cylindrical indenter is 0.9, whereas a flat surface would be 1.

This product between IK was recommended to be between 0.45-0.55(K.A.Blenkarn 1970) and was decided empirically. This methodology was used at early stages of structure design, and was derived from small scales laboratory indentation tests done for bridge piers(S.Løset 2006)however later measurements of ice loads in the field of wide offshore structures presented that Korzhavin's formula significantly overestimates the loads and it was found that in order for the equation to yield comparable results the contact factor has to be in the range of 0.02-0.13 which is really low.

Korzhavin's formula is based on the ice load measurements on small piles. The diameter of these piles was several times less than the offshore structure diameter. Therefore, the scale of observations is insufficient. When scale increases, the ice strength decreases significantly. It is now evident that a lot more parameters are affecting the ice actions The Korzhavin formula is a generally used formula and mentioned in the API recommendation and it is even the main formula in the Russian code SNIP. The problem with the Korzhavin formula is that there is a lot of parameters that is not considered (S.Løset 2006):

- It does not consider different possible failure modes
- It does not take account the fact that usually failure cannot develop absolutely simultaneously over the whole contact area.
- It does not consider the existence of the scale effect
- The unconfined compressive strength cannot characterize the whole stress field around the structure.

A more appropriate formula which also is simple is the one which has been used in the recent year:

$$F = pA$$

Here the *p* represents the effective pressure over the nominal contact area *A.* The pressure is calculated out from experiments when investigating the relationship F/A. Since it determined from experiments all of the factors influencing the ice action is included(S.Løset 2006):

- Failure mode
- Freezing conditions
- Ice edge roughness and real ice/structure contact area
- Size effect
- Linear characteristics of ice and structures
- In plane dimensions of ice features
- Structure's compliance
- Fracture toughness
- Form of the structures cross section

This scenario often dictates the design of the structure with respect to ice action. Some of the factors will be discussed in the following.

Failure mode

The failure mode that the vertical monopod experiences can be divided into two groups:

- Failure near the structure
- Failure some distance of the structure

Failure like creeping, crushing, cracking and spalling (flaking) is typically failure modes that happens near the contact-zone between the ice feature and the structure. Failure that happens some distance of the structure is typically bending and buckling. According to Kärna and Jochmann (2003) the probability of experiencing bending failure is more than 80% if the ice thickness is thinner than 0.15m. If the ice is thicker than 0.35m, the probability of experiencing crushing failure is more than 70%. Due to the fact that the probability of buckling is higher for thin ice, h <0.15m, then it follows that buckling will more likely happen during early year ice, rather than multiyear ice because of the thickness(Cannaert and Muggeridge,1988). Following formula was proposed for buckling action was proposed by Sodhi and Harnza (1977).

$$F_b = \rho g l^3 \{\frac{D}{l} + 3.32\left(1 + \frac{D}{4l}\right)\}$$

Where the characteristic length is:

$$l = \{\frac{Eh^3}{[12\rho g(1-v^2)]}\}^{\frac{1}{4}}$$

E - Youngs's modulus and v – Poisson's number. Experiments done by Kato and Sodhi(1983a,b) has shown that it is more likely to experience a combination of failure modes than just a pure failure mode alone.

Freezing conditions

If the platform is located in an area with low current and ice movement, there is a possibility that the structure itself will freeze into the ice.

When the ice is frozen to the structure, the contact between the structure and the ice is considered perfect. One will get a higher ice action due to the fact that the contact area between the ice feature and the structure is considered imperfect due to probable gaps and protrusions in the ice. Another factor to consider is that usually a vertical mono-pod will only experience action from one side of the structure when the moving ice feature hits the structure. If the structure is frozen to the ice and the ice starts to move, the structure will experience action from the ice that is pushed on to the structure in the front and action from the ice that is pulled in the back. The total action may then increase by a factor of 1.5-2(S.Løset 2006). A final thing to consider with respect to freezing conditions is that the ice cover might form a collar of ice around the structure due to the higher thermal conductivity of the structure. The thickness of the collar might be much greater than the thickness of the ice that surrounds the structure. As a result the global action will be higher due to the pressure of the ice will act over a larger area.

If the structure is located in waters with tide, the tidal motion will cause cracks between the structure and the ice, eliminating the ice actions from frozen ice.

Figure 13 Freezing ice stuck to a pillar. (Løset and Marchenko 2009)

Size effect

When doing a small scale test of the strength of ice like the experimental tests done in this thesis, it is natural to assume that one simply could scale the properties according to the ice dimensions dealt with, for example in a full scale experiment between a structure and ice. However it is shown that the strength of the ice is dependent on the size. This phenomenon is called the size effect. Following factors influences the size effect (S. Løset 2006).

- Flaws and the flaw hierarchy
- Ice non-homogenity
- Non-simultaneous failure
- Fracture mechanism

Flaws and flaw hierarchy

The largest dominating factor for the size effect is considered to be the existence of flaws in ice Freudenthal (1968) showed that if flaws and weak chains are distributed at random over some volume over a material, the likely hood of weak points to occur increases if the volume of the material increases. The crack hierarchy is also an important factor. Depsey et. Al (1995) and Adamson et al.(1995) showed that flaws exist in ice at different scales. It is likely that if the diameter of the structure is large, one will experience a greater number of flaws of different dimensions that influences the ice actions.

Non-homogeneity

Ice is not a perfect homogenous piece of material. Considering a large structure, it is likely to encounter a weak point in the ice that surrounds or crashes against the structure.

Non-simultaneous failure

Kry (1978) recognized that size effect observed in full-scale measurements may be attributed to non-simultaneous failure. It was suggested that independent zones in the ice at the water line, approximately as wide as the ice thickness, fail non-simultaneously during ice crushing. Non simultaneous failure occurs when fracture has initiated close to a structure or if the initial leading edge of the ice is highly irregular.

Fracture mechanisms

Kaplan (1961) and Bazant (1976-2002) developed an approach to explain the relationship between the size effect and flaws. Considering two different sized beams that has a crack just in the middle. According to geometrical similarity if one scales up the smaller beam the length of the crack on the larger beam should be longer than the smaller one. However, the force needed to propagate the larger crack,F_1 must be larger than the force needed to propagate the smaller one,F_2. As a result the larger beam will fail earlier then the smaller beam.

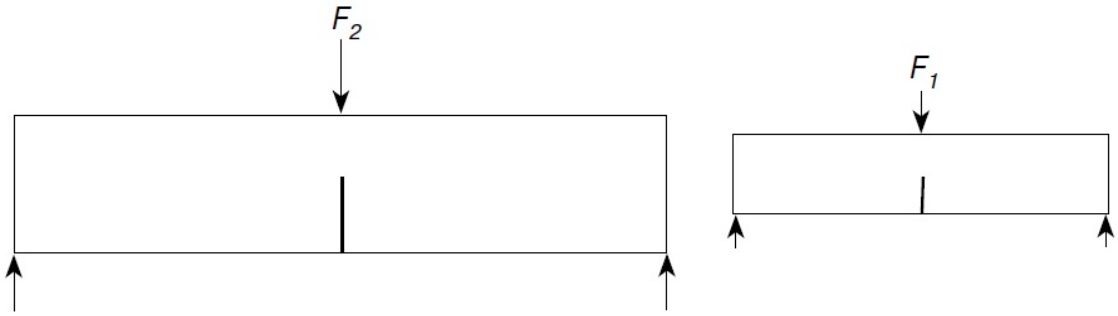

Figure 14 Fracture mechanisms (Løset et al. 2006)

Boundary conditions

Boundary conditions contribute to the size effect indirectly by following factors (Løset 2006):

- The properties of the ice sample may differ from those of the internal material; and different stress/strain fields may exist at the sample core and its surface.
- A stress singularity at the intersection of the crack edge with the sheet edge
- A stress concentration on the protrusions in the sample end or at the ice sheet edge
- Different time dependent effects like diffusion transport of heat, etc.

3.3.2.2 Limit momentum scenario

If the ice floe does not have enough kinetic energy and comes to a halt, we can write the equation of equilibrium as(S.Løset 2006):

$$\frac{1}{2}M_{tot}V^2 = \int_0^x \sigma_m(A_c)A_c(x)dx$$

The left hand side represents the kinetic energy of the ice sheet. M_{tot} = M+ΔM, where ΔM is the added mass due to ice interaction with water. The above equation is assuming that the ice failure happens simultaneously over the whole contact area A_c when the normal stress over this area reaches a maximum value of σ_m dependent on A_c integrating from zero to the maximal structure penetration of the ice, *X*.

Experiments shows that if the contact area is bigger than $2m^2$, then the maximum stress σ_m do not depend on the contact area and the equation above can be written as:

$$\frac{1}{2}\rho_{eff}A_i h V^2 = \int_0^x \sigma_m A_c(x)dx$$

Where A_i is the initial ice feature area, $\rho_{eff} = \rho_i + {}^{\Delta M}/_{A_i}$ which is the effective density. To calculate the ice action assuming that both the ice feature and the structure have a cylinder shape with diameter D_i and D_s and there is full contact between the structure and ice the Ice action corresponding to the maximal structure penetration can be expressed as:

$$F_m = 1.33h(\rho_{eff}D_s)^{0.33}(\sigma_c D_i V)^{0.66}$$

Depending on where the structure hits the ice floe, center of gravity of the ice floe and direction of motion, the ice might also immediately after penetration rotate around the structure. The energy of the ice feature will not only be spent on the ice failure, but also the rotation. So this case is considered as a lower ice action than when an ice floe comes to a halt.

3.3.2.3 Limit force scenario

If an ice feature comes to a halt in front of a structure like described earlier, environmental forces like wind and waves might drive surrounding ice features towards the structure causing a built up pressure which eventually might lead to a ridge or compressed ice creating a large ice action on the structure. It has been (Croasdale 1980) suggested following formula for calculating this type of ice action:

$$F_{lf} = \frac{1}{2}(C_c\rho_w V_c^2 + C_w\rho_a V_w^2)A_f + F_f$$

C_c is the drag coefficient for the current, C_w, is the drag coefficient for the wind, $\rho_a$is the air density, ρ_w is the water density, V_c, V_w is the velocity of current and wind. A_f is the stopped feature in plane area and F_f is the action of the surrounding ice along the border of the ice feature.

There are four forces in action in this scenario. Wind, current, thermal expansion of the ice and the direct ice action. Driven by the environmental forces itself, the ice action from the limit force scenario cannot be larger than the fluid forces and the forces transmitted through the ice cover.

3.3.2.4 Splitting scenario

Splitting of an ice feature might occur if the dimensions of the ice feature is not too large(S.Løset 2006). When the structure penetrates the ice, both compressive and tensile stresses act on the ice which leads to a formation of a crack. If the crack propagates it may lead to the ice feature to split in

parts. According to (S.Bhat 1988) and (D.S. Sodhi 1995)the action induce splitting can be determined as:

$$F/(hK_1L^{0.5}) = 3.3$$

K_1 is the fracture toughness. The above equation is valid the length to width ratio (W/L) of the ice feature is in the range of 0.75-125. If W/L >1.5 the ice is more likely to fail by crushing.

3.3.2.5 Global Ice action on vertical structures

In the situation where a sheet of ice interacts with a fixed vertical structure one can determine the global ice action as recommended by ISO19906. The global ice action is a product between the global pressure and the nominal contact area which is determined by the product of the ice thickness, h, and the width of the vertical structure, w.

$$F_G = p_g hw$$

The global pressure is defined by data from full-scale measurements in Arctic waters. Based on studies and measurements done, following formula is recommended for calculating the global pressure:

$$p_G = C_R(\frac{h}{h_1})^n(\frac{w}{h})^m$$

Were the global average ice pressure is expressed in MPa and valid when the aspect ratio *w/h >2*.

w – width of the structure [m]
h – thickness of the ice [m]
h_1 – reference thickness of 1 m
m – empirical coefficient of -0.16
n – empirical coefficient equal to :

$-0.50 + \frac{h}{5}$, $h \geq 1.0m$ *and* -0.30 , $h \geq 1.0m$

C_r – strength parameter [MPa]

The parameters *n, m* and *C_r* is derived from full scale data.

From what one can see from the previous formula is that the part after the strength parameter dictates the mentioned size effect of the ice.

The parameter C_r is the strength parameter that depends on the ice properties, which again depends on the location of the ice due to the temperatures and freezing degree days of the location of interest.

The ice strength parameter *C_r* is estimated to be 1.8 MPa in temperate sea areas where there are about 1000 freezing degree days per winter season and 2.8 MPa in Arctic areas where there are about 4000 freezing degree days per winter season.

If however, there are evidence which indicate that the ice strength is different from the pre estimated value of the area of interest, one have to reconsider the ice strength parameter and adjust it to local conditions. In the latter case following formula is suggested:

$$C_R = C_{R0}\frac{\sigma}{\sigma_0}$$

C_{RO} – is the strength parameter for the reference area which is affected by local conditions. 2.8 MPa for Arctic conditions.

σ – is the obtained strength index for the area of interest. Can be found by small-scale experiments of compressive strength measures. An example is shown in the experiments section in this thesis.

σ_0 – is the strength index for the areas where the strength parameter, C_{R0} ,has been obtained. This can be found by using the following formula from the Russian code of standards, SNIP 2.06.04-82(96):

$$\sigma_0 = \left[\frac{1}{N}\sum_{i=1}^{n}(C_i)^2\right]^{\frac{1}{2}}$$

The ice sheet divided into a number of layers, n, where the temperature and salinity profiles are obtained. Based on the salinity and temperature profile the brine volume fraction can be determined from the following formula:

$$V_b = S\left(\frac{49.18}{|T|} + 0.53\right)$$

where S is the salinity of the ice melt and T is the temperature expressed in degrees Celsius. With the obtained brine volume, $V_{b,}$, one can find the strength coefficient C_i from table(fig 15).

ν_b	0,001	0,010	0,025	0,050	0,100	0,200
C **(MPa)**	8,4	6,0	3,4	1,6	1,0	0,8

Figure 15 Ice strenght coefficient as a function of brine volume (ISO 19906)

Then the strength coefficient can be inserted in the formula to obtain the average strength index σ_0.

3.3.3 Ice action on structures with inclined surfaces

When dealing with structures with inclined surfaces we experience two types of failure mode during the interaction between the structure and ice, circumferential and radial cracking. The order in which the failure happens may determine the maximal load applied to the structure from the ice interaction. Depending on the structure width the structure will be prone to either circumferential or radial cracking. Structures with width of about 100m is likely to experience circumferential cracks at first, whilst narrow structures with the width of about 10 m are likely to experience radial cracking at first.

The process of interaction between the ice and the sloping structure may happen as shown in fig 16. (S.Løset 2006):

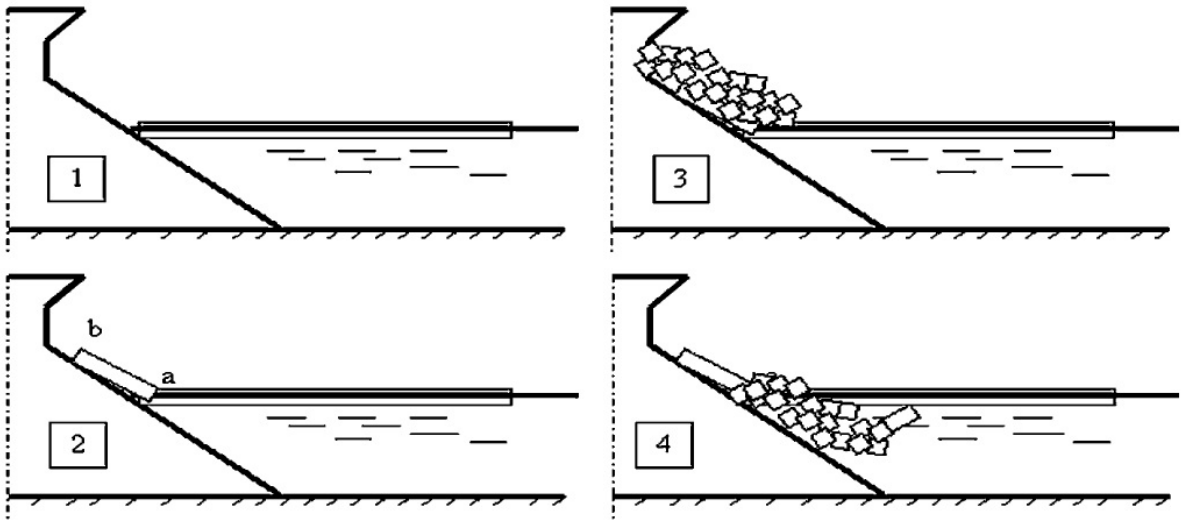

Figure 16 Ice inter action with a slopig structure (Løset et al. 2006)

An ice sheet with thickness ***h*** moves in with a certain velocity ***v*** and slides along the surface structure. The ice then fails by flexure and gets divided as shown in (2). By environmental forces the pieces of ice continues to be driven against the structure, causing the process to repeat itself, making smaller and smaller blocks of ice to slide and ride up the sloping structure surface as shown in (3). Some of the blocks of ice will roll back and accumulate on the ice sheet creating a vertical force on the sheet of ice. If the weight load from the blocks are heavy enough the sheet of ice will break and the blocks of ice will submerge. Ice pieces left on the slope of the structure will accumulate and create a rubble which again interacts with the ice sheet. The whole process will then repeat itself as long as the environmental forces and ice still exist. Due to that the ice feature that moves and interacts with the sloping structure fails by bending, rather than crushing the ice load against the structure will be lower due to the fact that flexure strength of ice is lower than the compressive strength. So structures with a sloping surface are usually more effective when it comes to reducing ice actions in comparison to vertical structures.

3.3.3.1 Global ice action on sloping structures

As mentioned, the design of the structure often dictates the failure mode of the ice interaction with the structure. There are several types of sloping structures; some of them are plane, conical or faceted, all of them with a slope angle of α. There is also a difference in which way the slope is directed, either upward or a downward slope.

When an ice feature interacts with a sloping structure, the ice loads are induced by both horizontal and vertical components.

$$F_H = N \sin\alpha + \mu \mathrm{N} \cos\alpha$$

$$F_V = \mathrm{N} \cos\alpha - \mu N \sin\alpha$$

where

- N is the normal component to the structure surface
- α is the inclination of the structure surface expressed in radians
- μ is the kinetic friction coefficient between the ice and the structure surface

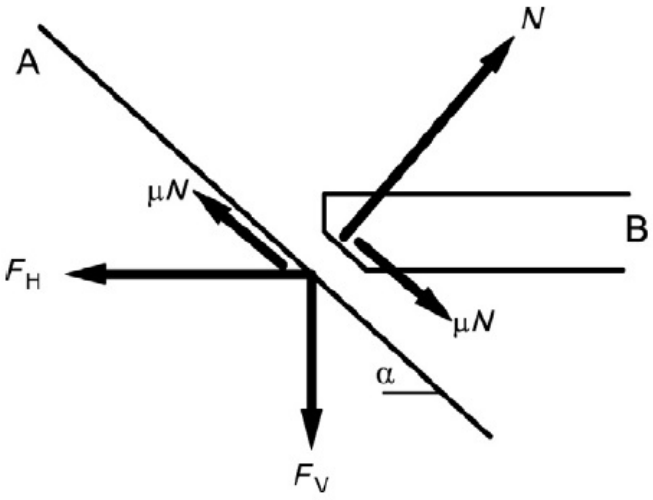

Key

A	sloping face of structure
B	encroaching ice sheet
N	normal component of reaction to ice action on structure
μ	ice-structure friction coefficient
α	slope of structure face from horizontal
F_H	horizontal component of ice action
F_V	vertical component of ice action

Figure 17 Forces on a sloping structure (ISO 19906, 2010)

When determining the ice actions on sloping structures ISO 19906 has described a method of solution based on the model of plasticity and the method based on elastic beam bending. Following models has been done to predict ice loads on sloping structures which includes:

- Croasdale (1980), 2D beam theory
- Ralston (1977),3D plate theory
- FEM simulations (Määttänen et al.)
- + several other models like Chao (1992)

The first method which is described in the ISO 19906 is the 3D plate model based on plastic limit analysis by Ralston (1977). In this model ice is treated as ductile material so the action considered is the flexural failure and the ride up actions due to ice pieces.

The horizontal and vertical forces in this model will be:

$$F_H = H_B + H_R$$

$$F_V = V_B + V_R$$

where the subscripts B and R is the action on the cone due to ice breaking and ride-up respectively. The derivation of the equations is shown in appendix 2 and is valid for both upward and downward - cones. For a downward braking cone the buoyancy effect comes into play and the density of ice ρ_i is replaced with $(\rho_w - \rho_i)$. The effect will then be on the vertical load and the overturning moment which will affect a floating structure.

The second model is suggested by Croasdale et.al. where the horizontal action component is determined by following equation:

$$F_H = \frac{H_B + H_P + H_R + H_L + H_T}{1 - \frac{H_B}{\sigma_f l_c h}}$$

where

H_B is the breaking load
H_P is the load required to push the ice sheet through the ice rubble
H_R is the load required to push the ice blocks up the slope through the ice rubble
H_L is the load required to lift the rubble on top of the advancing ice sheet prior to breaking it
H_T is the load to turn back the ice block at the top of the slope

The derivation of the horizontal action components is shown in appendix 1.

Due to the complexity of the prior models a simple 2D beam theory (Croasdale 1980) is shown in the following to show the effects of the slope angle, surface friction and ice thickness on the action load.

From Croasdale (1980) we have that the vertical load is defined as

$$V = 0.68\sigma_f W \left(\frac{\rho_w g h^5}{E}\right)^{\frac{1}{4}}$$

and the horizontal load defined as

$$H = 0.68\sigma_f W \left(\frac{\rho_f g h^5}{E}\right)^{\frac{1}{4}} \frac{\sin\alpha + \mu\cos\alpha}{\cos\alpha - \mu\sin\alpha}$$

where

W is the width of the beam along the waterline of the surface
E is the Young's modulus
μ_f is the flexural strength of the ice
g is the acceleration due to gravity
h is the thickness of the ice

The force needed to push the ice blocks up the slope would be

$$P = \frac{Z}{\sin\alpha} hW\rho_i g(\sin\alpha + \mu\cos\alpha)$$

where
ρ_i is the density of ice
Z is the height reached by the ice on the slope

the horizontal load would then be

$$H = (V + P\sin\alpha)\left[\frac{\sin\alpha + \mu\cos\alpha}{\cos\alpha - \mu\sin\alpha}\right] + P\cos\alpha$$

if we substitute V and P and simplify the terms:

$$C_1 = \left[\frac{\sin\alpha+\mu\cos\alpha}{\cos\alpha-\mu\sin\alpha}\right],\ C_2 = \left[\frac{(\sin\alpha+\mu\cos\alpha)^2}{\cos\alpha-\mu\sin\alpha} + \frac{\sin\alpha+\mu\cos\alpha}{\tan\alpha}\right]$$

we get following equation where the load over the contact width can be expressed as following:

$$\frac{H}{W} = \underbrace{\sigma_F(\rho_w g h^5)^{\frac{1}{4}}C_1}_{Breaking\ force} + \underbrace{(Zh\rho_i g C_2)}_{Ride-up\ force}$$

To test the relationship between loads and, friction and angle in the following spread sheet the With of the structure is sat to 1 m to show the force per m in Kn.:

Input parameters				
σf	700000	Pa		
σc	1200000	Pa		
ρw	1023	kg/m^3		
ρi	900	kg/m^3		
E	9E+09	Pa		
g	9,81	m/s^2		
μ	0,3			
z	5	m		
D	1	m		

GBS with slope

	Degrees	Radians	Degrees	
α	45	0,78539816	60	1,0472
C1	1,262857143		2,876432957	
C2	2,626396616		4,884439241	

	α=30°		α=60°	
h	Fh/D (N/m)	Fh (kN)	Fh/D (N/m)	Fh (kN)
0	0	0	0	0
0,1	13210	13	25242	25
0,2	27031	27	51876	52
0,3	41161	41	79214	79
0,4	55515	56	107063	107
0,5	70049	70	135322	135
0,6	84735	85	163926	164
0,7	99553	100	192830	193
0,8	114488	114	222003	222
0,9	129530	130	251417	251
1	144668	145	281054	281
1,1	159897	160	310895	311
1,2	175210	175	340926	341
1,3	190601	191	371136	371
1,4	206065	206	401514	402
1,5	221600	222	432051	432
1,6	237200	237	462739	463
1,7	252864	253	493570	494
1,8	268588	269	524539	525
1,9	284370	284	555640	556
2	300207	300	586867	587
2,1	316098	316	618216	618
2,2	332040	332	649682	650
2,3	348032	348	681261	681
2,4	364072	364	712949	713
2,5	380159	380	744744	745
2,6	396291	396	776642	777
2,7	412466	412	808639	809
2,8	428684	429	840733	841
2,9	444944	445	872922	873
3	461244	461	905203	905

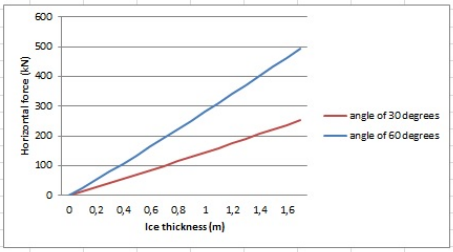

Summary

GBS with slope

α	45 °	α	60 °
Horizontal force at ice thickness (1 m)			
145	(kN)	281	(kN)
Horizontal force at ice thickness(2 m)			
300	(kN)	587	(kN)
Horizontal force at thickness(2,5 m)			
380	(kN)	745	(kN)
Horizontal force at ice thickness(3 m)			
461	(kN)	905	(kN)

in the above spreadsheet we can see that the load per meter increases both by ice thickness and angle. Adjusting the friction coefficient to 0.2 from 0.3 will yield following results:

Input parameters		
σf	700000	Pa
σc	1200000	Pa
ρw	1023	kg/m^3
ρi	900	kg/m^3
E	9E+09	Pa
g	9,81	m/s^2
μ	0,2	
z	5	m
D	1	m

GBS with slope

	Degrees	Radians	Degrees	
α	45	0,78539816	60	1,0472
C1	1,02		2,010120831	
C2	2,121320344		3,413364126	
	α=30°		α=60°	
h	Fh/D (N/m)	Fh (kN)	Fh/D (N/m)	Fh (kN)
0	0	0	0	0
0,1	10669	11	17640	18
0,2	21832	22	36252	36
0,3	33245	33	55357	55
0,4	44839	45	74818	75
0,5	56578	57	94566	95
0,6	68440	68	114555	115
0,7	80408	80	134755	135
0,8	92471	92	155141	155
0,9	104620	105	175697	176
1	116848	117	196407	196
1,1	129148	129	217261	217
1,2	141516	142	238247	238
1,3	153947	154	259359	259
1,4	166437	166	280588	281
1,5	178984	179	301928	302
1,6	191585	192	323373	323
1,7	204236	204	344919	345
1,8	216937	217	366561	367
1,9	229683	230	388295	388
2	242475	242	410117	410
2,1	255310	255	432024	432
2,2	268186	268	454013	454
2,3	281103	281	476081	476
2,4	294058	294	498226	498
2,5	307051	307	520445	520
2,6	320081	320	542736	543
2,7	333146	333	565096	565
2,8	346245	346	587525	588
2,9	359378	359	610019	610
3	372543	373	632578	633

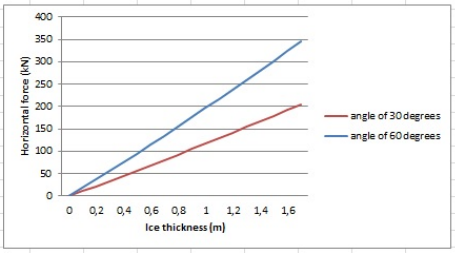

Summary

GBS with slope

α	45	°	α	60	°
Horizontal force at ice thickness (1 m)					
117	(kN)		196	(kN)	
Horizontal force at ice thickness(2 m)					
242	(kN)		410	(kN)	
Horizontal force at thickness(2,5 m)					
307	(kN)		520	(kN)	
Horizontal force at ice thickness(3 m)					
373	(kN)		633	(kN)	

the above table shows that a higher friction coefficient increases the load. As expected from the equations. Another observation is that the effect of the friction coefficient becomes significant with steeper slopes than 45˚. An obviously steeper angles gives more crushing which leads to higher loads. So it is important to have a gentle slope as possible and a smooth contact surface between the ice and the structure.

3.3.4 Ice actions on multi legged structures

When we look at multilegged structures, it has been shown that the ratio of the spacing between the structure columns and the diameter of the column itself (Q/D) has the influence of the ice action. If the ratio Q/D>5, it can be assumed that the influence of the surrounding columns does not have a considerable effect on the ice action. For Q/D<5, the action decreases in the normal direction relative to the line of the columns, while the ice action increases in the transversal direction. The magnitude of the total load remains the same; however the direction of the action is changed. For Q/D =1 the maximum action decreases at an angle of 8-12˚degrees. Fig 18 shows the average direction of load θ_a versus the pile spacing.

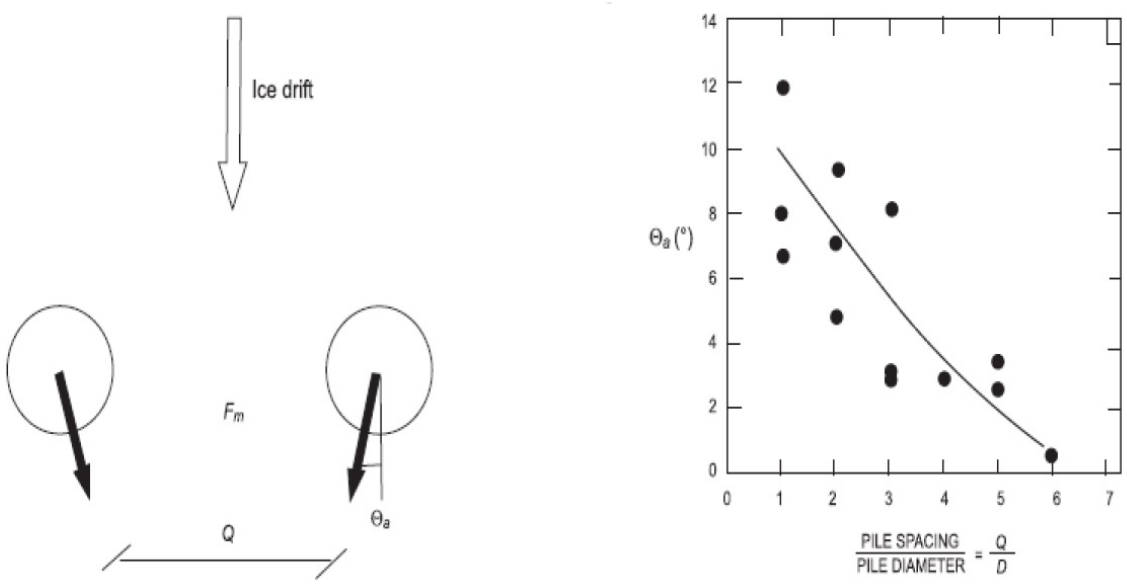

Figure 18 Illustration of drifting ice towards multilegged structure (S. Løset AT-327)

Depending on the direction of movement of the ice feature relative to the structure, the columns on a multileg structure can be fully or partly sheltered by the columns in front. This means that the ice action will differ on the sheltered columns in comparison with the columns in front which interact with the ice first. Since the ice is likely to be broken up, the ice loads on the sheltered columns will be considerably lower. It has been showed (T.Nawata 1985) by laboratory experiments that in a four legged rectangular plane model that if the ice movement was parallel to the front legs the actions of the back legs did not exceed more than 6-7% of the actions on the front legs. The action on the back legs if the ice movement was near diagonal relative to the structure was approximately 35 %. So when designing for ice loads of an multileg platform one has to be considerate about the distribution of the platform legs since that will affect the ice loads.

3.4 Icing

Infrastructures in the arctic are also vulnerable to icing. Icing is formed due to wave and wind action on the ships and platforms combined with low air temperature and low surface water temperature. Drifting ice consists of ice sheets, drift ice, ice blocks and icebergs etcetera. Both types are most common during late winter and early spring.

There are two types of icing(S.Løset 2006): sea spray icing and atmospheric icing. Icing is the phenomenon where moisture or water freezes on to a surface above sea level at freezing

temperatures. The source of the water can be rain, wet snow, super-cooled water droplets, sea spray and “green water”. Green water is large amounts of water coming over the bow as the ships breaks the waves.

The most common source of icing is from spray generated by waves breaking on the structure or ship(Y.P. Borisenkov 1972). In the Arctic Ocean spray alone is responsible for 50% of the icing events, spray with atmospheric ice accretion 41% and atmospheric ice accretion alone 9%. The mass of accumulated ice tends to be much lower from atmospheric sources than the mass from sea spray. The high porosity of the ice accretion from atmospheric icing makes it less of a problem than icing from sea spray, even though it can accumulate much higher up on structures and ships.

Even relatively small amounts of icing can be cause problems with slippery decks, ladders, and handrails. Equipment with moving parts can be rendered useless such as winches, valves, and derricks. Radar antennas are easily affected by icing and thus making incoming ice harder to detect, this will reduce the ability to detect icebergs and other floating hazards. Firefighting equipment and life rafts can also be rendered useless, potentially leading to a life threatening situation. The biggest direct threat caused by icing is that it will reduce the freeboard and raise the center of gravity, Brand

(2005), in extreme cases this can make the ship topple over or experience heavy tilt.

Figure 19 Icing on K/V Nordkapp 1987 (Løset et al. 2006)

One example is discussed by(R.F. Carlson 1981): A 620 gross ton ship arrived in port after experiencing heavy icing. The maximum thickness was measured to 0.3 m, the total mass of the ice was estimated to 27 metric tons and the center of gravity of the ice was calculated to be 2.84m above sea level. The ship was designed to be able to have icing or cargo of 27 metric tons with a center of gravity of 3.03m. If the ship had accumulated more ice it could have become so unstable that it would capsize, as other ships in the north Atlantic and around Alaska have done Carlson et al, (1981).

Icing requires three factors to be fulfilled: a source of water droplets, a relative movement between the surface and the droplets and a fast enough heat removal from the liquid as to allow it to freeze and adhere to the surface (S.Løset 2006).When the droplets hit the structure they will freeze in two different stages. The first stage is the instantaneous freezing as the droplets spreads out as a result of the impact with the surface. In the first stage the heat is transferred from the freezing water to the

remaining water. In the second stage the remaining water freezes by transferring heat to the surroundings by means of radiation, conduction, and evaporation.

The total time it takes for a droplet to freeze can be calculated using a heat transfer equation and making necessary assumption. The freezing time can then be used to predict the type of ice that will be formed by the droplets on the surface(L.Makkonen 1984):

$$\Pi = \frac{\tau_f}{\Delta\tau}$$

Where τ_f is the freezing time and $\Delta\tau$ the time between droplets. When Π is close to zero soft rime is formed. When Π approaches one but is still less than one hard rime is formed. As long as Π is less than one it is referred to as dry growth and if Π is more than one it is called wet growth. Ice formed by wet growth will be much harder and denser than ice formed by dry growth. When icing occurs with salt water, in addition to air pockets the ice will also contain pockets of brine. Ships in the arctic ocean are subject to all forms of icing but icing from sea spray is the most common and also the most severe.

There are three sources of sea spray (S.Løset 2006),the most important is from when the bow impacts the waves. The two others are from spume and from wind catching some of the green water and takes it over the ship. Spumes usually happen when wind speeds are higher than 8-10 m/s. The two later are believed to be insignificant compared to spray from bow impacts. The latent heat in the green water is sufficient to keep it from freezing if it flows of the ship fast enough, this will melt and flush away ice that has formed on the deck. However if drainage systems are clogged with ice the green water will stay on the deck and can form a thick layer of ice.

Icing form during a mass or thermal limited process. Thermal limited means that there is more water available than can be frozen between the sprays. Mass limited means that all the available water freezes between the sprays. There is also the case when both are matched perfectly meaning that the heat transfer needed to freeze all the available water is matched perfectly between prays. Ryerson et al. (2000) divided the ship into three regions: the thermally limited region defined as where $\Pi > 1$, the mass limited region where $\Pi < 0.5$, and the maximum limited region $0.5 < \Pi < 1$. The mass limited region is usually above the spray region and at the aft of the ship where the spray from the waves impacting with the bow can't reach. Thermal limited is more likely to be on the bow especially for bigger ships. The maximum region is likely to be a bit behind the bow where there is a better balance between spray flux and heat removed by the atmosphere.

Atmospheric icing is possible throughout the year in the Arctic region because the air temperature can drop below 0 °C. Mulherin, (1996) observed that atmospheric icing was observed 30-90 days of the year in Kara Sea, Laptev, East Siberian, and Chukchi Seas. Atmospheric icing occurs when fresh water in the form of rain, snow, fog, or super cooled droplets freezes and adheres to a surface. As a result of atmospheric icing, 1-2 cm (max 6 cm) of ice can accumulate on the higher parts of the ship(S.Løset 2006).

An important way to protect an operation from hazards associated with icing is to be able to predict when and where there is the highest risk of icing. In order to make good predictions, accurate data is required. Overland et al, (1989) suggested using the predictor *PR* to predict where there where a high risk of icing.

$$PR = \frac{U_A(T_F - T_A)}{1 + 0.4(T_W - T_F)}$$

Where the following parameters are used: U_A wind speed, T_F freezing point of sea water, T_A temperature of the air and T_W temperature of the seawater. *PR* is then converted to cm/h using a factor determined using data from open water in Alaska.

The most important and most effective countermeasure to icing is to avoid a situation when icing can occur. Seeing that this is not always possible it is important to design ships and platform so that they are equipped to deal with the ice. The first important factor is the size of the ship, a small ship will get more spray coming over the bow because of their lower freeboard and greater heave frequency. The bigger ships are less likely to be completely covered with spray from the bow. Also ships with greater freeboard and greater bow rake will deflect more of the spray and thus reducing the amount that ends up on the deck. The deck layout is the next important factor; fewer objects on deck will reduce the area that the ice can start accumulating on. A way to prevent crucial areas to get iced over is to have active heating melting the ice. This can give good results on smaller areas but should not be used on big surfaces. There are also ice-phobic coatings that can be applied to the exposed areas of the ship, they do however have problems associated with them. The treated area becomes slippery, the coating is quickly worn out, and they are still expensive.

3.4 Methods of Ice property studies

When participating class of UNIS course AT-332, autumn 2013 I performed series of different experimental tests in order to investigate the properties of ice. Following experiments where made:

- Medium scale Indentation test in the field
- Small scale Indentation test in the cold laboratory
- Uniaxial compression test of ice

In this section of the thesis each experiment is described and discussed.

3.4.1 Experimental testing of Ice

3.4.1.1 Field indentation test

Site and experimental set up:

In this part of the report the indentation test of fresh water ice in the field is described.

The test site was located at a small freshwater lake nearby Mine 7 in the outskirts of Longyearbyen at the 29th of October 2013.The lake was frozen and the weather conditions at the site was windy with air temperatures around -10 C . Three indenter tests were performed on the lake ice that day. However only two beam tests where recorded.

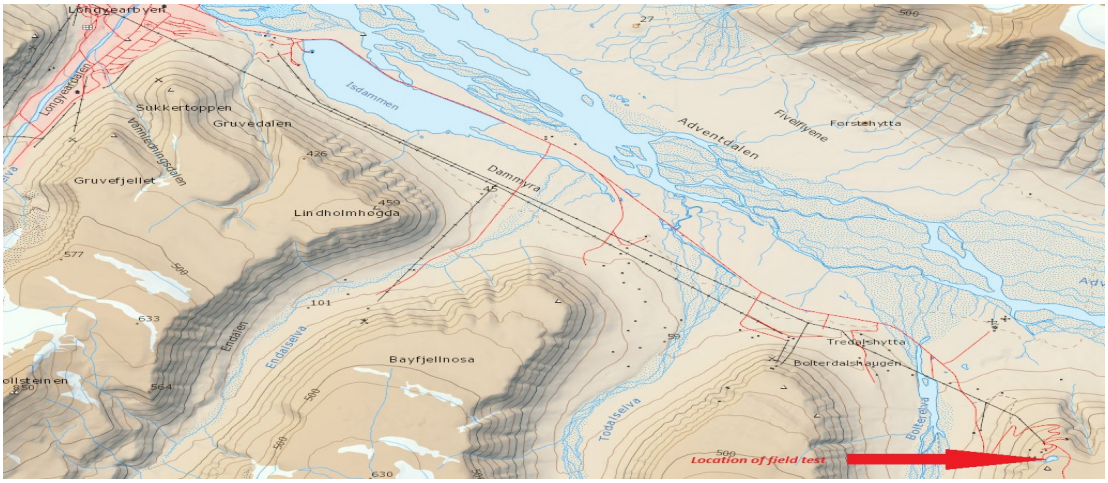

Figure 20. Location of fieldwork [http://toposvalbard.npolar.no/].

The two indenter surfaces had a half cylindrical shape with a diameter of 0,35m and height of 0,7m and were held together with two pistons driven by a hydraulically compressor, and it was lifted on chains and mounted on a steel frame which was assembled together at arrival to the lake. A load cell attached to the pistons was measuring the uniaxial force of the cylinder The indenter surface is measured by the load cell both on the upper part of contact surface and the lower part of contact surface, from now on called cylinder A and cylinder B respectively. A computer was recording data and was used to control the actions of the indenter test (see fig 21). It was continuously recording every 0,01 seconds. The power source of the indenter was a portable

The rig itself was pushed around manually from one test site to another. The test sites where made by drilling and carving holes in the ice and so it would fit the indenter. The rig was placed in such way that the indenter itself was located above the hole, and then lowered into the hole by the chains it was hang on.

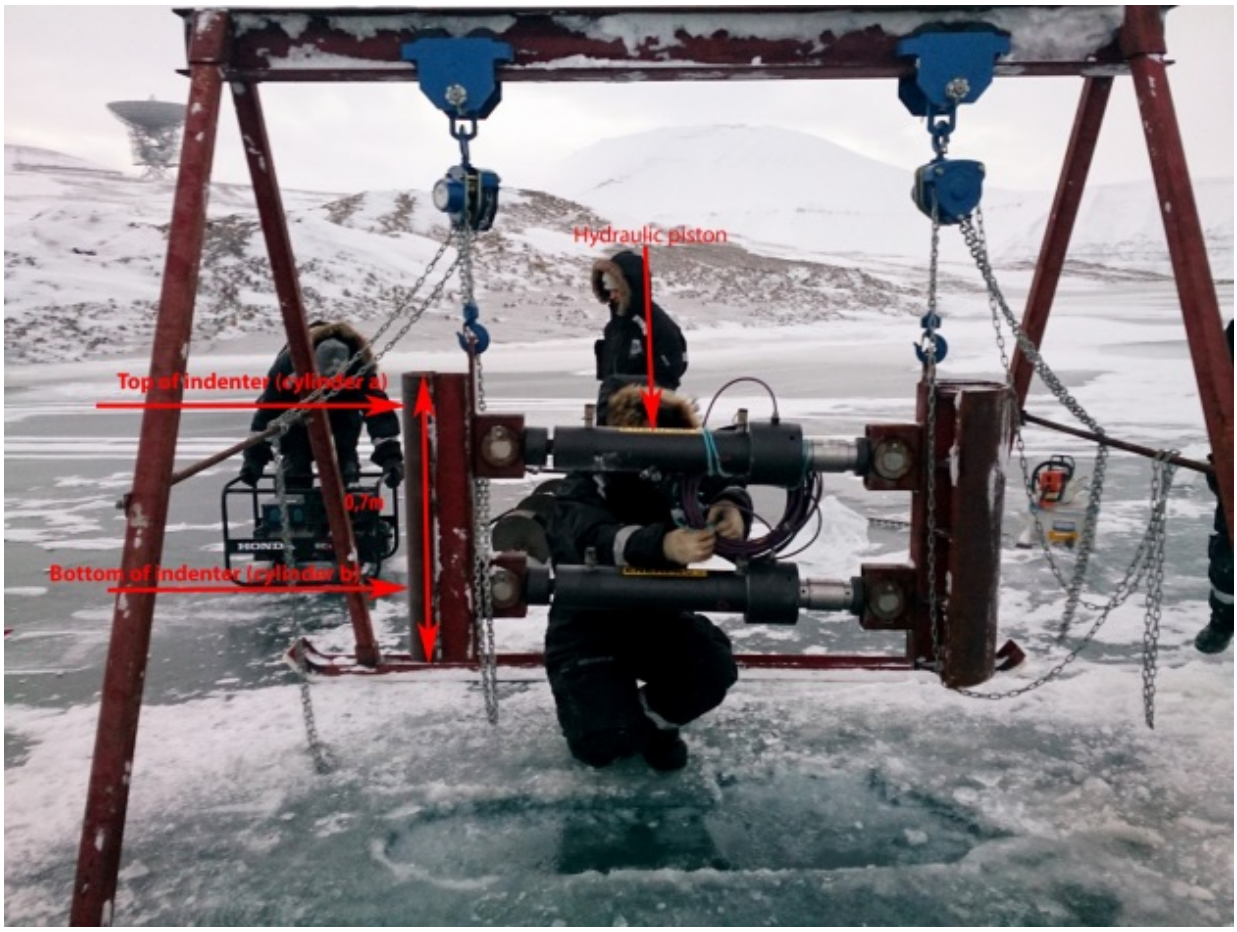

Figure 21. Indenter used in field.

The experiment is done with beams that have fixed ends and a short time load from the indenter is applied and gradually increased until breakthrough takes place.

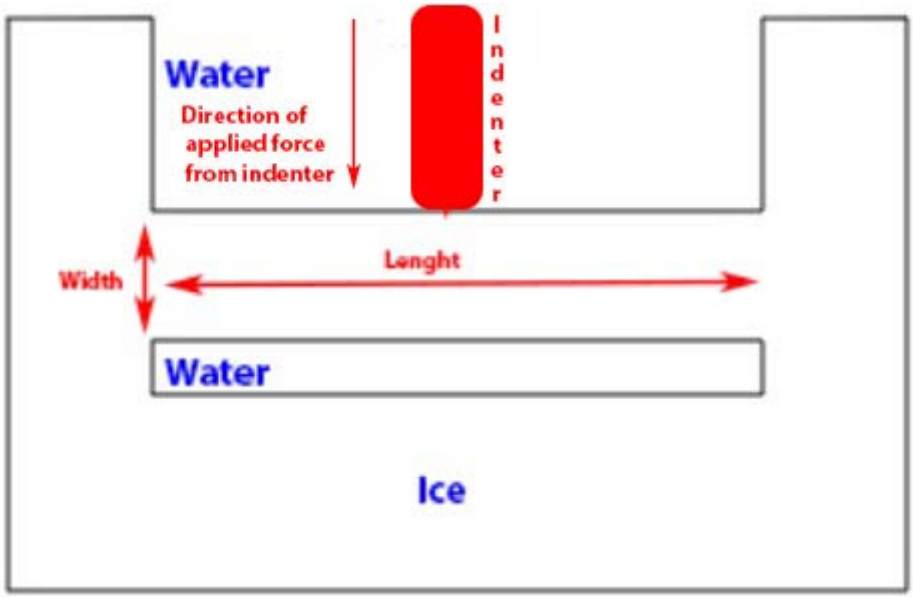

Figure 22 Scheme of experimental set up.

The two ice beams where carved out in front of the indenter hole with fixed ends and space on the backside to allow it to fracture. The width of the beams where 0,4 m and 0,8 m, and the length of the beams where 2 m. The height of the beams were 0,3m.

Results:

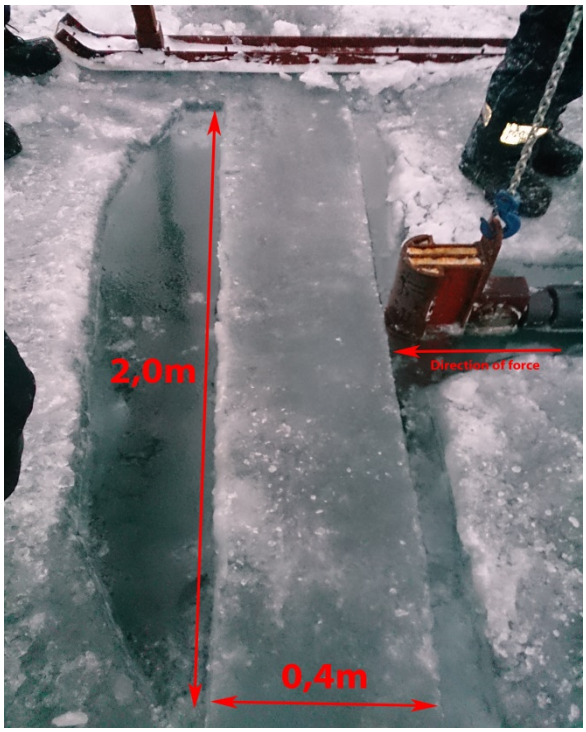

Figure 24 First beam test before indenter applied force.

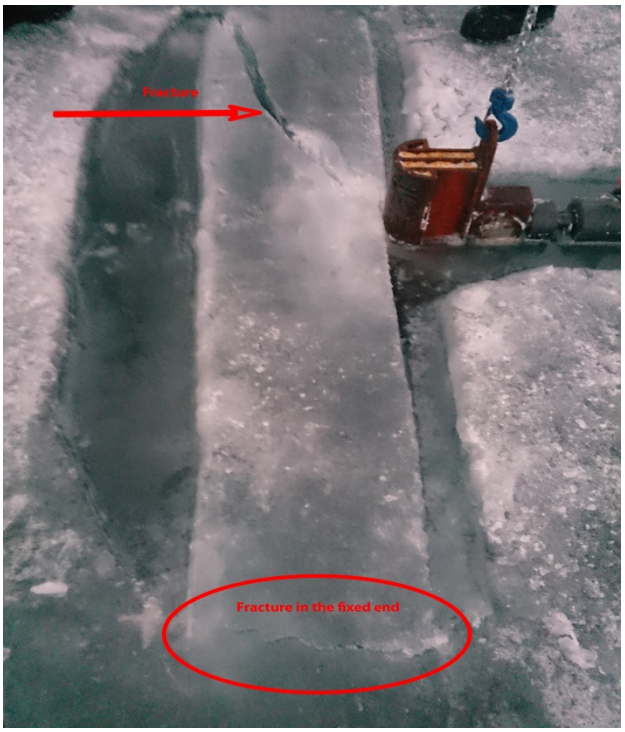

Figure 23 First beam test after fracture of beam

The first beam test was of the 0.4m wide beam. There was no visible creep of the ice when the indenter pushed on the ice, but it started to flake in the beginning before a crack formed nearly straight away almost with no further penetration of the indenter surface on to the ice. One of the fixed ends of the beam was also fractured from the surrounding ice as shown in **Feil! Fant ikke referansekilden.**.

At the point of fracture the pressure applied was about 2MPa which is indicated as the peak of following graph (fig 25).

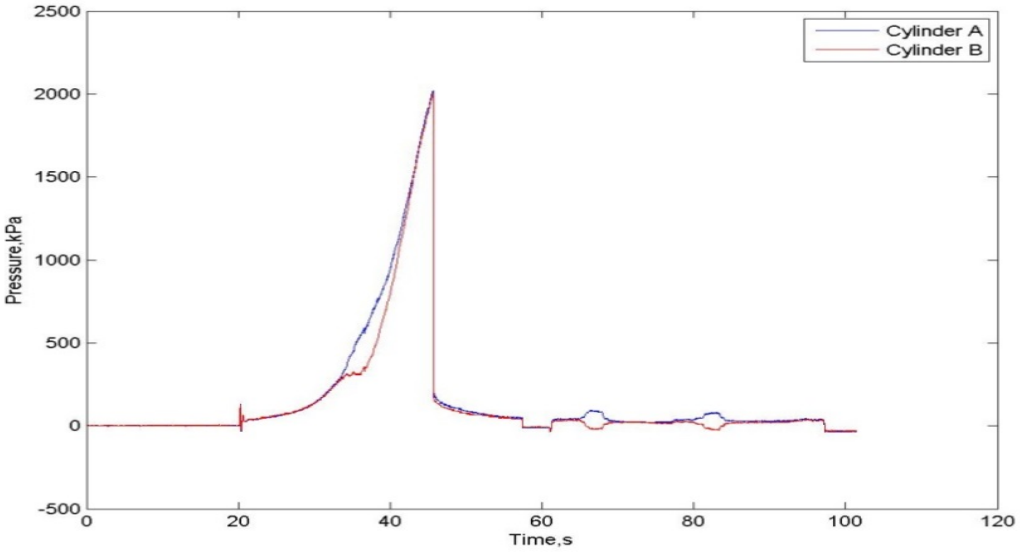

Figure 25. Pressure vs time first beam test.

The second beam test was done with the thicker beam of 0.8 m. Here there was no apparent immediate fracture, but the indenter penetrated the ice and some flaking on top of the ice happened. After a while a surface fracture propagated identical as the first beam test.(fig 26).

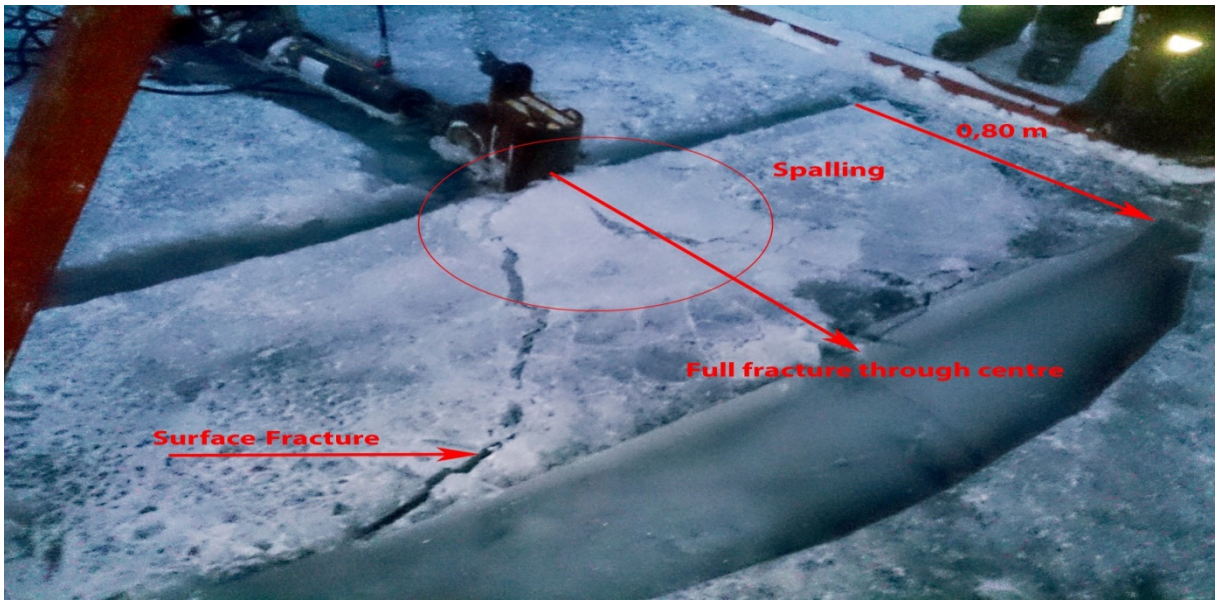

Figure 26. Fracture of second beam test.

The full fracture however were in the centre of the beam. This was visible after the top layer of ice was bruched away. As we can see from the graph(fig 27) is that while performing the indentor test the indenter itself tilted so that the load distribution was not even through out the total height of

ice. The maximum pressure value reached approx 4 MPa.

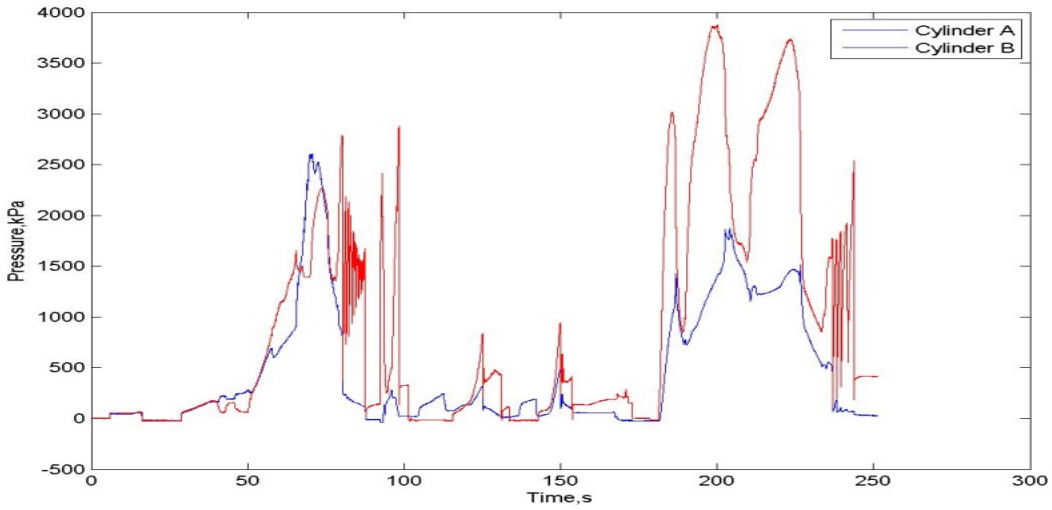

Figure 27. Pressure vs time second beam test.

Following table shows the maximum loads in the ice beams:

Width of beam [m]	Thickness of ice [m]	Max load [kN]	Max Displacement [mm]
0.4	0.3	56,7	90
0.8	0.3	104	150

Discussion and analysis

As one can see is that the first beam test that was 0,4 diameter wide resisted 2 MPa pressure before fracture. There was virtually no creep of the ice before it started fracturing, which shows brittle behavior of the ice. If one takes a look at the displacement of the cylinder (fig 28), they act similarly, which indicates that the indenter distributed the load quite evenly throughout the height of the ice beam.

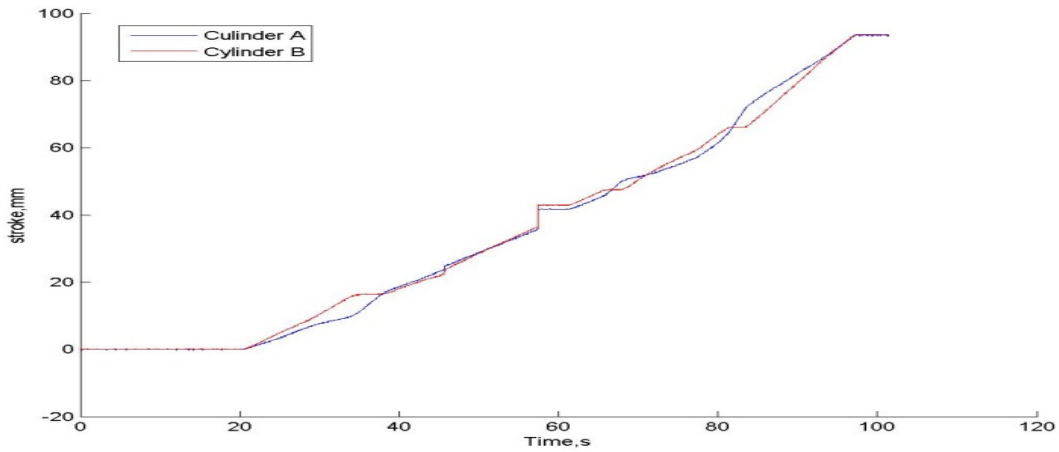

Figure 28. Displacment vs time first beam test.

The second beam test was twice as wide (0,8m) and the top pressure applied was measured to 4MPa. However, the beam started flaking on the surface at the beginning of the test, no fracture went straight through at first. From the load distribution of the graph for beam test two the indenter distributed the load unevenly which indicated that the ice sheet fractured different relative to the height of the ice sheet. One can also see that cylinder A sometimes did not move.

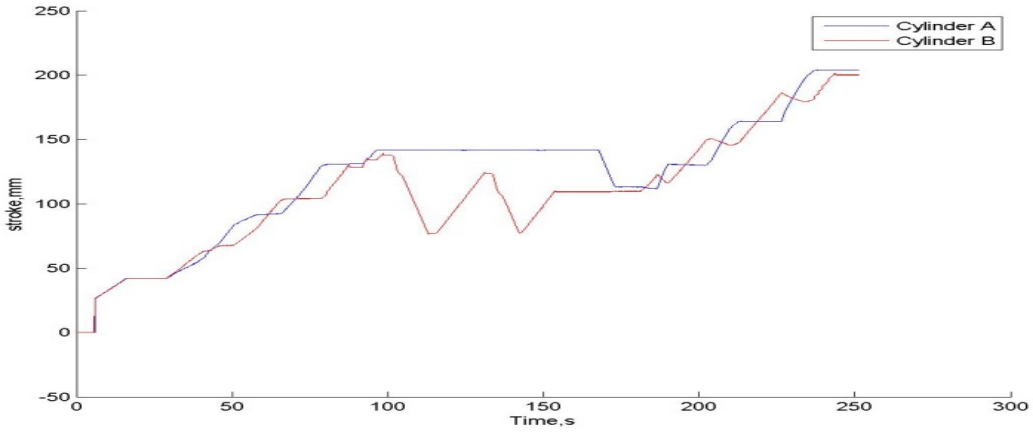

Figure 29. Displacement vs time second beam test.

This was due to the stopping and adjusting the indenter vertically, however it lead to an unevenly pressure distribution with respect to orientation. The last fracture that fractured straight through the sample yielded at the pressure of 4MPa.

The splitting of the ice beam through the middle was however an expected failure of the ice beam.

If one looks at ice floe acting on a circular stationary construction that has characteristic dimensions not large, one would expect a splitting of the floe through the middle of the ice floe from where the construction is situated. When the indenter penetrated into the ice it creates lateral normal stresses in the ice which induces formation of a tensile stress in front of the indenter. This leads to growth of the crack.(**Feil! Fant ikke referansekilden.**) In our case, splitting developed as the final stage of a limit stress scenario after some spalling of the ice beam.

The difference of the result of these two beam tests shows us that the width of the beam was one of the crucial factors for fracture behavior. Another factor was that the indenter did not apply the pressure evenly, which resulted in several types of failure mechanism in the ice there of spalling of the top layer of the ice. Sodhi and Chin (1995) did experiments that concluded that if the ratio W/L(width and length of ice sheet) is less than 1,5 and applied pressure is 2 MPa the ice will fail by splitting, just as we experienced in this experiment. If W/L>1,5 the ice will fail by crushing[1.2].

3.4.1.2 Laboratory indentation test

Motivation

After a medium scale test performed in the lake, a small scale indenter test was carried out in the cold laboratory at UNIS. The indenter test was also done together with Group #2 . The aim was to facilitate a practical understanding of the problems with performing small-scale indentation test inside a laboratory. Important factors such as load measurements and noise level are considered as important.

Theory

The theory of failure mechanics for the indenter test was discussed for the field indentation test. The following formulas are used for calculation in this experiment.
Korzhavin's formula is used for estimation of stress:

$$\sigma = \frac{p}{(I \cdot m \cdot k \cdot \chi)}$$

Where I-indentation coefficient, m-shape coefficient which is set to 1 since it is a straight indenter surface, k-contact coefficient set to 0.7, χ-strain rate function, p-pressure of the ice,_σ-compressive strength of ice.

p is the compressive stress which can be calculated as:

$$p = \frac{F}{b * h}.$$

The indentation coefficient is found by:

$$I = \left(\frac{B}{b}\right)^{1/3}, where$$

B is the width of the ice sheet.

The strain rate function is then found by:

$$\chi = \left(\frac{\dot{\varepsilon}_0}{\varepsilon}\right)^{1/3} = \left(\frac{v_0}{v}\right)^{1/3},$$

where v is the laboratory velocity value and v_0 is set as 1 m/s

Experimental set-up

This experiment was performed in UNIS using the ice tank in the Cold Lab. The dimensions of the tank are 1.5 x 1 x 0,7 m(see Figure 30) The tank was filled with seawater from Adventfjorden The tank is equipped with a heating system in the walls and bottom which holds the water at freezing point. This ensures that the water is freezing from the surface in a downward direction.

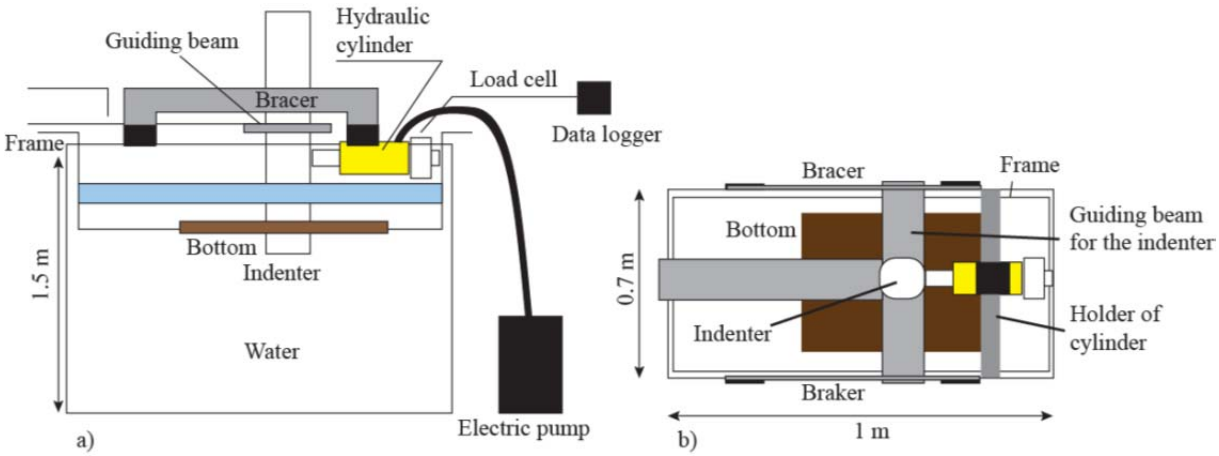

Figure 30. Scheme of the indentation test in the ice tank: side view (a) and in-plane view (b). [2.1]

When a sheet of ice is frozen over at the surface the hydraulical piston pushes the indenter beam forward against the sheet of ice with a chosen rate of speed and force. The force load and time is recorded by the data logger.

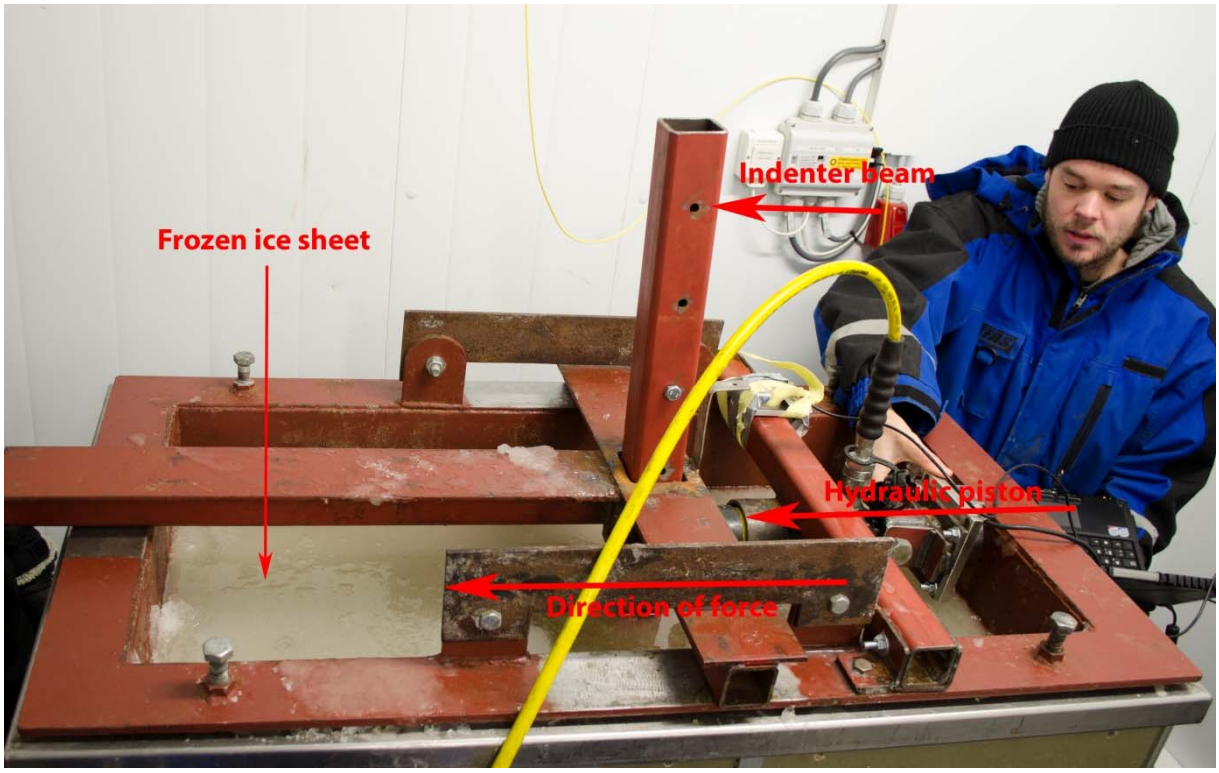

Figure 31. Picture of icetank with indenter set-up.

An accelerometer was also attached to the indenter beam for recording the acceleration of the indenter.

Results

The data taken from load cell is presented on the figure 15. Power spectrum of the data is shown on the figure 16 (on y-axis arbitrary units and logarithmic scale)

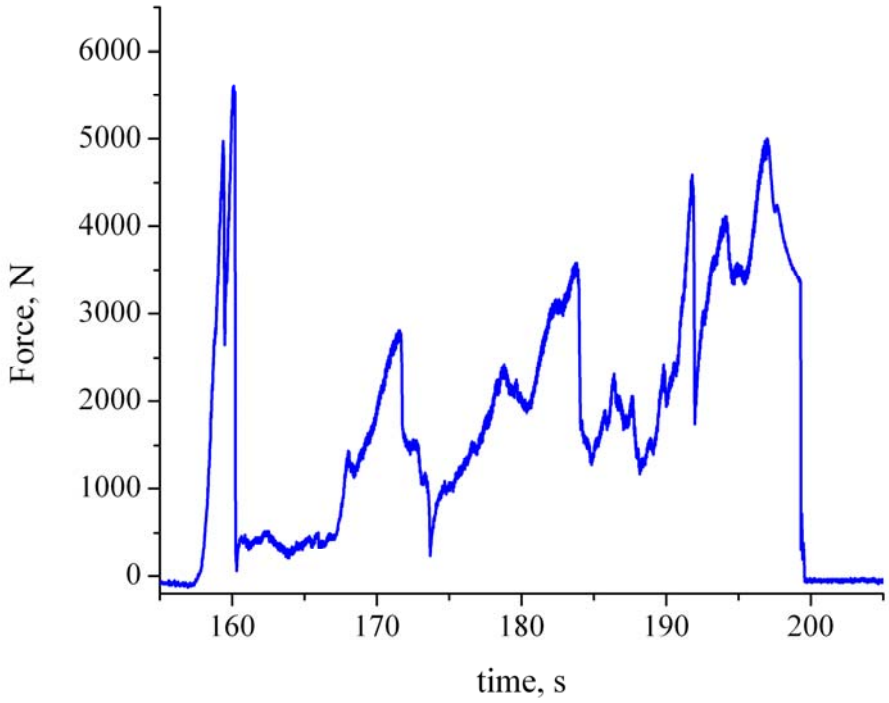

Figure 32. Data from load cell.

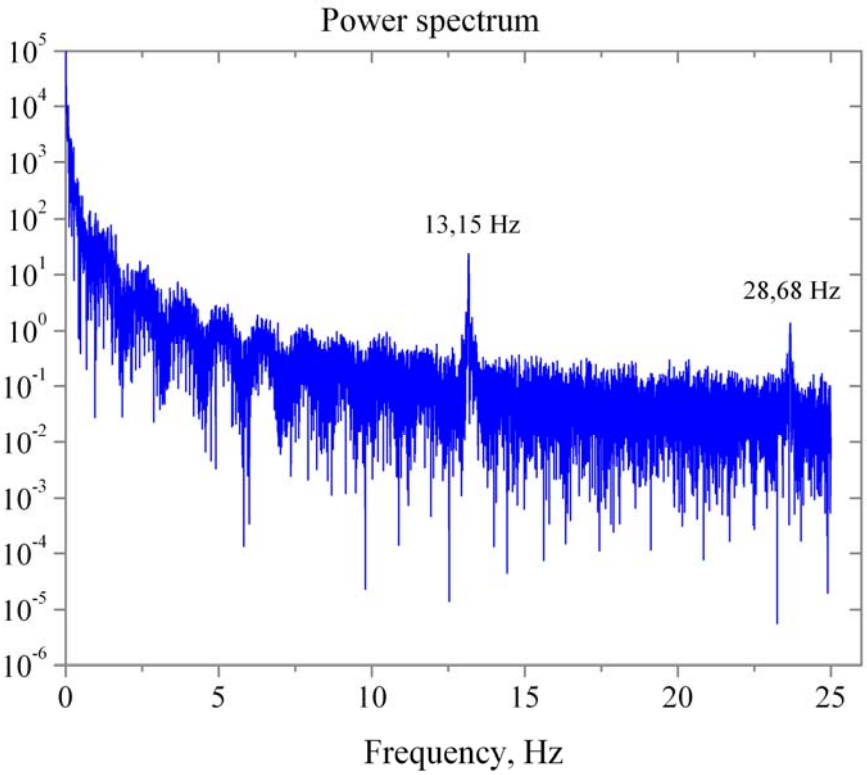

Figure 33. Power spectrum of the data.

Discussion and analysis

The speed of the indenter was 0.11m/43s = 0.0026 m/s

Maximum load equals to 5.6 kN.

According to the Korzhavin's equation:

$$\sigma = \frac{F}{\left(\frac{B}{b}\right)^{\frac{1}{3}} \cdot m \cdot k \cdot \left(\frac{v_0}{v}\right)^{\frac{1}{3}} \cdot b \cdot h} = \frac{5600}{\left(\frac{0,7}{0,06}\right)^{\frac{1}{3}} \cdot 1 \cdot 0,7 \cdot \left(\frac{1}{0,0026}\right)^{\frac{1}{3}} \cdot 0,06 \cdot 0,055}$$

Where: B – width of the ice sheet (width of the ice tank);

b – size of the structure (width of the indentor);

m – shape coefficient (1 for flat indentor);

k – contact coefficient (chosen to be 0.7);

$\frac{v_0}{v}$ – strain rate;

h – thickness of ice;

F – maximum load.

By using presented parameters, strength of ice can be estimated to be equal to

$$\sigma = 147\ kPa.$$

For analyzing frequency components of the load signal a Fourier transform was applied, the results can be seen at Figure 16. Power spectrum shows two distinct peaks: 13.15 Hz and 28.68 Hz. These frequencies correspond to periods of 0.076 and 0.035 seconds respectively.

Frequency of 28.68 Hz can be connected to the process of ice crushing.

According to the Hooke's law

$$\sigma = E\ \varepsilon.$$

Stress was estimated using Korzhavin's equation

$$\sigma \approx 150\ kPa.$$

Let's consider elastic modulus for sea ice to be equal to 0.9 GPa (the value which is close to what we obtained in other laboratory work for sea ice). Now we can estimate strain:

$$\varepsilon = \frac{\sigma}{E} = \frac{150\ kPa}{0.9\ Gpa} = 1.67 * 10^{-4}.$$

Length of the ice sheet (distance between the indenter and the end of the ice tank) was about 0.6 m, than according to definition of strain:

$$\varepsilon = \frac{\Delta x}{x}.$$

Therefore, $\Delta x = \varepsilon * x = 1 * 10^{-4} m$. Taking into account the velocity of the indenter of 2.7*10^{-3} m/s it is possible to calculate time needed for indenter to pass this distance.

$$T = \frac{\Delta x}{\vartheta} = \frac{1 * 10^{-4} m}{2.7 * 10^{-3} m/s} = 0.037\ s$$

This period corresponds to the frequency of 27 Hz which is very close to the value from power spectrum (28.68 Hz).

Frequency of 13.15 Hz can be related to the frequency of the structures such as natural frequency of the indenter or vibrations of ice tank. Since speed of sound of ice is about 3 m/s, about 5 m/s for steel and geometrical dimensions **of the structures are about 0.1-**1 m, natural frequency of **these structures can be about 3-**50 Hz.

3.4.1.3 Uniaxial compression test

Motivation

Uniaxial compressive test has large application in ice engineering practice. Number of field studies and laboratory experiments were carried out to characterize sea ice behavior under compressive loads ([3.1, 3.2, 3.3]). These tests are usually performed under constant strain rates. This regime is connected to short transient loadings and following failure. As well these experiments provide relative information on mechanical properties such as compressive strength and Young modulus of sea ice.

Since internal structure of sea ice which is a complex material that primarily consists of pure ice, inclusions of water with dissolved salts (brine) and air pockets, than it is always important to relate obtained mechanical characteristics to thermo dynamical properties such as temperature and salinity and with a volume of pores reside in sea ice.

As for compressive strength there is a distinct effect of porosity on horizontal strength,. especially brine pockets which can be viewed as concentrators of stress. Investigators report that compressive strength reduces as the amount of pores in sea ice is increasing. For example, in [3.2] suggested that sea ice loses its strength when porosity of higher than 0.2 for load in vertical direction.

This work was intended to carry out compressive uniaxial tests on sea ice samples collected during field work in April of 2013 in Barents Sea. Stress-strain relation was used to obtain vertical compressive strength and Young modulus. Salinity, density and temperature of each sample were measured. The brine and the air volumes was calculated and related to mechanical properties of sea ice.

Theory

The stress applied to an ice sample can be found basing on load as

$$\sigma = \frac{F}{A} \tag{1}$$

Here F is an applied force, A is an surface area of specimen.
From measured deformation relative displacement or strain is readily available,

$$\epsilon = \frac{\Delta L}{L_0} \tag{2}$$

where ΔL is a change in length and L_0 is an initial length.

Sea ice specimen can break down in either two modes which imply different failure mechanism. During the ductile failure maximal load is followed by a softening when the ice sample gradually loses its strength. While the brittle behavior is characterized by abrupt load drop and immediate lost of strength. The maximum load that sea ice sample can support in uniaxial compressive tests is called compressive strength.

Other important characteristics of sea ice mechanical properties is Young's modulus or elastic modulus. Considering ice sample as a perfect isotropic elastic material before failure Hooke's law will read,

$$\sigma = E\epsilon \tag{3}$$

Than it follows that Young's modulus can be obtained by taking derivative of stress-strain curve and further defined as the steepest gradient before it has been reached the yield point.
As it was suggested before both of these properties are highly dependent on internal structure of sea ice. Let define the porosity of material as ratio of volumes,

$$\nu_b = \frac{V_b}{V} = \frac{\rho S_i}{\rho_b S_b} \tag{4}$$

where V_b and V are the brine and total volumes respectively. ρ - the density of sea ice and ρ_b is the density of brine. Here it is assumed that all salts are dissolved in brine pockets.
It is clear that porosity will highly depend on brine density which can be found only by employing empirical relationships which have general form as

$$F_i(T_i) = \alpha_{i,0} + \alpha_{i,1}T_i + \alpha_{i,2}T_i^2 + \alpha_{i,3}T_i^3 \tag{5}$$

Here i can take values from 1 to 4. From F_1 and F_3 one can obtain $\rho_b S_b$ for $T > -2.0^{\circ}C$ and $T < -2.0^{\circ}C$ respectively. While F_2 and F_4 are used to find $\frac{\rho_b}{\rho_i}$ which are needed for fractional air volume, ν_a

$$\nu_a = \frac{V_a}{V} = \frac{V - V_b - V_i}{V} = 1 - \frac{V_b}{V} - \frac{V_i}{V} = 1 - \frac{V_b}{V} - \frac{m}{\rho_i V} = \left| m_i = m_t - m_b = \rho V - \rho_b V_b = \rho V - \frac{\rho S_i}{S_b} V \right| = 1 - \frac{\rho}{\rho_i} + \frac{\rho S_i}{\rho_b S_b}\left(\frac{\rho_b}{\rho_i} - 1\right) \tag{6}$$

In (6) density of pure ice is included which is temperature dependent as well and is given as

$$\rho_i = 0.917 - 1.403 \cdot 10^{-4} T_i$$

Now using empirical relations (6) the final formula for fractional brine and air volumes are written,

$$\nu_b = \frac{\rho S_i}{F_1(T_i)}, \quad \nu_a = 1 - \frac{\rho}{\rho_i} + \rho S_i \frac{F_2(T_i)}{F_1(T_i)} \tag{7}$$

which are functions of directly measured quantities, density, temperature and salinity of sea ice.

From known fractional volumes one can estimate compressive strength for vertically loaded ice samples. There are two empirical relations. First is given in [3.2],

$$\sigma_{c,v} = 160(\dot{\epsilon})^{0.22}\left[1 - \left(\frac{\nu_T}{0.2}\right)^{0.5}\right] \tag{8}$$

and the second estimate by [3.1],

$$\sigma_{c,v} = 24\left[1 - \left(\frac{\nu_T}{0.7}\right)^{0.5}\right]^2 \tag{9}$$

Here ν_T - total volume of pores in an ice sample, $\dot{\epsilon}$- strain rate.
For Young modulus suggested empirical relation (Weeks and Assur, 1967) is given as

$$E = E_0(1 - \nu_b)^4 \tag{10}$$

where E_0 is Young's modulus for freshwater ice and in the order of 10 *GPa*.

Description of experiment

Experiments on uniaxial compressive loading of columnar sea ice were carried out in C215 Cold Lab 1, UNIS on the 30th of October, 2013. The experimental procedure consisted of preparing a specimen from ice cores and making geometrical measurements. The cores were cut using a mechanical saw to length of L_0 = 175 *mm*. Further, samples were weighed by electrical weights, their average diameter were measured with a Vernier caliper. Temperature of sea ice was obtained as well. After measurement procedures the samples were then placed between two plates of pressure machine.

In overall 5 compression tests were conducted. The first three samples were tested in "Knekkis" pressure-tensile machine (**Figure 34**). Here two additional elastic compliance plates were placed on both ends of the specimen to increase friction. The fourth test was conducted in similar to "Knekkis" machine but used in field studies and has the name of "Kompis" (34).The last test was carried out again with "Knekkis" but without reducing frictional shear forces on samples.

Figure 34. , "Knekkis" – laboratory pressure-tension machine.

Figure 35. "Kompis" – pressure machine for field studies.

"Knekkis" and "Kompis" are specially designed for performing uniaxial compressive tests. In both machines the lower steel plate is moving upward with a constant velocity while the force is measured by a load cell mounted under the loading plate. The displacement is measured between the two steel plates.

For "Knekkis" the control program "Svalkryp 3.0" was used to set input parameters which are velocity, air temperature, length, diameter and weight.

The constant strain rate was set either to $1 \cdot 10^{-3} \frac{1}{s}$ or $0.7 \cdot 10^{-3} \frac{1}{s}$. From this the corresponding input parameter to the software, velocity, was calculated by

$$v = \dot{\epsilon} L_{0.}$$

After the sample failed it was left in a plastic box to melt overnight. The next day the salinity of the received solution was measured to find sea ice salinity.

Results

In a compression test performed, there was a region where linear law dependence between strain and stress was observed. At this region sea ice followed Hooke's Law and deformations were recoverable since it corresponds to elastic deformations. At the point of maximum stress the linear regime terminated and after sea ice sample showed plastic behavior, the deformations became unrecoverable once the load would be removed. Both of these regimes are illustrated by Figure 36 where the first region corresponds to elastic deformations and region 2 to plastic behavior.

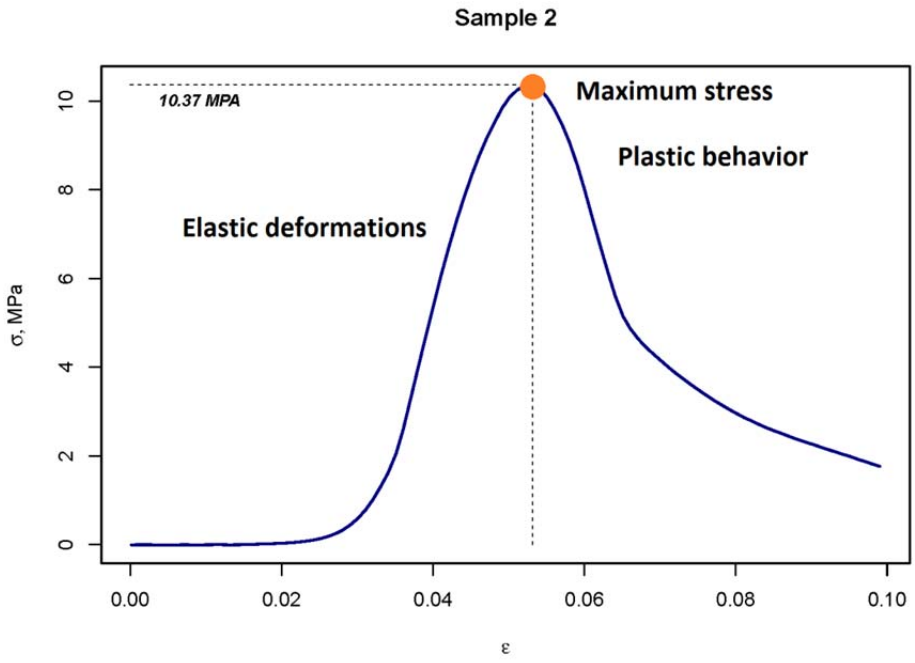

Figure 36. Typical stress-strain relation observed during experiments.

After transition to plasticity all of the samples had shown ductile behavior. Its manifestation was in a softening of sea ice and was characterized by steady reduction of its strength. Through this regime sea ice was not able to sustain applied load and failure had occurred. This was seen as developing of zones with cracks accumulation. Such zones (milky features) differed in color, becoming whiter with time, their texture was different from surrounding material. These areas of nucleation was occurring along all surface of the specimen .It can be speculated that large number of micro cracks were developed, but their propagation were restricted by relaxation of stresses under a slow compressive loads. Though these cracks continued to develop and at some moment specimen was broken. In most cases the major failure appeared in the middle of sample with angle around 45 degrees to direction of load .

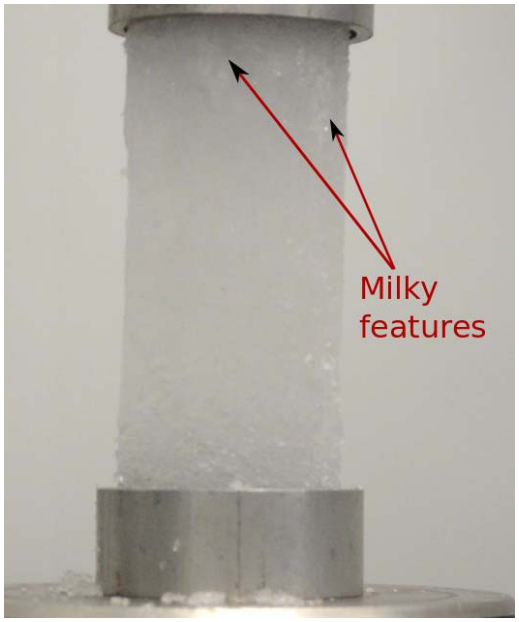

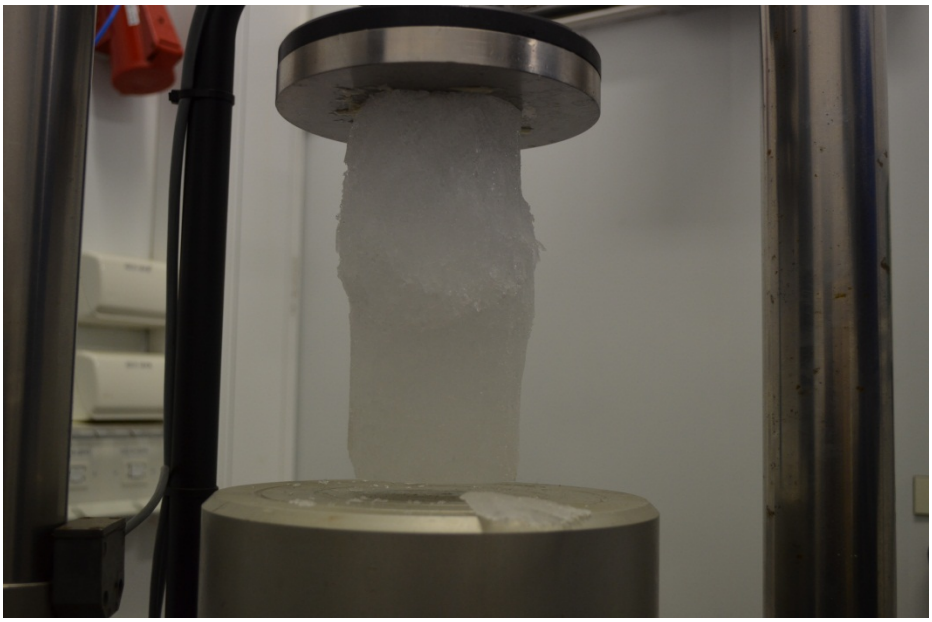

Figure 37 (a) Nucleation of cracks during ductile behavior. (b) Developed splice cracks. (c) Failure in the middle.

For Sample 3 was observed slicing at the lower end. But due to additional friction the appeared sections were confined and that is were still under load instead of being sliding apart. So the obtained results were satisfactory.

For comparison the sample 5 was tested without compliance plates , i.e. additional friction affecting on sides was not presented. This was seen as a bit different failure mode. The cracks did not developed at the ends. Nevertheless the major failure occurred in the middle portion of the specimen.

The sample 4 was tested with Kompis machine and its behavior was unusual in a sense that failure mode was reached faster as well as breaking of the material occurred in unusual way. The probable reason for this might be in an initial crack inside of the specimen since failure appeared along the length of the sample .

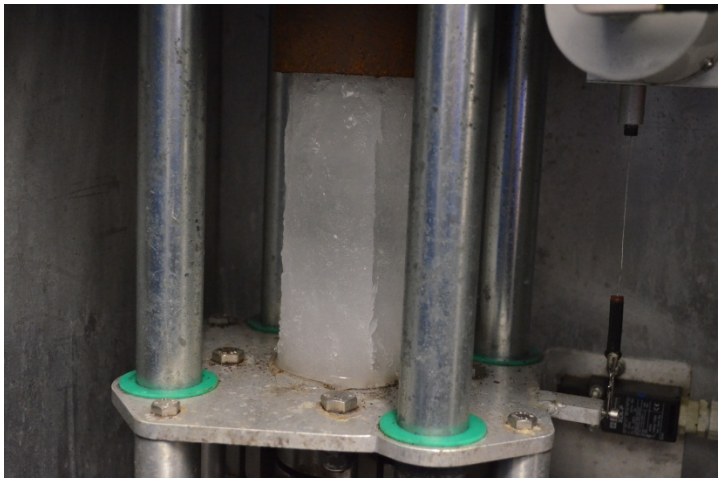

Figure 38. Failure of Sample 4.

From the obtained stress-strain relations number of quantitative parameters might be obtained. As was mentioned before the maximum stress that the sample could sustain corresponds to compressive strength of material, i.e. the maximal force under which the material can recover to its initial state without reduction in its mechanical properties. For example, for experimental results on fig 36 the maximum strength was found to be a bit higher than 10 *MPa*.

Further, since the initial regime of deformation is described as an elastic compression one can obtain the elastic modulus from Hooke's law as

$$\sigma = E\epsilon, E = \frac{d\sigma}{d\epsilon}$$

Thus, the Young modulus will define the inclination of the stress curve in relation to deformation.

The 39 shows results for all specimens except fourth when unrealistic behavior was observed. Here in the lower panel it is presented obtained Young modulus as maximum inclination of the first curve. The first three samples had shown relatively same results. For sample 4 both compressive strength and Young modulus are small which supports idea of initial fracture. The sample 5 was tested without compliance plates which reduced artificial stiffness, thus increasing Young modulus. Though, compressive strength is comparable with other results. These results are summarized in **Table 1**.

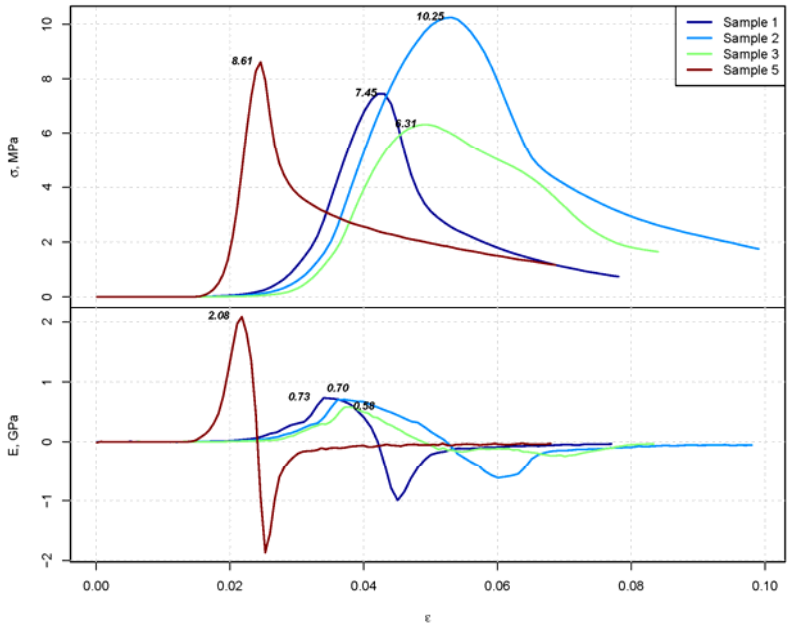

Figure 39.The measured stress-strain relations and calculated Young modulus.

Sample #	Diameter, mm	Strain rate, 1/s	Mass, g	Density, kg/m^3	Salinity, psu	T	σ_c, MPa	E, GPa
1	72.3	$1 \cdot 10^{-3}$	655.2	0.91	4.47	-9.3	7.45	0.73
2	71.9	$1 \cdot 10^{-3}$	655.68	0.92	4.57	-9	10.37	0.72
3	72.1	$7 \cdot 10^{-4}$	650.83	0.91	4.39	-11	6.35	0.58
4	71.3	$1 \cdot 10^{-3}$	657.37	0.94	5.83	-8.6	0.98	0.13
5	72.1	$7 \cdot 10^{-4}$	649.75	0.90	3.32	-10.2	8.66	2.09

Table 1. Measured and calculated properties of tested sea ice samples.

Discussion

Since for all specimens salinity, temperature and density were measured it was possible to obtain porosity basing on empirical relations defined for sea ice (eq. 7). These results were incorporated into empirical relations known for vertical compressive strength and Young modulus (eqs. 8-10). **Table 2** summarizes these estimations.

Sample #	Brine porosity	Total porosity	Strain rate, 1/s	$\sigma_{c,meas}$	$\sigma_{c,eq.8}$	$\sigma_{c,eq.9}$	E_{meas}, GPa	E_{10}, GPa
1	0.026	0.038	$1 \cdot 10^{-3}$	7.45	19.67	14.08	0.73	9.0
2	0.027	0.028	$1 \cdot 10^{-3}$	10.37	21.82	15.31	0.71	8.94
3	0.022	0.036	$7 \cdot 10^{-4}$	6.35	18.67	14.37	0.58	9.13
4	0.037	0.037	$1 \cdot 10^{-3}$	0.98	19.93	14.22	0.13	8.596
5	0.018	0.032	$7 \cdot 10^{-4}$	8.66	19.48	14.87	2.09	9.31

Table 2. Measured and estimated mechanical properties of the samples.

In all sea ice cores porosity was not larger than 4% meaning that the samples were relatively solid. The highest salinity and temperature was measured for sample 4. But its porosity was not the highest. At the same time it had maximal density. Nevertheless its mechanical properties were the smallest what is believed due to initial defect. For the rest of the samples there is no direct relation in measured mechanical properties with porosity For example, the largest measured uniaxial compressive strength corresponds to the smallest to porosity (Sample 2), while the highest porosity corresponds rather to average value of compressive strength (Sample 1). Nevertheless, from obtained data it is seen a trend that higher porosity corresponds to smaller compressive strength.

This corresponds to a general view that pores in sea ice affect its internal mechanical state as concentrators of stress. As amount of such discontinuities increase it is expected that material will have smaller strength under load. For temperature dependence such trend is not clearly seen since the temperature range is rather small to discuss its effect. In case of salinity it is seen slight decrease of sea ice strength with amount of salt presented in the samples. This is not surprising since for sea ice it is assumed that all salt amount is in brine pockets, i.e. porosity will be larger as salinity will increase.

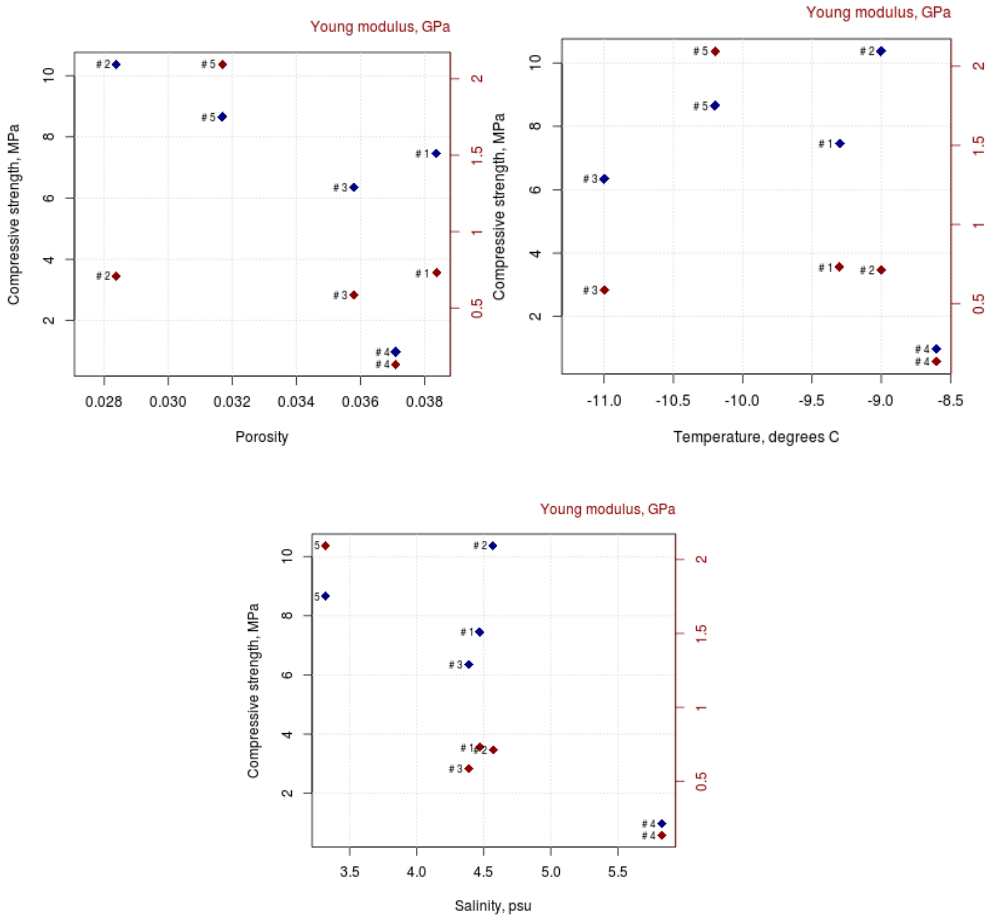

(a) (c) (b)

Figure 40. The relations of total porosity (a), temperature (b) and salinity (c) to compressive strength and Young modulus.

In contradiction to dependence of compressive strength to mentioned properties of sea ice, Young modulus shows almost no relation. Though here it should be differentiated porosity used for compressive strength which includes both volume of air and brine pockets. While if only brine porosity is considered than from Table 2 follows that Young modulus decreases with brine volume for the first three samples that were tested under the same conditions. This corresponds to the known empirical relation (10) which suggests large drop in elastic modulus with large amount of salt.

Comparison of obtained results and empirical relations for both compressive strength and Young modulus shows that the results are much smaller than it could be empirically predicted from physical properties. Though it is noticeable that the relation proposed in [3.1] is more applicable to this study.

It gives approximately two times larger values while for estimates following [3.2] it is 2.5 times larger. In this comparison it is again seen unrealistically small compressive strength for Sample 4 which is order of magnitude smaller than empirical estimates.
The most striking results come from comparison with estimation of Young modulus. Here the difference is order of magnitude smaller than one can find by (10). One reason for this can be envisaged from the last experiment where compliance plates were removed as Young modulus had increased by several times. Hence, introduction of additional stiffness into testing environment results in underestimated values of elastic modulus. From summation of strains and application of Hooke's law it can be shown that

$$E_{meas} = \frac{1}{1+{E_{ice}}/{2E_{plate}}}$$

Here Eice represents actual elasticity of ice while Eplate is an elastic modulus of compliance plates. From this relation it is easy to see as soon as plates stiffness is becoming comparable to Young modulus of ice, i.e. 9-10 GPa the error in measured values become larger. For example, if Eplate = 1 GPa, Emeas becomes 80% smaller. But as soon as Eplate is much larger than one of ice the error tends to zero and for Eplate = 20 GPa the error becomes around 18%.

Conclusion

The carried out uniaxial compressive tests on sea ice samples from Barents Sea had shown pure ductile behavior. With measured physical properties such as salinity, temperature, density it was possible to consider some of effects of these quantities on mechanical properties which can be summarized as

1) Compressive strength in large relation to porosity of the material. Large amount of discontinuities in pure ice matrix decrease amount of sustainable load.
2) Since porosity is directly affected by temperature and salinity through density of brines, sea ice shows the same type of dependence on these values.
3) Young modulus is largely susceptible to changes in volume of brine pockets.
4) Initial defects in sea ice can largely decrease its mechanical properties.
5) Elastic stiffness of loading machine should be known a priori for accurate measurements of Young modulus.
6) The empirical estimates based on large number of experiments can be used as an upper limit of mechanical properties.

3.4.2 Numerical study of Ice

The COMSOL Multiphysics provides a finite element analysis for various physical and engineering applications. COMSOL Multiphysics also offers an extensive interface to MATLAB and its toolboxes for a large variety of programming, preprocessing and post processing possibilities.

The second feature, MATLAB LiveLink allows us to run the same model but with different parameters (e.g. geometrical sizes) on the fly. In order to do this one can create and run a model in COMSOL with certain parameters and after save a model as an M-file.

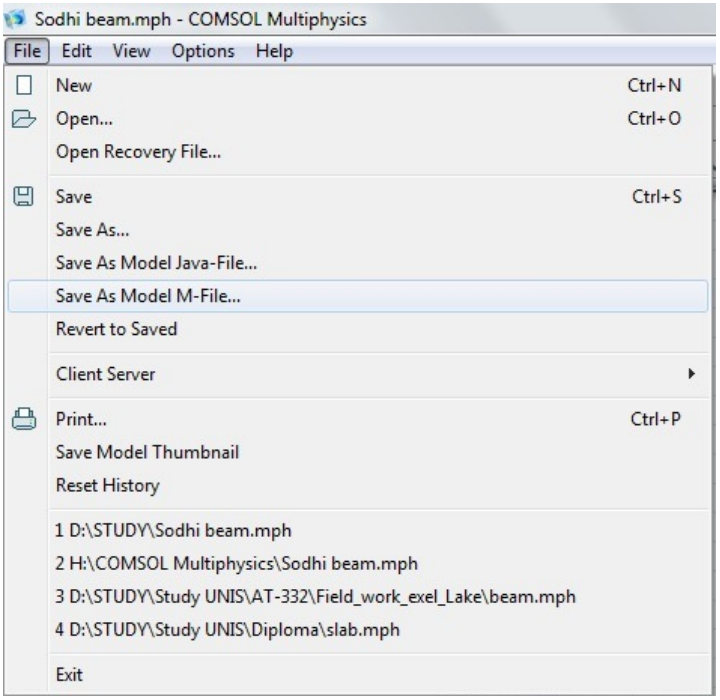

Figure 41. COMSOL screenshot.

Next step to run a model with different parameters is to modify this M-file. First, one should declare parameters that are wanted to manage as input parameters. For that it is necessary to choose a name of function and to write input parameters within brackets instead of “model” (42). In 42 we declared three parameters to manage. These are a1, a2 and filename.

```
   function out = model
function out = sodhi_beam1(a1, a2, filename)
```

Figure 42. MATLAB screenshots.

After one can just write a name of function with certain parameters on MATLAB command line and the result will be the same as you run a model with these very parameters in COMSOL.

Methods

The object of interest in our work is 3-point-loading test of the two dimensional ice beam and studying the intensity factor distribution along cross sections which include loading points.

On 43 half of the beam is shown which considered to be modeled in COMSOL Multiphysics. Length of the beam is 7 m, thickness is 0.75m. By dividing the beam into elements made it possible to assign different boundary conditions: symmetrical (blue), free (red), fixed (yellow) and floating (green).

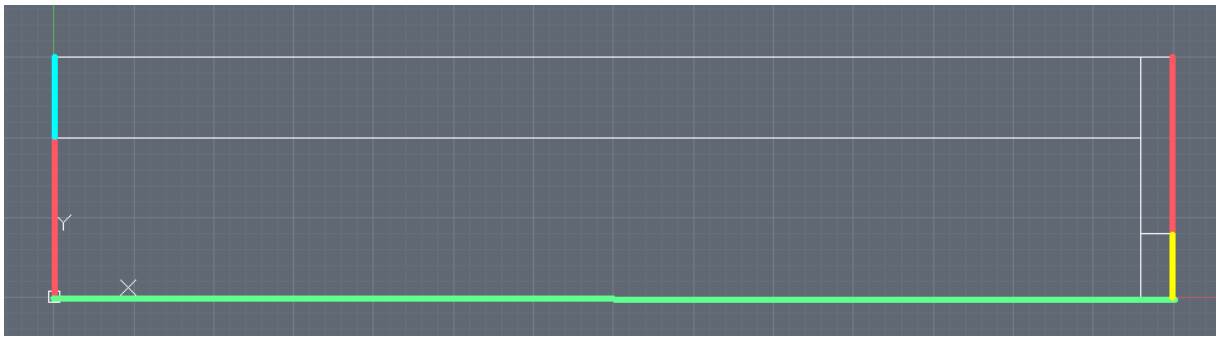

Figure 43. COMSOL model geometry.

Running this model in COMSOL gives us stress distribution along cross sections which match to cracks (free boundary conditions). It is known that maximum stress can be calculated using following equation:

$$\sigma_x = \frac{K_I}{\sqrt{2\pi r}}, where$$

K_I is intensity factor which shows how the material resists fracture propagation; r is the distance between maximum stress and the crack tip. After running a model and finding maximum stress and r one can easily calculate intensity factor. Thus we have a dependence of intensity factor on initial crack sizes. Typical stress distribution is shown on fig 44.

However in almost all cases r is equal to zero due to bad resolution of mesh used in this simulation. That is why it was decided to take r always equal to 5 mm and to fit stress growing curve with quadratic polynomial. In Appendix 3 one can find MATLAB scripts to perform simulations.

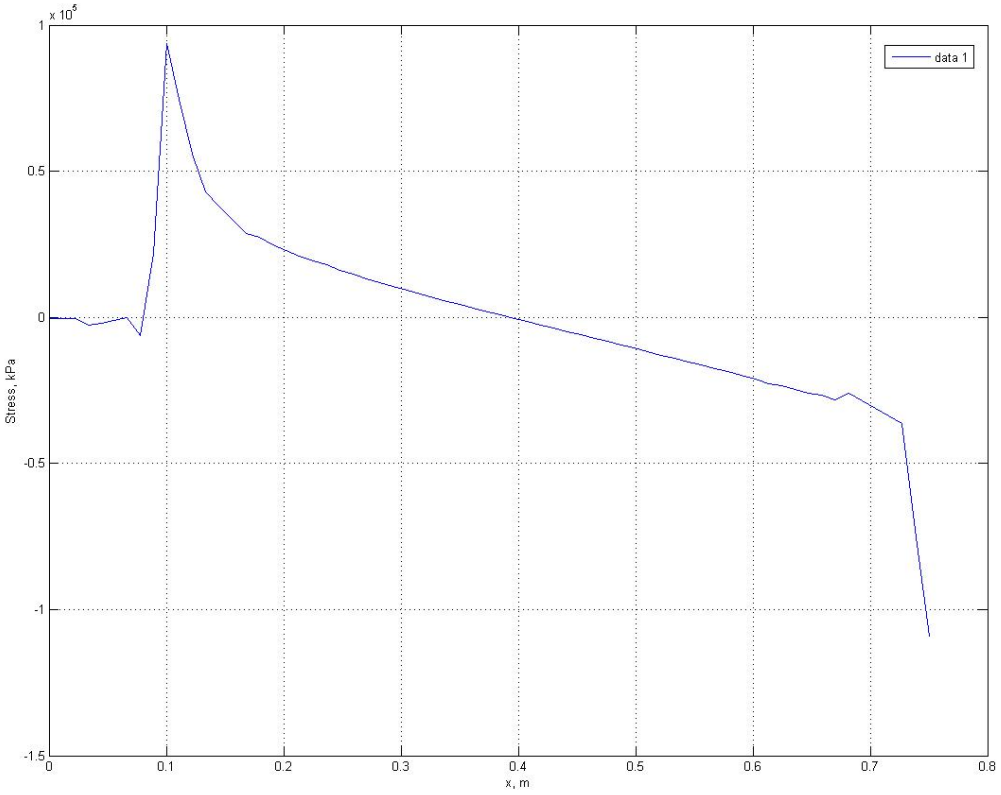

Figure 44. Stress vs y coordinate.

Results and discussion

Here we show intensity factors vs crack sizes a1 and a2 for middle cross section (45) and for edge cross section (46).

One can see that intensity factor for middle cross section depends strongly on middle crack size and slightly on edge crack size. Other way round the case is with intensity factor for edge cross section. It depends strongly on edge crack size and slightly on middle crack size. That seemed to be expected.

Now using this surfaces one can intersect them with a plane ($z = K_{Ic,}$ fracture toughness) and obtain a set of crack sizes when initial crack in this very cross section will propagate. Also a boundary of this set gives us a curve which shows critical crack sizes when initial crack in chosen cross section is starting to propagate.

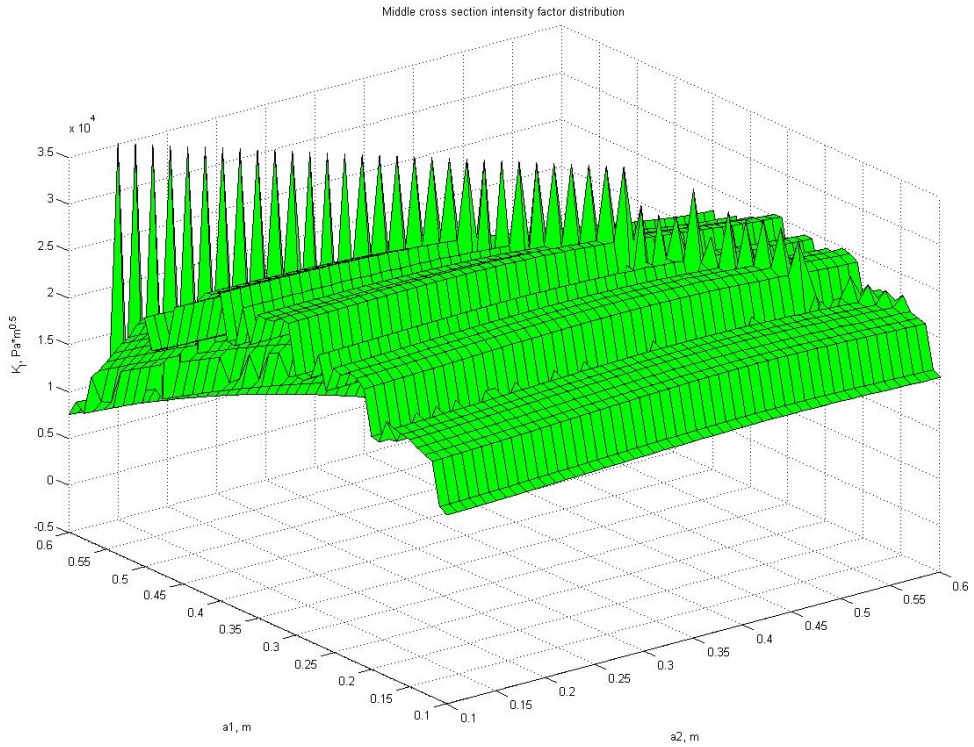

Figure 45. Middle cross section. Intensity factor vs crack sizes.

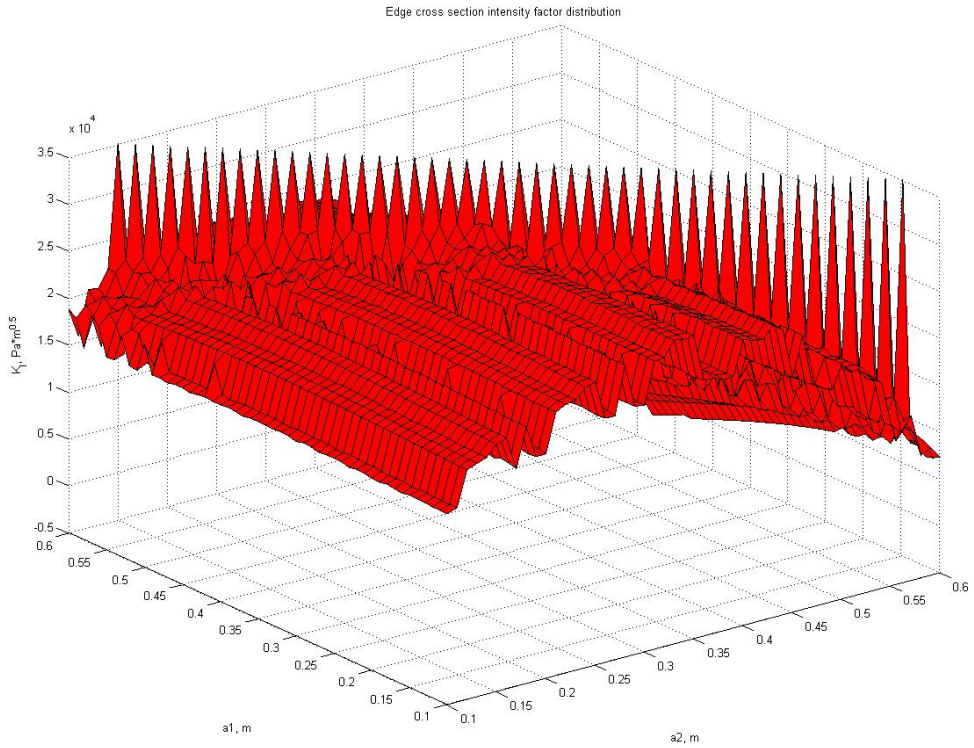

Figure 46. Edge cross section. Intensity factor vs crack sizes.

3.4.2 Basis theory references for the lab week reports

[1.1]: TJO Sanderson,1988, Ice mechanics, Risks to offshore structures.

[1.2]:S.Løset, N.Shkhinek, T.Gudmestad, V.Høyland, Actions from ice on Arctic offshore and coastal structures.

[1.3]: AT-327 Cource material, S. Løset slides.

[2.1]: A. Marchenko, D. Onishchenko, Ice piling up and ice loads on narrow structures: laboratory experiments and modeling of kinematics ,2013.

[3.1]: Moslet, P. O. Field testing of uniaxial compression strength of columnar sea ice

[3.2]: Timco, G. W., and R. M. W. Frederking. Compressive strength of sea ice sheets.

[3.3]: Weeks, Wilford F., and Andrew Assur. The mechanical properties of sea ice.

4 FPSO specific design

The ice actions on a FPSO is not that different than of a bottom-founded structure, however the calculations might be more complex due to the fact that the mooring line loads are also a factor. However, when designing for a FPSO one does not need to design the construction itself to withstand the load from a worst case scenario, for example in the event of an incoming iceberg. This is due to the fact that the mooring system cannot handle relatively huge loads so it is more important to implement good ice management and disconnection systems in order to evade extreme ice features. The FPSO that designed for and used in non-ice environments cannot handle the high Arctic conditions and must be built or modified accordingly. In the following the specific design features for an FPSO in an ice environment will be reviewed.

4.1 Ice Vaning

The ability for a FPSO to weathervane comes with the usage of a single point mooring system and a rotating turret. For arctic conditions the spread mooring system should then be excluded for a ship shaped FPSO due to the ice build-up that might occur if the ice has a drifting direction towards the broadside of the floater .Usually a FPSO has icebreakers that break up the surrounding ice so that the ice is broken up in floes so the ice features are of a lesser scale. But if ice management fails or is nonexistent it is important to design for situations where the ice might be unmanaged and the ice actions might be more severe.

4.1.1 Ship shaped FPSO

A ship-shaped FPSO can take advantage of that the knowledge of design that the ice breaker has. A number of efforts have been made to estimate the performance of ships in ice and are mostly based on empirical relations from full-scale data or model-scale tests. The ice actions on the FPSO are highly governed by the failure mechanism at the ice structure interface. In arctic conditions a ship shaped FPSO must be able to ice vane, meaning that the ship is able to adjust the direction in such way that the bow faces the drift direction of the ice. In such a situation the contact surface between the ice and the FPSO is as small as possible and causing the ice to fail by bending, rather than crushing which would give a much higher load. The bow is in most cases shaped like a downward cone for a ship shaped FPSO so the incoming ice will interact in an identical way as the situation for a sloping structure.

The turret placement dictates much how well the FPSO ice vanes. In the case of the best ice vane performance the turret should be placed by the bow of the FPSO. The turret can also be placed mid-ship, however the ability to ice vane will be reduced and must be aided by thrusters to get the FPSO into position. This solution however reduces the vertical displacement and the adverse effect on the mooring line tensions, which the solution with the turret at the bow would have. A solution where the turret is placed one third of the vessel length back from the bow would improve the mooring line safety factor by 15 to 18 %(Chakrabatri S, 2005).

Another solution is to use a dynamic positioning system rather than a mooring system to keep the FPSO in a desirable position. This eliminates the need to design for the mooring strength to withstand the ice loads.

4.1.2. Circular shaped FPSO

A circular or buoy shaped FPSO would not need to ice vane due to its geometry. The ice loads would be the same where ever the loads would hit the boat. This means that the FPSO does not have to rotate and can be moored to a fixed position without needing to rotate.

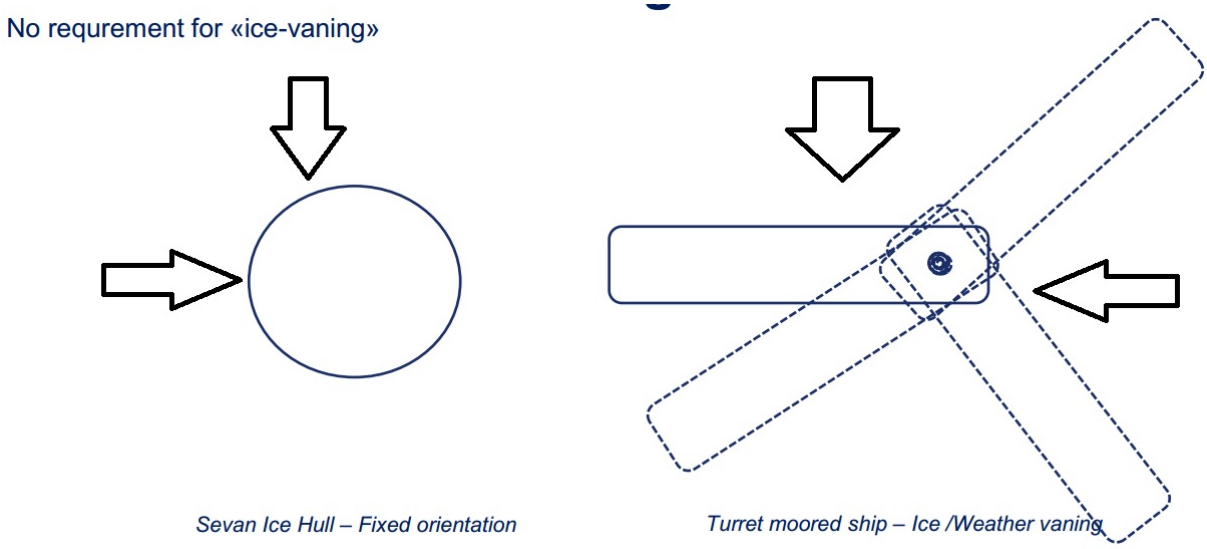

Figure 47 Circular vs Ship-shaped FPSO (Sevan marine)

4.2 Varying ice drift

According to ice charts, the drift ice covers varies from open waters in the summer to very close drift ice in the winter. However the drifting ice does not always have a constant drift direction. Influences from tidal currents and winds play a role in a locally fluctuating ice drift direction. From the first dynamic positioning operations in ice in Sakhalin, 1999 (Keinonen et al. 1999), they experienced how the ice was shifting directions driven by tidal currents and wind. The ice was typically travelling in an

oval loop about once a day (fig 48). These conditions must be taken in consideration in the design of the FPSO.

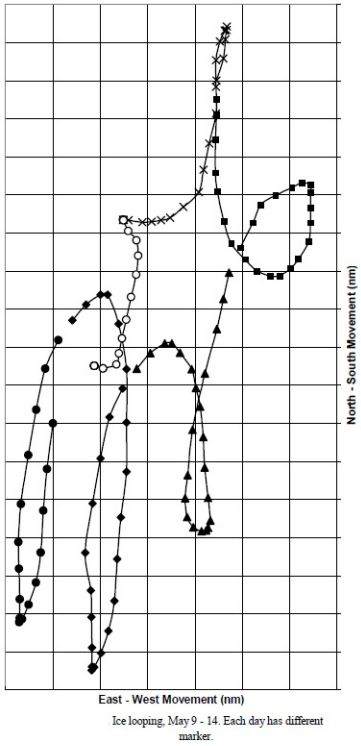

Figure 48 Ice looping during the DP operation in Sakhalin (Keinonen et al 1999)

4.2.1 Ship-shaped FPSO

For a ship-shaped FPSO the varying ice drift is a big issue. Drift patterns are hard to predict and in an Arctic environment with sea-ice the drift patterns may affect the action level in general. A gradual change of direction of the ice drift will allow the floater to ice vane. But if the ice comes to a halt like for the limit momentum scenario, and then suddenly changes direction, this may lead to a high action situation and overloading of the mooring system. If for example ice is at a halt and surrounding the floater, and then suddenly the ice starts to drift in an adverse direction compared to the heading of the bow, the floater will be subjected to a broad side ice load. If the ice vane do not immediately act then, depending on the ice feature a severe load will act on the side of the boat.

Ordinary tankers are not built for this situation due to that they are normally straight vertical on the sides. The failure mechanism would be crushing, which creates high ice loads on the side of the tanker and the moorings. A purpose built FPSO is built with downward sloping sides so that the ice feature in a situation as just described, would be to fail by bending resulting in lower loads. However if the load is high enough the ice feature might start to rubble at the broadside of the ship if the ship does not ice vane fast enough. This is a situation one wants to avoid, and is usually avoided by good ice management.

5.2.2 Circular shaped FPSO

For a circular shaped FPSO the shifting of ice drift direction is not much of an issue. From an environmental point of view that could be considered more environmental friendly due to that the floater does not need thrusters to rotate.

4.3 Ice management

Ice management systems are used to reduce the severity or frequency of ice action on an offshore structure. To have an effective ice management system the following prerequisites need to be fulfilled: A system to detect, track, and forecast ice within the area of interest, this can be done with satellites, airborne surveillance or radar/visual observations from the instillation or ice management ships; A system to evaluate the threat level of a situation, normally it evaluates the situation in terms of potential consequences to the instillation; Physical ice management such as ice breakers where it is required. Performance of the ice management system can be evaluated by studying the effects it has on the following parameters of the incoming ice: The ice feature dimensions drift speed, mechanical properties, ice pressure, and metocean conditions.

In order to manage icebergs it is important to understand the physics that determine their drift. According to Løset and Carstens, (1993), the drift of an iceberg is governed by the pressure distribution acting on its surface.

The force from the current is given by:

$$F_w = \frac{1}{2}\rho_w C_w A_w \mid u_w - u_i \mid (u_w - u_i)$$

where A_w is the exposed area to the current, ρ_w is the density of the water, C_w is the water drag coefficient (normally about 1.5), and $(u_w - u_i)$ is the relative velocity between the iceberg and the current. In (S.Løset 2006) it is shown that if the iceberg is assumed to be surrounded by a current field composed of a slowly varying residual current and a sum of components derived from the deterministic tidal potentials the drift of the iceberg is mainly driven by the pressure of the residual current. If the wind is also assumed to be stochastic the iceberg will approximately drift along the residual surface current. Big icebergs go deep enough that it becomes important to consider that the current systems might change significantly from the bottom of the keel to the surface.

The force from the wind is given by:

$$F_a = \frac{1}{2}\rho_a C_a A_a \mid u_a - u_i \mid (u_a - u_i)$$

where A_a is the cross section area above the water line and normal to the flow. The parameters are the same as for the current case except that they are for air. Air drag will also cause a force that acts on the horizontal surface of the iceberg; it is however often ignored because it is often relatively small. The wind speed will start to have a significant effect when it is stronger than about 10 m/s.

One of the most common techniques to manage level ice and ice ridges is to have the icebreaker either circle the instillation or break the incoming ice upstream into floes, or reduce the size of already existing floes. This method has been shown to perform well Jolles et al.(1997). It is important to have an icebreaker designed to be able to handle the worst conditions expected at the instillation. It is also preferable to have at least two icebreakers in case the primary breaks down. If ice conditions are more severe than the ice management system can handle the production must be stopped and in worst case the structure may have to be disconnected.

There are different types of icebreakers available and the azimuth model has proved very useful. The propellers are able to turn 360° and therefore provide full thrust in all directions; this means that their maneuverability is much higher than a normal icebreaker both in open water and in level ice. Keinonen and Lohi (2001) concluded that this makes the icebreakers more efficient and versatile.

Ice management usually divides the area surrounding the instillation into three zones(S.Løset 2006).

Zone #1: Possible ice feature detected, evaluate the situation to assess how serious it is.

Zone #2: Dangerous ice feature is approaching and risks colliding with the structure causing damage, ice management needs to be deployed.

Zone #3: Collision is unavoidable, production need to be stopped and structure may have to disconnect.

Each of the zones has a time frame within which actions has to be taken, for example the time for zone #3 may be the time it takes to stop production and disconnect.

The following key elements are required to have a good ice management system. Satellite information, weather information, airborne ice reconnaissance, drift buoys, available vessels, visual information. Satellite information, weather information, and airborne ice reconnaissance will provide the basis to analyze the current situation and predict future possible dangers. The airborne reconnaissance will also be able to get precise measures of ice thickness, ice concentration, intensity of ice ridges, and detect icebergs, bergy bits, and growlers. It can also deploy drift buoys that will provide exact measurements of local currents and drift patterns. If the situation is determined to require active ice management icebreakers have to be deployed. Ice management will be harder in the high arctic due to the lack of light during large parts of the year.

All kinds of icebergs can be found in the arctic sea as several iceberg campaigns between 1987-1992 have shown (S.Løset 2006)they can be too big to be towed, broken or even pushed by ships. However many icebergs can be towed enough to deviate from the instillation and thus keeping the operation going.

Offloading from a FPSO is also a challenging factor to design for when operating in the arctic. When transferring petroleum from one vessel to another there is always risk involved an in the arctic especially the risk increases due to environmental conditions. Critical issues can be the risk of collision between two objects and the ability to quickly and safely disconnect in the event of an incoming ice feature. Four categories for structure types can be chosen for offloading in arctic conditions (Gudmestad et al. 2007):

- Platform
- Tower
- Single Anchor Mooring
- Turret loading

The platform is bottom-founded and is usually equipped with a loading arm and offloading/onloading from a moored tanker. This design has its risk where the tanker can collide with the structure if the environmental conditions are severe. If this solution is used the design for the structure should be design in case of a colliding incident. The tanker might be pushed by the ice towards the structure so the tanker should be equipped with thrusters or be surrounded by good ice management in order to operate safely.

The tower can be an oil terminal like the Varandey in the Pecora Sea. Equipped with a loading-arm that exports the oil to the tankers. The tower resembles very much offloading solution of the platform.

Figure 49 Varandey offloading terminal (http://neftegaz.ru)

The SAL system is often used for the FPSO where a tanker is connected to the floater for offloading. There are several designs of this system depending on the region where it is supposed to operate in but what they all have in common is that they require an extensive ice management. The ability to ice vane is vital in this solution.

The turret loading is a system which is fully subsurface that the tankers can connect to for offloading. As for the SAL system, the ships ability to ice vane is a critical to avoid huge ice action.

All of these solutions have their pros and cons but they all reveal that if one wants to offload in arctic conditions it will require a really good ice management.

For the deeper waters in the arctic it is no use to build platforms and towers, this will be to cost full. For instance in the western Barents sea all the fields like Snøhvit, Goliath and Johan Castberg takes advantage of either FPSO units or full well stream to shore. The water depth of these fields are over 300 meters some of the fields like in the Pechora where the Varandey oil terminal is or the monster sturdy platform Prirazlomnoye only has to deal with a water depth of approximately 20 meters.

A proposed concept for arctic conditions is the Arctic Tandem Offloading Terminal (ATOT). This concept was tested at the Hamburg ship model basin (HSVA). The concept consists of a moored offloading icebreaker connected to a moored offloading tanker. During calm sea conditions and open waters the offloading can happen by a distance of approximately 60m. During heavy and medium ice conditions the two floaters close together and performs the loading. If ice conditions is severe then the tanker is disconnected and the offloading ice breaker offloads the petroleum alone. This concept is proven as a good soulution for year-around operation in heavily ice infested waters (Aksnes et al.2008)

5 Possible FPU's for the Shtockman

In the following a review of the loads and challenges a FPSO might encounter in a field like Shtokman.

5.1 Region information

The Shtokman gas condensate field (SGCF) is located in the Barents Sea approx. 650 km offshore NW of Murmansk. This is supposedly the world's largest gas field and the SGCF phase 1 development has gone on for years before it got frozen and postponed due to a decline in the gas demand marked in Europe. The uncertainty of the project lies within the huge economic cost and challenges it takes to develop an offshore field in such a harsh environment. Now the company shareholders Statoil and Total has left the project because they find the challenges of developing an offshore field in Shtokman at the moment not economical profitable even though it is one of the world's largest offshore fields. Statoil however has signalized in the media that they would consider to join the project if one comes up with a better field solution. But today Gazprom is alone in owning the rights

of Shtokman.

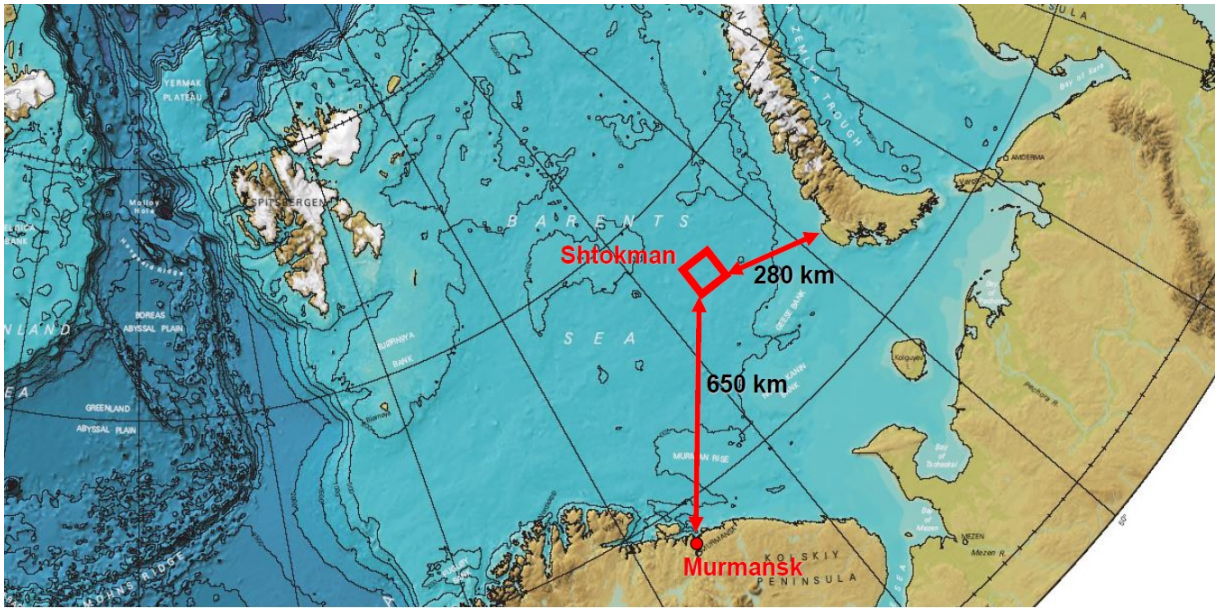

Figure 50 Shtokman field (Liferov AT-327, 2013)

The challenges of this project can seem to out weight the opportunities. The climate conditions in this field are so severe and unpredictable that to make a design for an offshore field solution is not straight forward and there is a lot of factors to consider. Just to make an comparison to other challenging we can present following table (Liferov P. AT-327 2013):

	Norwegian sea	Sakhalin-Sea of Okhotsk	Barents Sea - Shtokman
Depth	280m	40m	***320m***
Distance from shore	200km	15km	***550km***
Wind speeds	38 m/s	37 m/s	***39 m/s***
Wave heights	29m	19m	***25m***
Temperatures	-17 ˚C	-44 ˚C	***-38 ˚C***
Days of darkness	No	No	***100 days***
Ice bergs	No	Yes	***Yes***
Sea ice cover	No	Yes	***Yes***
Icing	Little	Yes	***Yes***

As we can see is there are similarities of condition to especially the Sea of Okhotsk. However the depth of the Barents Sea is much more deeper and that excludes the use of some of the structures used in more shallow waters such as an Gravel island or a Gravity Based Structure (GBS) Hibernia.

Predicting the ice environment in the Barents Sea is difficult due to there is a large inter annual variability, but it is estimated that sea ice is drifting in to the region 3 out of 10 years (fig 51).

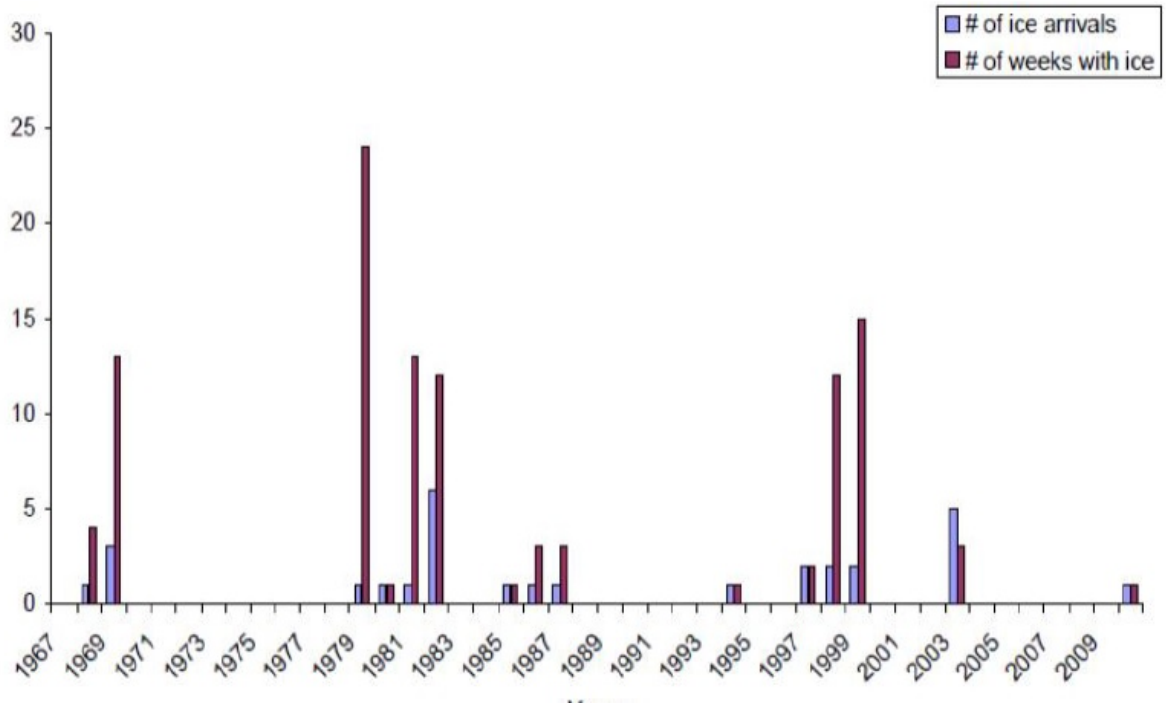

Figure 51Occurences of ice in Shtokman (Liferov at-327. 2013)

The event of an incoming iceberg is also a factor one have to consider. For the last 50 years it is observed over 220 icebergs, in 2002, 15 ice bergs have been observed close to Shtokman where 2 of them where weighing about 3 mill. tons. Probability of an iceberg impact is predicted to be less than once in the 50 years life of the project, in general it is around 50 times less probable to encounter an ice berg than in Canada's grand banks but 30 times more likely to encounter sea ice in the Shtokman compared to the Grand Banks.(Liferov P. Metge M 2009). The keel depth of the ice ridges that one might encounter in the Barents Sea can stretch up to 21 m.

5.2 Design considerations

When deciding on what kind of production units to use with respect to ice following considerations should be taken into consideration (Liferov P. AT-327 2013).

- Production can be performed when sea ice is within the operational limits of the structure.
- The structure should be designed to resist most of the ice actions.
- Ice management is required to detect ice threats to reduce the downtime of the production unit.
- Detection of sea ice and ice bergs is a necessity
- Disconnection must be within the design but should only be used as a last resort.

Today we have only a limited experience of a operating in deeper arctic waters. Today the Deep Arctic water fields (over 100 m) are located in the Barents Sea, Orphan Basin; outside of New Foundland and offshore of Greenland. The technology is still developing but a few concepts has today been found feasible to operate in arctic deep arctic waters.

With those depths in mind there is really only two types of field production types for deeper arctic waters, the subsea to shore concept and the floating production platform/units with subsea wells. Due to the distance from shore of the Shtokman field, the subsea to shore solution would demand serious investments so the use of a FPSO unit has been considered as the most profitable option in terms of transport of the petroleum. For example the distance from shore is over twice as large as the Snøhvit field (232 km from shore) that uses a subsea to shore solution.

5.3 Platform concepts for deep arctic waters

The concepts which are found usable in the deeper arctic waters are the following (Aggarwal et al.2011):

- FPSO (Ship-shaped)
- FPSO (Buoy)
- TLP
- Semi-submersible
- SPAR

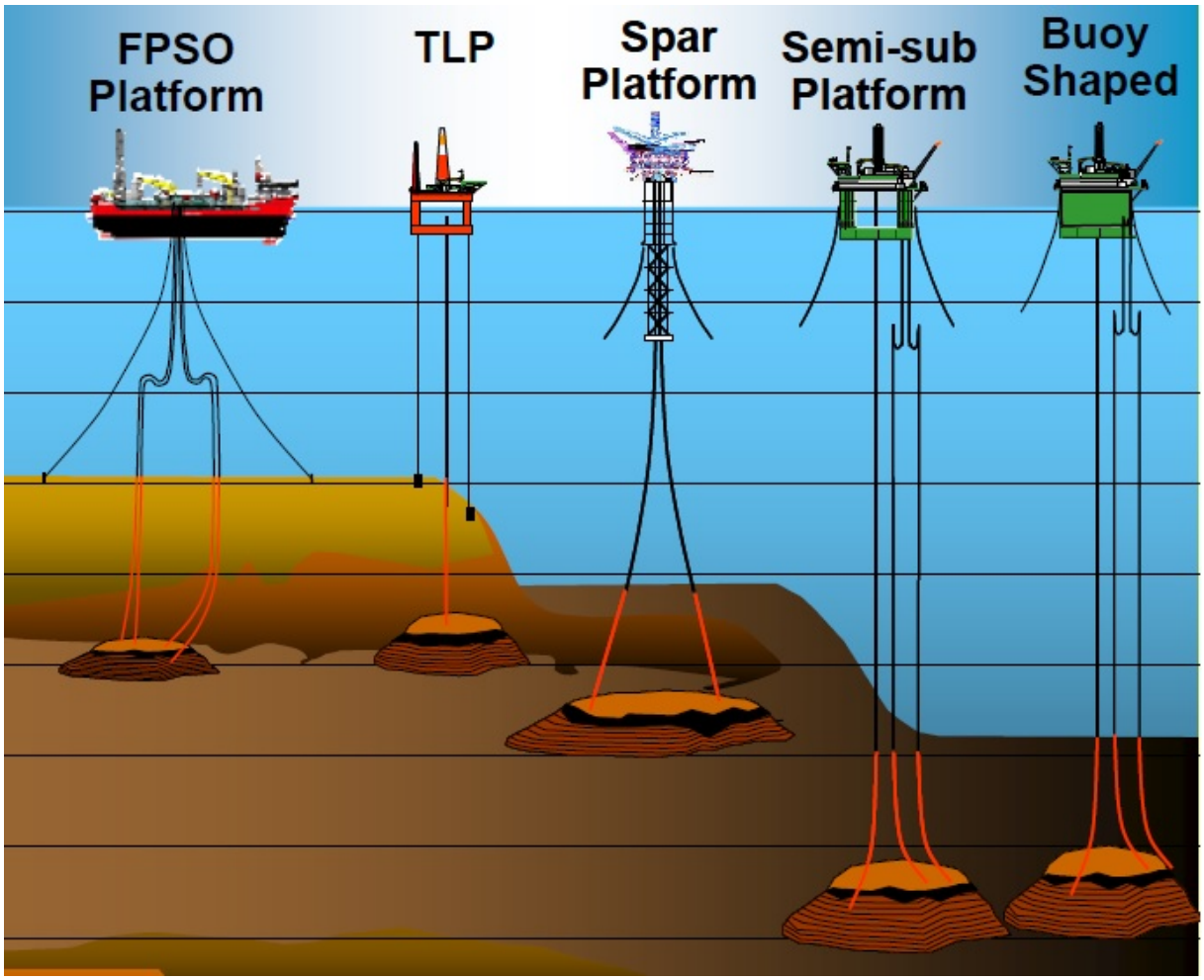

Figure 52 Different floater consepts for deeper arctic waters (Aggarwal R. D'Sousa R. 2011)

FPSO (Ship-shaped)

The ship-shaped FPSO has been proven qualified and is used in the Grand Banks at the Terra Nova field. The water depth of Terra Nova is around 90-100m and it was not considered economically robust enough to support a GBS. The Terra Nova FPSO is equipped with a quickly disconnectable turret, mooring and riser system and is designed to withstand a hit from a 100000 tons iceberg moving at 0.5 m/s.

The Terra Nova FPSO is implemented with an ice management system which covers early detection, monitoring and deflection of incoming ice features. So far there has been no need for disconnection of the Terra Nova FPSO. The ship can also rely on dynamic positioning rather than mooring in certain cases, which in some cases has its advantages.

A FPSO concept has its advantages with that it does not require towing if it wants to move from location. It can also quickly disconnect if needed. However the FPSO is vulnerable to icing. The importance of ice management is imperative because it affects the FPSO ability to weathervane. If this fails the side of the ship will experience huge loads in a worst case scenario.

FPSO Buoy

The buoy-FPSO has its obvious advantage with that it is circular shaped. The loads will then be similar on all sides. Sevan marine has developed a concept called the FPSO Ice and is constructed especially for ice infested waters with a semi enclosed top deck which is designed to resist against icing. The need for ice management will be limited because of it does not need to weathervane. The mooring system used in the Sevan FPSO-Ice is a disconnectable riser and mooring buoy, so there is no need of a turret. The buoy can operate with two drafts, depending on the environmental conditions. In ice infested waters the draft will be lowered in such way that the downward facing cone will be at the waterline to handle the ice action. In open waters the ballast tank will be drained so that the buoy wil be raised to the vertical draft is at the waterline. This will handle the waves better, minimalizing the heaving of the floater.

TLP

This system has a single column design and moored with vertical lines. A modified TLP is also moored laterally and can be called as a hybrid TLP concept. A single column is favorable it terms of geometry and is not that different than of a Bouy shaped FPSO. However, the possibility of it operating in two different drafts is not available and its disconnection procedure is complex.

Semi –Submersible

A semi-submercible has multiple columns that are cone shaped with a downwards slope so that incoming drifting ice will fail by bending. This type of platform is covering a huge deck area compared to the other solutions and is considered as a good solution if the ice drift only drift one way. Then the columns behind the columns that are facing the ice drift are sheltered so that no ice loads is acted on them. However, in a situation where the ice drifts in different directions, which it usually does in the Barents Sea, the ice might jam in between the columns causing an accumulation of ice under the platform. The total ice load on the platform must then be calculated for the entire width of the platform due to the accumulated ice will now act as a wall for the incoming ice. In a worst case

scenario the failure mode will be that of an vertical structure and the force acted on the semi-Semi-submersible would be $F = pA$. In this scenario one would need to disconnect, however the mooring system of this is complex so the disconnecting would not be performed quickly.

SPAR

Instead of the traditional spar that had several columns bundled, the SPAR designed for the Arctic has only one column due to the risk of ice jamming in between the columns. The SPAR designed for the arctic is also modified in such way that the draft is adjustable to both open water (vertical draft) and ice waters (conical draft). The original SPAR design is too wide since the ice loads on the column would be too high for the moorings to handle. So a SPAR for the arctic would need a conical transition with a smaller diameter near the waterline. Due to the length of the SPAR hull and the heavy top weight the transportation and disconnection procedure of the SPAR is a complex task.

5.4 Evaluation of proposed platform concepts

All though all of the proposed FPU's are operational, if we look at the design consideration the disconnection procedure is a vital point and is the one thing that might separate them.

Only two of the units proposed, the FPSO's both ship-shaped and Buoy, are able to disconnect in a timely manner due to the fact that they can rely on a single point mooring system and are quite easy movable either by thrusters or by towing. The reason for the need to disconnect is if the ice loads exceeds the mooring capacity or if an icebergs gets trapped in the mooring lines. The probability of that these scenarios might happen is low (Liferov AT-327, 2013) but it must be taken into consideration in the design.

The disconnection procedure is based on a forecast of the mooring load. When an ice feature pushes on the structure, the production unit will be offset from its original position. The Sevan FPSO –ice is design to disconnect when the offset is 10% of the water depth. The ship-shaped floater has its advantage that it can easily transport itself after disconnection, whilst the Buoy shaped unit must be towed away from location. Many authors and companies has come to the conclusion that the FPSO'S is the best solution for deeper arctic waters.

5.5 Ice loads on the FPSO unit from unmanaged ice.

In order to define the limits of what one could expect the loads from unmanaged ice should be calculated. With unmanaged ice one can consider a huge ice sheet with a certain ice thickness drifting towards the FPSO. With managed ice the ice will be broken up in parts and the global loads would be smaller. To give numerical values to what the FPSO'S has to be able to withstand some examples of calculations will be given.

5.5.1 Level ice

In the case of drifting level ice acting on the structure following calculations can be done.

Circular-shaped FPSO

For a circular-shaped FPSO one simply can use the formula for calculating ice loads on a sloping cone seen in 4.3.3.1 and replace the density of ice with the buoyancy ($(\rho_w - \rho_i)$.Typical parameters is

shown in the appendix as performed in a KRCA spreadsheet (Croasdale K. Palmer A. 2012). The mooring loads on a circular shaped FPSO with a water line diameter of 70m is as following:

Ice thickness	Horizontal load
1,5 m	14.88 MN
2,0 m	17.69 MN
3,0 m	24.33 MN

Ship-shaped FPSO

For a ship-shaped FPSO the load at the bow is calculated the same way as the circular FPSO. The load on the side of the boat is determined by the pressurized ice around the boat and the friction of rubble and ice passing along the ship. $F_{side} = p\mu hL$, where p is the pressure of the ice, μ is the friction of ice and rubble, h is the ice thickness and L is the length of the ship.Following loads is calculated for the ship-shaped FPSO with a width of 200m and a beam of 50m, the parameters are found in the appendix (Croasdale K. Palmer A. 2012):

Ice thickness	Total load
1,5 m	4.71 MN
2,0 m	8.91 MN
3,0 m	17.43 MN

From what we can see from the result above the loads is not that different from each other. However the circular FPSO does not have to weathervane and the ship shaped structures does. If an instant load hits the side of the ship shaped FPSO the load would be the pressure on the side multiplied with the nominal contact area. However the arctic design FPSO has typically a downward slope at the waterline on the side of the boat. Initially the ice will fail by bending. The problem arises if the ice starts to rubble into pieces and ice accumulates. This would increase the load significantly depending on the ice feature and may lead to disconnection or damage to mooring or hull. Typical loads on the broadside would be as following (Croasdale K. Palmer A. 2012)

Ice thickness	Horizontal load
0,5 m	12.2 MN
1,0 m	26.0 MN
1,5 m	40.6 MN
2,0 m	55.7 MN

The load at 2m ice thickness is over 4 times as much as the bow. This is something to consider in the design of the FPSO. This is and first year ridges are probably the designing limit of what a FPSO should withstand from without trying to disconnect.

5.5.2 Ice ridges.

The determination of loads on a structure from ice ridges has been a difficult topic for years. The problem lies within that there is usually uncertainties about the properties of the ice ridge. An idealized ice ridge consists of a sail which is the top part, the consolidated layer which is virtually solid ice and the keel that which consists of ice blocks frozen together with water in between

together with water in between.

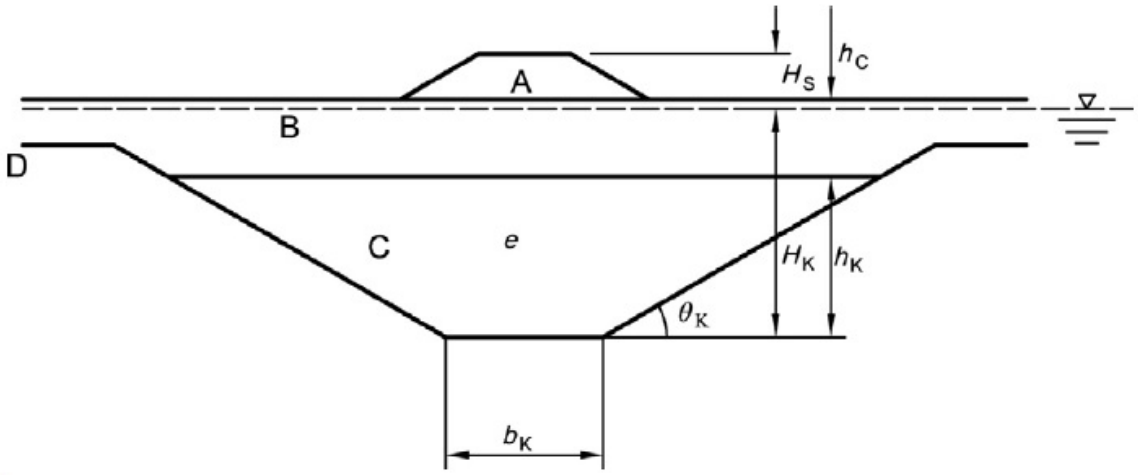

Key

A	ridge sail
B	ridge consolidated layer
C	ridge keel
D	level ice
H_s	sail height
H_k	keel depth
h_c	consolidated layer thickness
h_k	distance between the base of the consolidated layer and the base of the keel
b_k	width of the base of the keel
e	keel porosity
θ_k	keel angle

Figure 53 Sketch of an ice ridge (ISO 19906)

According to ISO 19906 the load from a first year ridge can be calculated as the horizontal load from the consolidated layer and the load from the keel. However when calculating loads for a ridge that hits a downward sloping structure one can assume that when either the keel or the consolidated layer fails, this is the maximum action on the structure. There are several textbooks and authors suggesting methods on how to calculate this.

When calculating the ice loads caused by a ridge it is common to present an idealized model of the ridge which only consists of the consolidated layer and the keel. The sail is assumed not to have a significant contribution to the ice action. For a downward sloping cone which can be used on both the bow of a ship shaped structure and the circular FPSO following method is a outline from Croasdale K and Palmer A. 2012.

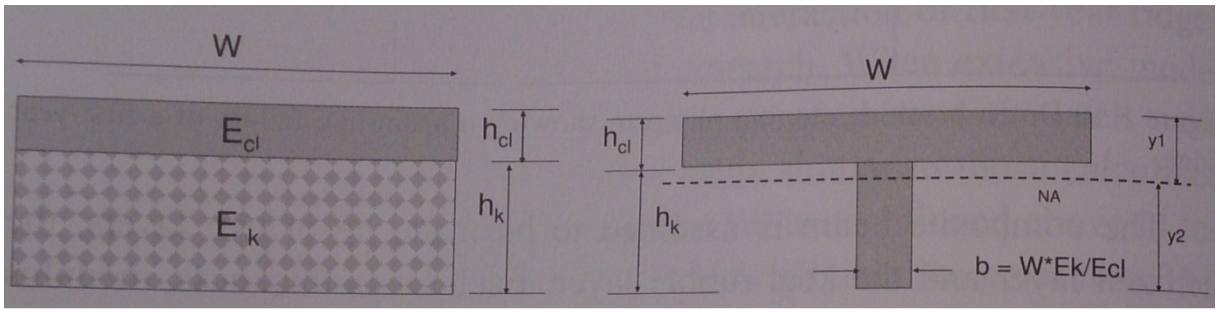

The figure above shows an idealization of an ice ridge with the parameters used for calculating the ice loads.

$$\boldsymbol{b = \frac{WE_k}{E_{cl}}}$$

the "b" represents the width of the keel which is an solid ridge equivalent of pure ice as shown in right of the last figure. E_k and E_c is the elastic modulus for the keel and the consolidated layer respectively.

The stress in the unmodified material is given as:

$$\boldsymbol{\sigma_{cl} = \frac{y_1 M}{I_T}}$$

$$\boldsymbol{I_T = \frac{W(h_{cl})^3}{12} + Wh_{cl}\left(y_1 - \frac{h_{cl}}{2}\right)^2 + \frac{b(h_{cl})^3}{12} + bh_k\left(\frac{h_k}{2} + h_{cl} - y_1\right)^2}$$

where M is the bending moment and I_t is the second moment of area of the transformed section

$$\boldsymbol{y_1 = \frac{W(h_{cl})^2}{2} + \frac{bh_k(h_{cl}+0.5h_k)}{(Wh_{cl}+bh_k)}}$$

y_1 represents the distance to the top surface from the neutral axis.

The stress in the keel area is found by:

$$\boldsymbol{\sigma_k = y_2\left(\frac{E_k M}{E_{cl} I_T}\right)}$$

To assess the critical bending bending moment values the maximum bending moment which creates a crack is found by:

$$\boldsymbol{M_1 = \frac{V_1 L_c}{4}}$$

Where L_c is the characteristic length and V_1 is the load at which the ridge fails:

$$\boldsymbol{L_C = \left(\frac{4E_{cl}I_T}{W\rho_w g}\right)^{0,25}}$$

combining the equations we have the load for the consolidated layer to fail by:

$$\boldsymbol{V_1 = \frac{4\sigma_{cl} I_T}{y_1 L_c}}$$

And the load to fail the keel of the ridge given by:

$$\boldsymbol{V_1 = \frac{4\sigma_k I_T E_{cl}}{y_2 L_c E_k}}$$

This is a pretty straight forward method, however the problem lies within the parameters used. There are huge uncertainties of the values of the flexural strength and modulus of the rubble mass that is in the keel. This is why one could never accurate determining the loads of ice ridges. The prediction of multi-year ridges are even more difficult to determine so that will not be described in this thesis.

7 Summary and Conclusion

General considerations

When thinking of choosing a platform concept one has to consider many different factors. It is necessary to analyze them together to determine if the design is technically feasible, reliable and economically possible. One has to make sure that the structure is able to maintain both vertical and horizontal stability under loads such as:

- Waves
- Currents
- Wind
- Ice cover
- Seismic
- Weight
- Accidental actions
- +++

In the arctic, it is assumed that the highest type of action is caused by ice features. When designing for these, it is not as simple as just calculating for the highest load possible and build accordingly. That would not be economically possible, so instead one calculates the probability of certain events might happened and then do the design accordingly.

When designing a structure it is important to:

- Define possible ice features existing in the region of field development
- Define all possible design scenarios
- Determine parameters of design ice features
- Choose a platform concept
- Calculate ice loads according to the probability of certain types of events happening.

This is not an easy task due to there is a great variety of floating ice forms, variety of the morphometric characteristics of ice features and the variable speeds the ice drift around with. The loads due to ice failure also depend on:

- Local ice strength
- Failure mechanism
- Possible freezing of ice to the surface of a structure
- +++

And for all of the ice actions the resistance of the platform needs to be higher than the ice action or even better, be able to avoid the event all together.

Production units

When it comes to the deeper Arctic waters the best solutions today is probably the choice of the ship-shaped or the circular FPSO. These options are more economically sustainable and are best suited for the deeper waters.

The interphase between the ice and the structure defines the level of ice action exerted on the platform. A vertical faced platform is subjected to higher loads than of a structure with a sloping interphase. From the calculations done in chapter 3.3.3 we saw that the effects of the friction coefficient become significant with steeper slopes than 45˚. An obviously steeper angle gives more crushing which leads to higher loads. So it is important to have a gentle slope as possible and a smooth contact surface between the ice and the structure. We see that the circular FPSO and the SPAR both have modified by implementing a downward sloping cone in their design to better withstand their capability to operate in icing conditions. The down side is that the ability to handle open water diminishes with a sloping draft. That's why a solution with two possible operating drafts is developed. An example is the Sevan FPSO. The ballast tanks are filled during icy waters and drained during open water conditions.

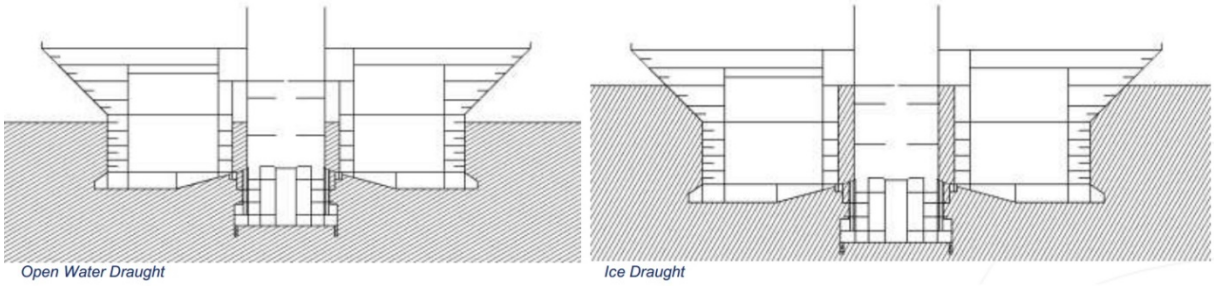

Figure 54 Draft possibilities for a circular FPSO. (Sevan Marine)

The ship-shaped FPSO has its advantages when it comes to transport without help. However the ship shaped FPSO requires a very good ice management due to its necessity to weathervane. The main point to choose a Ship-shaped FPSO is that we actually know it works. The Terra Nova FPSO has been operating sucsessfully in the Grand Banks, while the Sevan FPSO –Ice design is still just a consept, not yet proven to work in the real world. Not long ago, desember 2012, the "mother" of all cylinder FPSO'S design benchmark , the Kulluk drillship, grounded of the coast of Alaska. It was during towing that it got ripped apart from a danker and startet drifting uncontolable in heavy wind and huge waves. No huge damage was done, but that only gives a reminder of how voulnrable platforms like that are in harch environment.

Arctic conditions

The petroleum industry have been drilling and producing oil and gas for several years with successful results. They have a lot of experience in drilling in harsh environment and icy conditions. But the knowledge about drilling in really deep waters 300+meters is limited and the solutions for doing that are few. If a deep-water field is close to shore 250-300km it is possible do a fully subsea solution like they have in Snøhvit. But for Stockman conditions where the distance is over 550km it is today not economical possible.

Properties of ice

It is evident that the lack of knowledge of certain properties of ice features like the ice ridge is a restraint when designing for the maximum loads the structures has to with stand. Due to the complexity of an ice ridge an estimation is done in order to design and this might lead to conservative designs of the production units which is costly in terms of economy.

Environment

One of the biggest challenges is the predicting of the future conditions of the High Arctic. All the predictions and probability estimations are done on historical numbers. With the fast changing climate one really don't know with a good certainty what kind of ice features or other weather condition one might encounter in the future. If you only take a look at the latest events in the world in terms of extreme weather, things are happening that we cannot predict. An to design an offshore field with an expected lifetime of 50 years to survive and operate safe in conditions like that is a outmost challenging task.

Personal note

The above concludes what I have learned from this thesis and my stay at Svalbard. From having no knowledge about field development and ice mechanics. I am satisfied of have learned the basics and to be aware of the challenges that the petroleum industry is facing with respect to the Arctic.

With that being said, I cannot help to have made up some personal opinions after studied for five and a half years. After 5 years of studying Petroleum technology I can only remember having a few lectures about environmental considerations in terms of oil spill and pollution from the oil industry. When I have been to lectures about the challenges and opportunities that the arctic faces, the last thing on the list is environmental considerations and response time. After my opinion this should be the first thing on the list.

The industry is predicting that the melting ice at the north pole will give more opportunities with regards to exploration of oil. That is probably right, however in order to start exploring and developing an offshore field all the way up there a huge infrastructure must be build. This will cost money, a lot of money. When the Macondo incident happened a few years back hundreds of boats and thousands of volunteers was part of the cleanup job on top of huge amount of coastguards and other organization. If an oil spill like that would happen in the arctic, several hundreds of kilometers away from shore a huge infrastructure must be built in order to have the same emergency response. And the response time would be huge due to the distance. I personally can't imagine the amount of economical investments needed for such to happen. And if it happens, a cleanup job in such a severe environment would be difficult due to the harsh environment. I can't help but thinking that maybe this will be the turning point where maybe the money should be invested on EOR from existing wells and new technology for the future.

References

A.J.Keinonen, P. L. (2001). "Azimuth Icebreakers for Ice Offshore." The 16th Int. Conference on Port and Ocean Eng. under Arctic Conditions: pp.877-880.

Croasdale, K. R. (1980). "Ice Forces on Fixed Rigid Structures." 1st IAHR State of the Art Report on Ice Forces on Structures, CRREL Special report: pp. 34-106,pp 180-126.

D.N. Mulherin, D. T. E., T.O. Proshutinskii,A.I.U,D.L.Farmer P.O.Smith (1996). "Development and Results of a Northern Sea Route Transit Model." U.S. Army CRREL Report 96-05.

D.S. Sodhi, S. N. C. (1995). "Indentation and splitting of freshwater Ice floes." Journal of Offshore Mechanics and Arctic Engineering. 117: pp.63-69.

J.E.Overland, C. H. P. (1989). "Prediction of Vessel Icing: a 1989 update." Proceedings of POAC'89.

K.A.Blenkarn (1970). "Measurements and Analysis of the Ice Forces on Cook Inlet Structures." Proceedings of the 2nd Offshore Technology Conference, Houston,Texas 2.

L.Makkonen (1984). Atmospheric Icing on Sea Structures. CRREL Report, U.S. Army.

Pauling, L. (1935). "The Structure and Entropy of Ice and of Other Crystals with some Randomness of Atomic Arrangement. ." J. Am.Chem.Soc. 57: pp. 2680-2684.

R.F. Carlson, J. P. Z., I.C. Hok (1981). "Engineering for Vessel Ice Accretion with particular Reference to Alaskan Fishing Fleet." Proceedings of POAC'81.

S.Bhat (1988). "Analysis of Splitting of Ice Floes During Summer Impact." Cold Regions Science and Technology 5 (1): PP.53-63.

S.Løset, K. N. S., O.T Gudmestad, K.V.Høyland (2006). Actions from Ice on Arctic Offshore and Coastal Structures.

S.Løset, T. C. (1996). "Sea Ice and Icebergs in the Western Barents Sea in 1987." Cold Regions Science and Technology 24(4): pp.323-340.

Sanderson, T. J. O. (1988). Ice Mechanics Risk to Offshore Structures.

T.Nawata, T. K., S. Yano,S Ishikawa (1985). "Model tests of Jacket Structure in Ice Tank." Proceedings of the ISOPE Conference: pp. 436-443.

W.Jolles, R. B., A.Keinonen (1997). "Model development of Vessel Approach Mooring Operations at Arctic Loading Terminals." Proceedings of the 16th International Conference on Offshore Mechanics and Arctic Engineering,Yokohama 13-18 April IV: pp.191-200.

Y.P. Borisenkov, V. V. P. (1972). "Basic Result and Prospects of Research on Hydrometeorological Conditions of Shipboard Icing." Cold regions Research and engineering Laboratory, Draft translation(TL411): pp.1-30.

Dempsey,J P Adamson, R. M and Mulmule,S (1995): Large scale In-situ Fracture of Ice. IN: Wittmann, F H.(ed). Vol. 1 (Proc 2nd Int conference on fracture Mech of Concrete structures (FraM-CoS-2),ETH, ZURICH,pp 575-648.

Kry, P. R. (1978): A statistical prediction of Effective Ice Crushing Stresses on Wide structures. Proceedings of the 4th IAHR Symposium. Vol 1.,pp.33-47

Arno Keinonen, Hal Wells, Peter Dunderdale, P.E. Dunderdale and Associates IncRoger Pilkington, Gordon Miller, Alexander Brovin, (1999),Dynamic Positioning Operation in Ice, Offshore Sakhalin

Gudmestad, O.T; Løset, S; Alhimenko, A.I; Shkhinek, K.N; Tørum, A; Jensen, A. (2007). Engineering Aspects Related to Arctic Offshore Developments

Aksnes, V. Bonnemarie, B. Løset, S. Lønøy, C.(2008). Model Testing of the arctic tandem offloading terminal-Tandem Mooring Forces and Relative Motions between vessels.

P, Liferov and M, Metge.(2009) Challenges with ice related design and operating philosophy of the Shtokman Floating Production Unit. POAC 09'

R, Aggarwal and R, D'Souza (2011), Deepwater Arctic- Technical Challenges and Solutions

Croasdale K. Palmer A. 2012. Arctic Offshore Engineering ch. 6.

Cource material AT-327, AT-332 and AT-301, UNIS Svalbard.

Cammaert, A. B and Muggeridge, D.B (1988). Ice Interaction with Offshore Structures, Van Norstand Deinhold,385pp.

Sodhi,D.s.(1979) Buckling Analysis of Wedge- Shaped Floating Ice Sheet. 5th POAC conference, Vol IV, pp 651-655

Kato, K and Sodhi, D. S.(1983a): Ice Action on Pairs of Cylindrical and Conical Structures. CRREL report 83-25, 35p

Kato, K and Sodhi, D.S. (1983b): Ice Action on two cylindrical and conical structures. The OTC 1983 Conference, OTC Vol 1.

Freudenthal, A.M (1968): Statistical Approach to the Brittle Fracture. chapter 6 in Fracture, Vol 2, ed. by H. Lie-Bowitz, pp 91-619

Swipa report 2011, Arctic Climat issues, AMAP.

S. Chakrabarti (2005), Handbook of offshore engineering

API RT2T, (2010), American Petroleum Institute

Ronalds, B.F, and Lim, E.F.H.(2001), "Deepwater production with surface trees" Trends and Facilities and risers. SPE Asia Pacific Oil and Gas conference Jakarta SPE 68761

S.Løset , Ice compendium(1998) course material AT-327.

Kärna, T. and Johmann, P.,(2003): Field observations of ice failure Models. 17th POAC conference, Vol 2, pp. 839-848

Appendixes

1.

The load component H_B is obtained from

$$H_B = 0{,}68\ \xi\ \sigma_f \left(\frac{\rho_w\ g\ h^5}{E}\right)^{0.25} \cdot \left(w + \frac{\pi^2\ L_c}{4}\right), \text{ where}$$

$$L_c = \left(\frac{E\ h^3}{12\ \rho_w\ g\ (1-\nu^2)}\right)^{1/4}$$

where E is the elastic modulus and ν is the Poisson ratio. Other parameters have been explained above.

The load component H_P is expressed as

$$H_P = w\ h_r^2\ \mu_i\ \rho_i\ g\ (1-e)\left(1-\frac{\tan\theta}{\tan\alpha}\right)^2 \cdot \frac{1}{2\tan\theta}$$

where h_r is the rubble height, μ_i is the ice-to-ice friction coefficient, e is the porosity of the ice rubble and θ is the angle the rubble makes with the horizontal.

The load component H_R is given by

$$H_R = w\,P\,\frac{1}{\cos\alpha - \mu\sin\alpha}\text{, where}$$

$$P = 0{,}5\,\mu_i\,(\mu_i+\mu)\,\rho_i\,g\,(1-e)\,h_r^2\sin\alpha\cdot\left(\frac{1}{\tan\theta}-\frac{1}{\tan\alpha}\right)\cdot\left(1-\frac{\tan\theta}{\tan\alpha}\right)+$$
$$+\,0{,}5\,(\mu_i+\mu)\,\rho_i\,g\,(1-e)\,h_r^2\,\frac{\cos\alpha}{\tan\alpha}\left(1-\frac{\tan\theta}{\tan\alpha}\right)+h_r h\,\rho_i\,g\,\frac{\sin\alpha+\mu\cos\alpha}{\sin\alpha}$$

The load component H_L is given by

$$H_L = 0{,}5\,w\,h_r^2\,\rho_i\,g\,(1-e)\,\xi\left(\frac{1}{\tan\theta}-\frac{1}{\tan\alpha}\right)\left(1-\frac{\tan\theta}{\tan\alpha}\right)+$$
$$+\,0{,}5\,w\,h_r^2\,\rho_i\,g\,(1-e)\,\xi\tan\phi\left(1-\frac{\tan\theta}{\tan\alpha}\right)^2+\xi\,c\,w\,h_r\left(1-\frac{\tan\theta}{\tan\alpha}\right)$$

where c and ϕ are the cohesion and the friction angle of the ice rubble. The final load component, H_T, that is needed in Equation (A.8-40) is given by

$$H_T = 1{,}5\,w\,h^2\rho_i\,g\,\frac{\cos\alpha}{\sin\alpha-\mu\cos\alpha}$$

Equation (A.8-40) has been modified from the original equation[A.8-16] to account for compressive stress in ice sheet as a result of the applied horizontal load, accounting for the denominator in Equation (A.8-40). This is considered by using the calculated value of the horizontal action to modify the flexural strength as follows

$$\sigma_f^{(1)} = \frac{F_H}{l_c\,h}+\sigma_f$$

where l_c is the total length of the circumferential crack, estimated as

$$l_c = w+\frac{\pi^2}{4}L_c$$

2

The following functions are defined for the solution:

$$f = \sin\alpha + \mu \; E_1 \cos\alpha$$

$$g_r = \frac{\sin\alpha + \dfrac{\alpha}{\cos\alpha}}{\dfrac{\pi}{2}\sin^2\alpha + 2\,\mu\,\alpha\cos\alpha}$$

$$h_v = \frac{f\cos\alpha - \mu\,E_2}{\dfrac{\pi}{4}\sin^2\alpha + \mu\,\alpha\cos\alpha}$$

$$W = \rho_i\, g\, h_r \frac{w^2 - w_T^2}{4\cos\alpha}$$

where α is the slope of the structure measured from the horizontal (in radians), w_T is the top diameter of the cone and h_r is the ice ride-up thickness ($h_r \geq h$). Effects of a rubble accumulation on the cone can be considered by using a value that exceeds the single sheet thickness for the ride-up thickness. The parameters E_1 and E_2 are the complete elliptical integrals of the first and second kind, defined as

$$E_1 = \int_0^{\pi/2} \left(1 - \sin^2\alpha \;\sin^2\eta\right)^{-1/2} d\eta$$

$$E_2 = \int_0^{\pi/2} \left(1 - \sin^2\alpha \;\sin^2\eta\right)^{1/2} d\eta$$

Assuming a single sheet thickness of ride-up ice, the horizontal ride-up action H_R and the vertical ride-up action V_R are obtained from the expressions

$$H_R = W\,\frac{\tan\alpha + \mu\,E_2 - \mu\,f\,g_r\cos\alpha}{1 - \mu\,g_r}$$

$$V_R = W\cos\alpha\left(\frac{\pi}{2}\cos\alpha - \mu\,\alpha - f\,h_v\right) + H_R\,h_v$$

The horizontal breaking action H_B and the vertical breaking action V_B are given by

$$H_B = \frac{\sigma_f\,h^2}{3}\,\frac{\tan\alpha}{1 - \mu\,g_r}\left(\frac{1 + Y\,x\ln x}{x - 1} + G\,(x-1)(x+2)\right)$$

$$V_B = H_B\,h_v$$

where $Y = 2{,}711$ for Tresca yielding or $Y = 3{,}422$ for Johansen yielding and $G = (\rho_i\,g\,w^2)/(4\sigma_f h)$. The parameter x is given by

$$x = 1 + \left(3\,G + \frac{Y}{2}\right)^{-1/2}$$

3

Matlab codes.

M-file generated by COMSOL (black letters) and after modified by us (red letters)

```
function out = sodhi_beam1(a1, a2, filename)
%
% sodhi_beam.m
%
% Model exported on Oct 30 2013, 22:55 by COMSOL 4.3.1.115.

import com.comsol.model.*
import com.comsol.model.util.*

model = ModelUtil.create('Model');

model.modelPath('I:\');

model.name('Sodhi beam.mph');

model.modelNode.create('mod1');

model.geom.create('geom1', 2);
model.geom('geom1').feature.create('r1', 'Rectangle');
model.geom('geom1').feature.create('r2', 'Rectangle');
model.geom('geom1').feature.create('r3', 'Rectangle');
model.geom('geom1').feature.create('r4', 'Rectangle');
model.geom('geom1').feature.create('uni1', 'Union');
model.geom('geom1').feature('r1').set('size', {'3.4' num2str(a1)});
model.geom('geom1').feature('r2').set('size', {'3.4' num2str(0.75-
a1)});
model.geom('geom1').feature('r2').set('pos', {'0' num2str(a1)});
model.geom('geom1').feature('r3').set('size', {'0.1' num2str(0.75-
a2)});
model.geom('geom1').feature('r3').set('pos', {'3.4' '0'});
model.geom('geom1').feature('r4').set('size', {'0.1' num2str(a2)});
model.geom('geom1').feature('r4').set('pos', {'3.4' num2str(0.75-
a2)});
model.geom('geom1').feature('uni1').selection('input').set({'r1'
'r2' 'r3' 'r4'});
model.geom('geom1').run;

model.physics.create('solid', 'SolidMechanics', 'geom1');
model.physics('solid').feature.create('spf1', 'SpringFoundation1',
1);
model.physics('solid').feature('spf1').selection.set([2 7]);
model.physics('solid').feature.create('pl1', 'PointLoad', 0);
model.physics('solid').feature('pl1').selection.set([3]);
model.physics('solid').feature.create('sym1', 'SymmetrySolid', 1);
model.physics('solid').feature('sym1').selection.set([3]);
model.physics('solid').feature.create('fix1', 'Fixed', 1);
model.physics('solid').feature('fix1').selection.set([12]);

model.mesh.create('mesh1', 'geom1');
model.mesh('mesh1').feature.create('ftri1', 'FreeTri');

model.view('view1').axis.set('xmin', '-0.20527414977550507');
model.view('view1').axis.set('ymin', '-1.9025318622589111');
model.view('view1').axis.set('xmax', '3.7052741050720215');
```

```
model.view('view1').axis.set('ymax', '2.402531862258911');

model.physics('solid').feature('lemm1').set('E_mat', 'userdef');
model.physics('solid').feature('lemm1').set('E', '2.28*10^9');
model.physics('solid').feature('lemm1').set('nu_mat', 'userdef');
model.physics('solid').feature('lemm1').set('nu', '0.33');
model.physics('solid').feature('lemm1').set('rho_mat', 'userdef');
model.physics('solid').feature('lemm1').set('rho', '920');
model.physics('solid').feature('spf1').set('kPerArea', {'0';
'10000'; '0'});
model.physics('solid').feature('pl1').set('Fp', {'0'; '-
8294.1*t/3.9'; '0'});

model.mesh('mesh1').feature('size').set('hauto', 1);
model.mesh('mesh1').run;

model.study.create('std1');
model.study('std1').feature.create('time', 'Transient');

model.sol.create('sol1');
model.sol('sol1').study('std1');
model.sol('sol1').attach('std1');
model.sol('sol1').feature.create('st1', 'StudyStep');
model.sol('sol1').feature.create('v1', 'Variables');
model.sol('sol1').feature.create('t1', 'Time');
model.sol('sol1').feature('t1').feature.create('fc1',
'FullyCoupled');
model.sol('sol1').feature('t1').feature.remove('fcDef');

model.result.dataset.create('cln1', 'CutLine2D');
model.result.dataset.create('cln2', 'CutLine2D');
model.result.create('pg1', 'PlotGroup2D');
model.result('pg1').feature.create('surf1', 'Surface');
model.result('pg1').feature('surf1').feature.create('def',
'Deform');
model.result.create('pg2', 'PlotGroup1D');
model.result('pg2').feature.create('lngr1', 'LineGraph');
model.result('pg2').feature.create('lngr2', 'LineGraph');
model.result.create('pg3', 'PlotGroup1D');
model.result.export.create('plot1', 'Plot');

model.sol('sol1').attach('std1');
model.sol('sol1').feature('st1').name('Compile Equations: Time
Dependent');
model.sol('sol1').feature('st1').set('studystep', 'time');
model.sol('sol1').feature('v1').set('control', 'time');
model.sol('sol1').feature('v1').feature('mod1_u').set('scaleval',
'1e-2*3.579455265819089');
model.sol('sol1').feature('v1').feature('mod1_u').set('scalemethod',
'manual');
model.sol('sol1').feature('t1').set('control', 'time');
model.sol('sol1').feature('t1').set('timemethod', 'genalpha');
model.sol('sol1').runAll;

model.result.dataset('cln1').set('genpoints', {'0' '0'; '0'
'0.75'});
```

```
model.result.dataset('cln2').set('genpoints', {'3.5' '0'; '3.5'
'0.75'});
model.result('pg1').name('Stress (solid)');
model.result('pg1').feature('surf1').set('expr', 'solid.sx');
model.result('pg1').feature('surf1').set('rangecolormin', '-40000');
model.result('pg1').feature('surf1').set('rangecoloractive', 'on');
model.result('pg1').feature('surf1').set('unit', 'N/m^2');
model.result('pg1').feature('surf1').set('descr', 'Stress tensor, x
component');
model.result('pg1').feature('surf1').feature('def').set('scale',
'996.3661457056616');
model.result('pg1').feature('surf1').feature('def').set('scaleactive
', false);
model.result('pg2').set('ylabel', 'Stress tensor, x component
(N/m<sup>2</sup>)');
model.result('pg2').set('xlabel', 'Y-coordinate (m)');
model.result('pg2').set('ylabelactive', false);
model.result('pg2').set('xlabelactive', false);
model.result('pg2').feature('lngr1').set('descr', 'Stress tensor, x
component');
model.result('pg2').feature('lngr1').set('unit', 'N/m^2');
model.result('pg2').feature('lngr1').set('xdata', 'expr');
model.result('pg2').feature('lngr1').set('xdatadescr', 'Y-
coordinate');
model.result('pg2').feature('lngr1').set('data', 'cln1');
model.result('pg2').feature('lngr1').set('expr', 'solid.sx');
model.result('pg2').feature('lngr1').set('xdataexpr', 'Y');
model.result('pg2').feature('lngr1').set('looplevelinput',
{'last'});
model.result('pg2').feature('lngr2').set('descr', 'Stress tensor, x
component');
model.result('pg2').feature('lngr2').set('unit', 'N/m^2');
model.result('pg2').feature('lngr2').set('xdata', 'expr');
model.result('pg2').feature('lngr2').set('xdatadescr', 'Y-
coordinate');
model.result('pg2').feature('lngr2').set('data', 'cln2');
model.result('pg2').feature('lngr2').set('expr', 'solid.sx');
model.result('pg2').feature('lngr2').set('xdataexpr', 'Y');
model.result('pg2').feature('lngr2').set('looplevelinput',
{'last'});
model.result.export('plot1').set('plotgroup', 'pg2');
model.result.export('plot1').set('plot', 'lngr1');
model.result.export('plot1').set('filename', filename);
model.result.export('plot1').run;

out = model;
```

Script for simulating via MATLAB LiveLink

```
for a1=[0.1:0.01:0.6]
    for a2=[0.1:0.01:0.6]
        filename = strcat('(2)',num2str(a1),'x',num2str(a2),'.txt');
        sodhi_beam1(a1,a2,filename);
    end
end
```

Script for data processing and obtaining intensity factor surface.

```
i = 1;
K11 = [];
for a1 = [0.1:0.01:0.6]
    j = 1;
    for a2 = [0.1:0.01:0.6]
        filename = strcat(num2str(a1), 'x', num2str(a2), '.txt');
        fid = fopen(filename);
        textscan(fid,'%s',28);
        data = textscan(fid, '%f %f',67);
        fclose(fid);

        x = cell2mat(data(1));
        Stress = cell2mat(data(2));

        [maxStress, maxIndex] = max(Stress);

        xx = x(maxIndex:maxIndex+2);
        yy = Stress(maxIndex:maxIndex+2);
        p = polyfit(xx, yy, 2);

        c = 0.005;
        maxStress = p(1)*(a1+c)^2 + p(2)*(a1+c) + p(3);

        K11(i, j) = maxStress * (2 * pi * c)^0.5;

        j = j + 1;
    end
    i = i + 1;
end

a1 = [0.1:0.01:0.6];
a2 = [0.1:0.01:0.6];
surf(a2, a1, K11)
```

4

Flexural strength of ice (kPa)	500	500	500	500	500	500	500
Specific weight of ice (kN/m^3)	8,89	8,89	8,89	8,89	8,89	8,89	8,89
Specific weight of water (kN/m^3)	10,10	10,10	10,10	10,10	10,10	10,10	10,10
Bouyant Weight (kN/m^3)	1,21	1,21	1,21	1,21	1,21	1,21	1,21
Young's modulus (kPa)	5,00E+06	5,00E+06	5,00E+06	5,00E+06	5,00E+06	5,00E+06	5,00E+06
Poisson's ratio	0,3	0,3	0,3	0,3	0,3	0,3	0,3
Bow Angle (deg)	30	30	30	30	30	30	30
Rubble angle of repose (deg)	20	20	20	20	20	20	20
Rubble friction angle (deg)	45	45	45	45	45	45	45
Rubble Depth (m)	15	15	15	15	15	15	15
Beam at Bow (m)	50	50	50	50	50	50	50
Ice-ship friction	0,1	0,1	0,1	0,1	0,1	0,1	0,1
Ice-ice friction	0,05	0,05	0,05	0,05	0,05	0,05	0,05
Ice thickness (m)	0,5	0,5	0,5	1,5	1,5	3	3
Rubble porosity	0,2	0,2	0,2	0,2	0,2	0,2	0,2
Cohesion of rubble (kPa)	2	2	2	2	2	2	2
Waterline length (m)	200	200	200	200	200	200	200
Pressured Ice (kPa)	5	15	30	5	30	5	30

Flexural strength of ice (kPa)	500	500	500	500	500	500	500
Specific weight of ice (kN/m^3)	8,89	8,89	8,89	8,89	8,89	8,89	8,89
Specific weight of water (kN/m^3)	10,10	10,10	10,10	10,10	10,10	10,10	10,10
Bouyant Weight (kN/m^3)	1,21	1,21	1,21	1,21	1,21	1,21	1,21
Young's modulus (kPa)	5,00E+06	5,00E+06	5,00E+06	5,00E+06	5,00E+06	5,00E+06	5,00E+06
Poisson's ratio	0,3	0,3	0,3	0,3	0,3	0,3	0,3
Cone Angle (deg)	45	45	45	30	30	30	30
Rubble angle of repose (deg)	35	35	35	20	20	20	20
Rubble friction angle (deg)	45	45	45	45	45	45	45
Rubble depth (m)	15	15	15	20	20	20	20
Waterline diamenter (m)	40	40	40	70	70	70	70
Ice-cone friction	0,1	0,1	0,1	0,1	0,1	0,1	0,1
Ice-ice friction	0,05	0,05	0,05	0,05	0,05	0,05	0,05
Ice thickness (m)	0,5	1,5	3	0,5	1,5	2	3
Rubble porosity	0,2	0,2	0,2	0,2	0,2	0,2	0,2
Cohesion of rubble (kPa)	5	5	5	5	5	5	5